4/4/77

INTERPRETATION OF GEOPHYSICAL DATA FROM THE BROKEN HILL AREA

Thesis submitted for the Degree of Master of Science

by

H.T. Pecanek, B.Sc. (Hons.)

Department of Economic Geology,

University of Adelaide.

This thesis does not contain any material previously submitted for any degree in any University by me, or any other person, except where due reference is made in the text of the thesis.

(Signed)

21st October, 1975.

ABSTRACT

Bulk density measurements determined from 2884 samples of diamond drill core from the metamorphic rocks of the Broken Hill lode sequence were used to construct subsurface density models which were used in computer modelling of the expected gravitational attraction. This was then numerically compared with observed gravity profiles with stations as close as fifty feet to produce residual gravity profiles. The detailed gravity survey covered an area of 20 sq miles whilst local traverses of two hundred foot spacing and regional traverses of half mile to two mile spacing extended coverage to 600 sq miles. Correlation between aeromagnetic, gravity and geological data was attempted.

CONTENTS

CONTENTS (contd.)

FIGURES

FIGURES (contd.)

FOLIO FIGURES

TABLES IN TEXT

APPENDICES

SECTION 1 GENERAL INTRODUCTION

The dimensions of geological samples ranged from handsize to regional scale. Many bulk density measurements were determined from diamond drill core only a few inches long. Using computer modelling of the subsurface density distribution these small scale measurements were compared with gravity data along traverses with station spacing from fifty to two hundred feet and almost seven miles in total length. These traverses were in turn compared with regional gravity traverses with station spacing from half a mile to one mile, and of length of the order of twenty miles. Finally gravity data was examined on a regional area basis and compared with regional geological maps and regional aeromagnetic maps.

This study was undertaken to determine whether other Broken Hill type orebodies could be detected using gravimetric data and also whether the country rock formations could be characterized by gravity anomalies. Other such studies had been conducted (O. Weiss, D.W. Smellie). These studies were conducted after the major gravimetric survey had been completed in 1949 by O. Weiss and Associates on behalf of the Zinc Corporation. Previous studies had suggested that the Broken Hill orebody could be detected using the gravimetric method, but no final report had been made on interpretations of the O. Weiss data. No other orebodies have been found using this method in the Broken Hill district. The author decided to undertake rigorous quantitative evaluation of the extensive gravimetric and density data and geological data. The University of Adelaide's CDC 6400 computer was used to calculate the expected gravitational anomalies of sub-surface density distributions. These distributions the author inferred for numerous density determinations made on unweathered diamond drill core and geological data. Such studies would be possible in other areas where diamond drill core was available near an orebody. However,

often in the literature the computer modelling technique is used to infer the density contrasts within the subsurface - or if density data from the subsurface are available then they are not used with the intensity of observations undertaken by the author. An extensive and detailed study was made of the variations in bulk density.

The results found by the author were not in accord with those found by previous workers. The author found that because of variations in bulk density of the country rock the gravity anomaly due to the orebody was effectively masked by those anomalies caused by the country rock. Other techniques such as filtering are not expected to have succeeded since the expected gravity anomaly due to the orebody has no strong spectral characteristics. The author suggests in other areas where subsurface unweathered samples are available and access to modern computer facilities is possible that theoretical expected responses be calculated to suggest whether an orebody could be detected by the gravity method.

Other results found by the author include the conclusion that rock formations in the Broken Hill area can be traced using gravity anomalies for over two miles in many instances, particularly where the excellent coverage provided by the O. Weiss survey exists. Excellent correlation with aeromagnetic data was also possible. Good regional gravity data would help reduce ambiguity in interpretation of regional aeromagnetic and geological data.

The Broken Hill lode sequence is characterized by a positive local anomaly and also regionally by an area of higher gravitational attraction. Regionally psammitic sequences such as granite gneiss and aplitic sequences were characterized by gravity lows. The largest positive gravity anomaly occurs in an area where only one shallow diamond drill hole exists. The anomaly can be tentatively correlated with a lode sequence. However, amphibolites outcrop in this vicinity.

The volume of lode sequence would have to be twice that in the Broken Hill lode sequence to account for this anomaly and the density of the rock must on average be at least as dense as the Broken Hill Lode Sequence.

ACKNOWLEDGEMENTS

I thank Professor D.M. Boyd for suggesting this project, and for many helpful directions during its course. I wish also to thank the Zinc Corporation of Broken Hill for permitting access to their gravimetric data and also access to core for further data collection. Particularly Dr. David Klingner and Ian Johnson of the Zinc Corporation deserve thanks in this respect. I would also like to express my appreciation to the Mine Manager's Association of Broken Hill for their field and travel allowance during collection of data in the Broken Hill area. Bill Laing and Roger Cammell of the University of Adelaide also deserve thanks respectively for assisting in the collection of geological and surveying data. I am grateful to Clifford Gurr of C.S.I.R.O. for allowing the use of radiometric absorption facilities for automated density determinations.

SECTION 2 BULK DENSITY DATA

2.1 Introduction to Bulk Density

In 1950 and 1951 L.A. Richardson presented approximately one thousand, nine hundred and fifty bulk density values in diagrammatic form (described in Appendix 1). He also presented average bulk densities for rock types commonly found in the Broken Hill Area. These averages are included in Table 1 which comprises of a list of averages which have been given by several workers. O. Weiss and L.A. Richardson were two consultants for Zinc Corporation in 1949. Rob Wood and G. Jenke were two Honours students at the University of Adelaide during 1972. Ralf Burkett was Acting Chief Geologist from North Broken Hill Limited in 1972. The author, who measured density variations within sillimanite gneiss in order to discover whether any bulk density variations within the country rock of the Broken Hill lode sequence might produce a gravity anomaly similar to the Broken Hill orebodies, has given some averages in this table. The author's realization of the dense Zinc Lode Horizon was important because it increases the gravity anomaly expected near the Broken Hill orebody. Also important to remark was the high bulk density of the amphibolite bodies.

The original copies of L.A. Richardson's diagrams are now not available nor are tables which list the original values. In order to use these results quantitatively and to present some of the data for comparison with the data measured by the author values were measured from dyeline copies. These copies are now too faint to be reproduced.

One thousand, one hundred and eighty four of the density values presented by L.A. Richardson are plotted on Folio Fig. 1. Also plotted on this figure are nine hundred and thirty four values measured by the author. The data was plotted by the ten inch Calcomp plotter connected to the University of Adelaide CDC 6400 computer. The plotter

took one thousand and seventy seconds to plot the data and the axes with labels. All values from any one borehole are represented by the same symbol. For each borehole the density values are plotted in the same sense, that of plotting more westerly values to the right of the graph with the horizontal scale as one inch represents four hundred feet. The vertical scale is one inch represents 0.2 gram/cm^3. Also diamond drill holes 1600 and 2200 are plotted one above the other to allow vertical correlation of density. Horizontal positioning was based on the positions of these diamond drill holes relative to the rock types indicated in geological section 262 of the New Broken Hill Consolidated Mine (Folio Fig. 4).

Before discussing some of the features of the bulk density variations along boreholes it is interesting to consider where these boreholes lie in relation to the Broken Hill lode sequence. The one thousand, two hundred density determinations from Section 62 were made on core from a volume containing the orebody. This volume had a cross-section of twelve hundred feet and a depth of two thousand, six hundred feet. Since most of this volume is occupied by lode, A horizon and the enveloping gneiss, these density values provide very good information on the density of the lode zone. Since density information on the lode zone is also available in Section 92 the change in bulk densities of the lode can be observed along strike.

The bulk density of A lode averages 0.16 gm/cm^3 lower in Section 92 than in Section 62. Also number 1 lens group and lead lode are absent. Therefore a smaller gravity anomaly due to the lode was expected over Section 92.

As a special study of the Broken Hill lode sequence in a section where no orebody was thought to exist Section 262 was sampled by the author for density determinations. Eight hundred and forty density determinations were made on core selected from two diamond

drill holes. These diamond drill holes, DD 1600 and DD 2200, intersected an equivalent part of the Broken Hill lode sequence for a majority of their length (see N.B.H.C. Geological Section 262, Folio Fig. 4). Therefore, correlation of average bulk densities was made between these diamond drill holes in order to gain a qualitative level of confidence for extending estimates of average bulk density downdip.

Also N.B.H.C. descriptions of mineralogy of core samples for density determinations were used by the author. These were used both quantitatively and semi-quantitatively. (See Section 2.4.1).

2.2 Interpretation of Density Data from the Broken Hill Lode Sequence

The first approach used by the author to interpret bulk density values was to examine the data one borehole at a time. In one such approach the density data were filtered by square ware filters of various band widths (Zurflueh). However, trends could not successfully be removed by this method.

In order to determine whether the density of the sillimanite gneisses were spatially related over distances of around one hundred feet the author constructed semi-variograms (Matheron, G., 1971). The semi-variogram compares the squared differences between the values measured at adjacent sample points with the squared differences between values sampled further apart. The semi-variograms showed that there was no spatial dependence of samples over the range thirty feet to one hundred and twenty feet - in other words at that range the density values may be treated as random. The main contribution towards the spatial dependence of density values from samples from the Broken Hill lode sequence was from a few amphibolite stringers. The most notable was a xixty feet wide stringer from the upper (west) amphibolite, formation 11, in Fig. 1. Therefore, the best estimate for the average density of sillimanite gneiss formations was the arithmetic average for densities found within the formations. The author found that in

TABLE 1 TABLE OF AVERAGE BULK DENSITY OF ROCKS FROM THE BROKEN HILL LODE SEQUENCE

Rock Type	O.W. Zinc	L.A.R. N.B.H.C.	R.J.W. U of A	G.P.J. U of A	R.B. N.B.H.	H.T.P. U of A
Pb Lode	3.59	3.58				
Zn Lode	3.22	3.22				
Enveloping Gneiss	2.80–2.90	2.89				
Zinc Lode Horizon					East 2.66	3.00
Granite Gneiss	2.72	2.72	2.74 (1)	2.70	2.75–2.80	
Sillimanite Gneiss	2.80	2.84	2.84 (2)	(2.83 (3) (2.80 (5)	2.75–2.85	2.83–2.80
Thorndale Gneiss	2.75	–				
Amphibolite	3.15	3.15			3.2 –3.35	3.2 –3.3
Pegmatite	–	2.65				
Potosi Gneiss	–	2.79				
Aplite	–	2.67				
Garnet–Haematite	–	4.00				
Schist	–		3.005			
Dolerite	–	–	3.06			
Garnet S/S	–	–	–	–	3.38	
Shears					2.81 also 2.92	
Lode					2.93	

(1) 2.74 gm/cm^3 average for 56 readings with a st. dev. 0.044
(2) 2.84 gm/cm^3 average for 82 readings with a st. dev. 0.095
(3) 2.70 gm/cm^3 average for 76 readings with a st. dev. 0.069
(4) 2.83 gm/cm^3 average for 63 readings with a st. dev. 0.15
(5) 2.80 gm/cm^3 average for 76 readings with a st. dev. 0.06

Section 262 the average bulk density of sillimanite gneiss was 2.83 gm/cm^3. As this average falls within the range reported by other workers (see Table 1) the average was used as basis for comparison for all densities. Since sillimanite gneiss was the most voluminous rock in the Broken Hill lode sequence this reduced the volume of rock to be considered anomalous in subsurface density models.

Initially the geometry of formations used in subsurface density models was that suggested by geological sections (e.g. Fig. 4 and Folio Figs. 2, 3 & 4). This was necessitated by the insufficient number of density values. In the rare cases where sufficient density control was available boundaries were based on major density contrasts.

2.3 Bulk Density of the Broken Hill Orebody

An average bulk density was assumed between the boundaries. Outside these boundaries the bulk density was assumed to be that of sillimanite gneiss common to the Broken Hill lode sequence. On re-examining density data collected by the N.B.H.C. mine the author realized that the Zinc Lode Horizon (see Fig. 1) has a density significantly larger than that of sillimanite gneiss. Thus the initial model was modified by inclusion of the Zinc Lode Horizon with geometry as drawn in Zinc Corporation Geological Section 30.

As there was sufficient information near the lodes in Section 62 a final model was based entirely upon the bulk density data.

L.A. Richardson from N.B.H.C. mine presented bulk density values in 1949 on diagrams which are now not available. Also no tables of the original values are available. Therefore in order to use this work quantitatively all values were read from duplicates. In Appendix 1 these diagrams and the small error incurred in rereading the bulk density values are described. All values were used to deduce the average density distribution. Folio Fig. 1 represents most of these

values and those determined by the author.

Folio Fig. 1 illustrates the high densities recorded in the lode rocks. Diamond drill hole number 131 contains both A and B lode. Density values as high as 4.3 gm/cm^3 were recorded. The end of DD 131 is in the Zinc Lode Horizon and the densities are plotted in Folio Fig. 1 above the minus 5800 feet feducial. These values are also greater than those common to sillimanite gneiss, which is extensively intersected by DD 1600 and DD 2200. The density values recorded on core from these boreholes are also represented in Folio Fig. 1. The Zinc Lode Horizon (Formation number 9 in Fig. 1) has an average density of 3.0 gm/cm^3, considering all diamond drills for which density determinations have been made.

In Folio Fig. 1 it may also be observed that along diamond drill 15 the bulk density values remain high between A lode and B lode. In diamond drill 107 the author observed an exceptionally high average density of 3.47 gm/cm^3 for just two hundred feet between A lode and lead lode. Generally the average bulk density for rock between lodes was greater than that for country rock. Thus as the initial model of the orebody zone was based on the geometry of the lodes as drawn in Section 62 (Folio Fig. 3) the total gravitational attraction of the orebody zone was underestimated. This underestimation was the greater gravitational attraction of the interlode rock over that of the country rock.

Since the number of densities recorded in the vicinity of the orebody in Section 62 was high the geometry of the subsurface density distribution could be defined using these observed density values. The averages for consecutive two hundred feet intervals were computed. These were then marked on Section 62. Three subdivisions were then made on the basis of the type of averages observed (see Fig. 4). The divisions were considered to be low, medium or high density divisions

of the Broken Hill orebody zone. The relatively low average of 2.98 gm/cm^3 was found at the near surface extremity of the orebody. Overestimation of the near surface division would have been more critical because gravitational attraction decreases as the inverse of the distance squared. Therefore this division was kept small. The second division contained the Zinc Lode Horizon over the greater volume. Also contained were the upper and thinner reaches of A lode and B lode, which are two divisions of the Zinc orebody. The average bulk density of this division was 3.02 gm/cm^3.

The lowest part of the orebody (not including the Zinc Lode Horizon) was found to have the highest bulk density (3.28 gm/cm^3). This was mainly due to the preponderant volume of lead lode and partly due to the presence of dense A lode and B lode. The geometry of these three divisions is illustrated in Fig. 4.

2.4 Bulk Density of the Lode Sequence

Figure 1 illustrates the disposition of formations in the Broken Hill Lode Sequence. No bulk densities were available for the footwall gneiss (Formation number 1) or for Formation number 2, a sillimanite gneiss which contains potosi gneiss stringers and banded iron formation. Therefore no density contrasts were assumed in the initial model.

The author made ninety-six bulk density measurements through and around the lower (east) amphibolite, Formation number 3. These measurements were made on core taken from DD 2310 in Section 84. This core is only 2400 feet along strike from Section 62 in which most density information is known. Therefore, this data is expected to provide a reasonable estimate of the average bulk density for the lower (east) amphibolite in that section. The average bulk density was 3.10 gm/cm^3 over an apparent thickness of four hundred feet. Apart

from the lode this amphibolite has the highest bulk density over volumes significant when related to gravimeter detection. In Fig. 2, at feducial minus 3500 feet, the anomalously high density of the lower (east) amphibolite can be seen. (Figure 2 illustrates the values for average bulk density over consecutive one hundred feet intervals.)

When a true thickness of four hundred feet was assumed for the lower (east) amphibolite the gravity anomaly predicted was much larger than that observed. The density contrast assumed was 3.10 gm/cm^3 for the amphibolite against sillimanite gneiss assumed to be 2.83 gm/cm^3 throughout the Broken Hill Lode Sequence unless specially re-defined. The geometry used was that shown in Section 62 (Folio Fig. 2).

If the geometry and thickness of the lower amphibolite as drawn in Section 30 (Fig. 1) was used in the subsurface density model the residual gravity anomaly was found to be smaller. This true width can be deduced from the apparent width of four hundred feet which was observed in diamond drill 2310, Section 84. The author observed that the angle of intersection of the axis of the core with the compositional layering was forty-five degrees - this compositional layering was defined by light and dark bands. The light bands were believed to be rich in quartz and feldspar.

To the east of the lower (east) amphibolite in DD2310 a high density rock called "potobalite" was intersected. "Potobalite" has amphibolite and a potosi gneiss composition. Over an intersection of seventy feet the "potobalite" was found to have a bulk density of 3.00 gm/cm^3 (Folio Fig. 1 at feducial -4880). It is possible that this unit causes a small observed gravity anomaly (Fig. 5 at feducial -1900 feet). A high density model for this "potobalite" has been successfully used by the author in Section 92 (Fig. 9).

The initial subsurface density model for the lower (east) amphibolite produced a large residual anomaly. However, re-examination of the geological evidence suggested modifications which produced a smaller residual anomaly. In many formations some feedback was allowed in that excessively large residual anomalies suggested in which way the model assumed was wrong.

In Section 92 DD 130 passes through Formation number 4 which is predominantly sillimanite gneiss. Between feducials 1100 feet and 2300 feet in Fig. 2 the average densities for 100 feet intervals of Formation number 4 are plotted. This twelve hundred feet long intersection has an average bulk density of 2.83 gm/cm^3. Therefore no anomalous density need be considered since sillimanite gneiss from the Broken Hill Lode Sequence averages 2.83 gm/cm generally.

It is interesting to observe that a relatively broad section of Formation 4, between feducials -3300 feet and -2000 feet, in DD 1600 has a higher than average density and is not encountered in DD 2200. In this stratigraphic position in Section 262 the geological section suggests that banded iron formation and a Potosi gneiss stringer are lensing out. Ian Johnson, Chief Geologist of Zinc - N.B.C.C. mines at Broken Hill, first pointed out the correlation of this density anomaly with lensing of rock types (pers. comm.). This produces a density anomaly of up to 0.02 gm/cm^3 in adjacent diamond drill holes. This anomaly emphasises the need for cross-correlation of density information in order to gain an intuitive confidence in the legitimate extrapolation of bulk density values both along strike and down dip.

The author was guided by Professor Boyd to measure densities along those adjacent diamond drill holes, namely DD 1600 and DD 2200. The author was pleased to have examined the correlation down dip. The correlation was good for densities from Formations 5 to 11. However, there was lensing of a higher density zone within Formation 4. No

other formations were common to both diamond drill holes. Also correlation along strike was possible using densities presented by L.A. Richardson in Section 92. These correlations will be alluded to as each formation is discussed. The ultimate validity of the density models is indicated by the success with which the observed gravitational field can be predicted (Residual Gravity, Section 3.3).

Figure 2 shows the broad correlation of average bulk density for Formations 5 to 9. A high density zone over 600 feet wide was defined on the basis of the density values. It has an average bulk density of 2.89 gm/cm^3. It can be seen in Fig. 2 between feducials -1400 feet and -900 feet for DD 1600, between feducials -1500 feet and -800 feet for DD 2200 and between feducials +170 feet and 2900 feet for DD 130. Much of this unit is composed of rock bulked as potosi gneiss. Since elsewhere potosi gneiss has a bulk density of 2.78 gm/cm^3 this may be taken as anomalous. Explanation may lie in the presence of banded iron formation. Also this high density zone lies in the lode horizon (where Formation numbers 7 to 9 could occur).

2.4.1 Geological Description of Core

The N.B.H.C. geological description of core was examined. The author attempted to correlate recorded visible variations in mineral composition with the bulk density.

Qualitative comparison of each density determination with core mineralogy was effected by plotting density values every tenth of an inch. The data was plotted on fourteen inch wide computer paper using the line printer. As samples were drawn at a regular spacing of ten feet and the printer prints six lines every inch, this represented a scale of one inch represents sixty feet. At each footage where the description of rock type changed an arrow was plotted by hand. Also between arrows the description was annotated. Coloured asterisks were

used to denote mineralization. It must be stated that the N.B.H.C. descriptions of core do not explicitly relate to ten foot intervals of core as the samples for density determination do. Rather they relate to various lengths of core some times of the order of two thousand feet. Such an example is the Hanging Wall Gneiss. For the sillimanite gneiss, from which came most of the core selected by the author, N.B.H.C. descriptions of core mineralogy related to lengths of up to seventy feet. Often apparent density contrasts or gradiations existed within such lengths.

Attempts were made to qualitatively correlate such variations with comments within the description relevant to that length of core. For example whilst the core from a particular length may be described as a sillimanite biotite garnet gneiss it may be commented that less sillimanite exists downhole and that the gneiss is more quartzitic downhole. In such a case the bulk density will be seen to decrease downhole. The comment that numerous interbeds of quartzite or quartz gneiss were present amongst sillimanite gneiss was often correlated with higher fluctuations in bulk density values than usual.

The semi-quantitative use of the descriptions of mineralogy for core consisted of first using the rock classification whether gneiss, schist, amphibolite or the special classifications potosi gneiss, granite gneiss and quartzite. Then the relative order of percentages in mineral composition were digitized from the sequence in the list of minerals written by the N.B.H.C. geologists before the rock type. Then the average density for each rock classification was taken for subclasses selected on the basis of mineral composition. This may have meant that when a mineral was selected as being first in the list it had a greater than usual percentage composition rather than actually occupying the greater volume of the rock. However, the averages do relate to the relative composition of the mineral selected. The results

TABLE 2 GEOLCGICAL DESCRIPTION OF CORE

Average Bulk Densities, Section 262

Rock Type	Major Mineral	M	Std	No.of Samples	Mineralized
Amphibolite		3.249		6	
	Quartz	2.939			
Sericite Gneiss	Gneiss	2.906	0.123	10	
	Schist	2.785		2	
Sillimanite Gneiss		2.856	0.083	318	2.885/0.098/32
	Feldspar rich	2.899	0.118	27	
	Garnet	2.865	0.074	112	
	Biotite	2.860	0.113	45	
	Sillimanite	2.846	0.077	80	
	Sericite	2.839	0.059	30	
	Quartz	2.805	0.055	29	
Potosi Gneiss		2.806	0.065	33	2.856 0.038 5
Quartzite		2.778	0.071	124	2.815 ± 0.067 15
	Garnet rich	2.816	0.090	4	

N.B. Densities measured in core from ZC DD 160C, Broken Hill

are summarized in Table 2.

For DD 1600 there are several factors relevant to the increase in density of the Potosi Gneiss. Firstly Potosi Gneiss containing traces of pyrite or phyrrhotite is on average 0.06 gm/cm^3, denser than the average for all Potosi gneiss including samples which are mineralized. Secondly, sillimanite gneiss is 0.03 gm/cm^3 for samples where mineralization was noted than for all sillimanite gneiss including samples where mineralization was noted. Thirdly the relative proportion quartz and garnet can change the density of the sillimanite gneisses. The sillimanite gneisses are gneisses which contain visible sillimanite crystals. Their actual composition varies over a whole range of compositions. It was noted by the author that the garnet rich variety tended to predominate in this high density zone. Also included in this high density zone is the Banded Iron Formation. Although this formation is only a few feet wide it may be indicative of the proximity of heavy elements. These may be evident in the form of iron in garnet, for example.

No definite correlation between density and original geological environment was possible. However, psammitic rocks tended to be less dense. It was postulated that for metamorphosed sedimentary sequences the more psammitic sections would be less dense, ranging from 2.67 gm/cm^3 for aplite to 2.72 gm/cm^3 for granite gneiss (Table 1), also that for metamorphosed pelitic sequences the density would be as high as 2.83 gm/cm^3 for sillimanite gneiss to 3.3 gm/cm^3 for amphibolite-rich gneisses.

2.4.2 Lode Sequence West of the Lode Zone

The lode zone in Section 262 included the upper Potosi Gneiss and was a composite of Formations five to nine (see Fig. 1). The average of the bulk density values found within these formations in Section 262 then served as the average for the whole high density zone.

The lower Potosi Gneiss in Section 262 (see Folio Fig. 4) was considered as a composite with Formation four.

Formation 10 is a sillimanite garnet gneiss. Different averages for the bulk density of this formation were found in Sections 62 and 92. The presence of pegmatites and an unconformable garnet quartzite and gneiss which is one hundred feet thick is believed to be the cause. The gravity data has a break in O. Weiss gravity line 2A above the formation in Section 92 and there is no anomaly above Formation 10 in line 1 in Section 62. Therefore there is no indication from the gravity data that this density anomaly extends significantly distant from DD 130. In Section 262 the average bulk density of core from DD 1600 was 2.83 gm/cm^3 over 500 feet. In the same section but for DD 2200 the formation averaged 2.83 over 500 feet and 2.79 over another two hundred feet.

Formation 11 is the west or upper amphibolite and is composed of amphibolite stringers and sillimanite gneiss (King and O'Driscoll, 1953). There are generally four to five stringers of amphibolite of variable width which cannot be correlated with assurance between boreholes. However, one amphibolite estimated sixty feet thick with average density of 3.20 gm/cm^3 can be correlated between DD 1600 and DD 2200. The selection of a width which incorporated a maximum anomalous density contrast was avoided. The geometry as presented in Section 262 Folio Fig. 4 and N.B.H.C. geological descriptions of the core were used to select the intervals of density data. The model proposed for the west amphibolite in Section 262 was 160 feet wide with average density 2.97 gm/cm^3. This high density zone can be seen on Folio Fig. 1 in DD 1600 between feducials -360 feet and -240 feet and also in DD 2200 between feducials -120 feet and zero.

Formation number 12 is a sillimanite gneiss. In Section 262 DD 1600 intersects this formation over a length of one thousand feet.

The average bulk density for this formation in Section 262 is 2.82 gm/cm^3. As the subsurface density models are related to a standard density of 2.83 gm/cm^3 Formation number 12 has only a density contrast of 0.01 gm/cm^3. The expected gravitational attraction is not significant so no model is necessary. However, in Section 92 Formation 12 averages 2.79 gm/cm^3 over a four hundred feet intersection with DD 130. The densities decrease towards the Hanging Wall Granite Gneiss, whereas in Section 262 the average density for 100 feet sections of core remain more constant over a length of 1000 feet. Such a difference is not unexpected because Formation number 12 has a width of 400 feet in Section 92 compared with a width of 2400 feet in Section 262.

In later models for Section 92 the density was averaged over Formations 11 and 12. The combined unit has an average density of 2.84 gm/cm^3 for 700 feet. This model produced no significant residual anomaly.

Formation number 13 is a granite gneiss called the Hanging Wall Gneiss. Density data was available for only the eastern side of the Hanging Wall Gneiss. However, the N.B.H.C. geological sections suggest that the gneiss is grossly homogeneous. Therefore the average bulk density measured on the eastern side was extended throughout the whole volume. This average was 2.72 gm/cm^3 when given by O. Weiss and L.A. Richardson and as 2.74 gm/cm^3 by R.J. Wood (see Table 1 and R.J. Wood, 1972). Since L.A. Richardson's individual density values were available they were reviewed by the author. Replotting the data illustrated the lower mean value and lower variance of the densities of Hanging Wall Gneiss. Densities averaged over 100 feet intervals from DD 130 Section 92 are illustrated in Fig. 2 between feducials 4200 feet and 6000 feet. The average density rises by 0.04 gm/cm^3 seven hundred feet inside the eastern boundary. The author considered that this high density band would be expected to outcrop only 500 feet west

of the boundary and would therefore correlate with a small gravity anomaly mentioned in the interpretation of residual anomalies (Section 3.3.1). However, apart from this small high density band the bulk density of the Hanging Wall Gneiss appeared the least variable when compared with other formations from the Broken Hill Lode Sequence.

2.4.3 Conclusions to the Interpretation of Density Data

The author has re-examined the density measurements carried out by N.B.H.C. and presented by L.A. Richardson. Whilst the average densities for rock within the lodes were correctly determined the author believes that at least one other important observation can be drawn from this data. The author has noted that the Zinc Lode Horizon (Formation number 9) has an average density slightly in excess of 3.00 gm/cm^3. As it has a volume and bulk density comparable to that of the lode and extends further towards the surface then intuitively it will produce a gravitational attraction comparable to that of the orebody. This means that if one assumes that the Zinc Lode Horizon is largest where there is an orebody present its presence enhances the likelihood that a residual positive anomaly will be observed over an orebody in the B.H. sequence. A second observation made by the author was that there were high densities recorded between lodes. Since the number of density determinations was large in the vicinity of the lodes it was possible to define the density distribution based only on the density determinations.

Average bulk density values were consistently correlated with formations from the Broken Hill Lode Sequence. It is unfortunate that a diamond drill hole (DD 305 geological section 92, Folio Fig. 3) passes through the upper amphibolite at a shallow depth above the Broken Hill orebody without density determinations having been made on the core. The core is now weathered. The author suggests that since

density determinations are relatively cheap when compared with the cost of drilling that determinations should be made every ten feet whenever it is probable that gravity data will be collected. In the case just mentioned a small residual anomaly exists close to the expected position of the anomaly due to the orebody.

Average bulk density for formations and the geometry of these formations as described in N.B.H.C. and Zinc Corporation sections were proposed for initial subsurface models. The author believes that the case studied here does not reach the maximum nor optimum potential use of density determinations to detect the type of orebody in question.

Not all spatially suitable boreholes were sampled for density determinations and now the core has weathered. In view of the cost of the gravity survey some corcession in the design of the drilling program (such as spatial location and individual hole length) could have been made - had the modern computer been available to help design optimum sampling to differentiate the anomalous density of the target from the anomalous density within country rock.

SECTION 3 RESIDUAL GRAVITY

3.1 Introduction to Residual Gravity

The Broken Hill Lode Sequence in the New Broken Hill Consolidated and Zinc Corporation Mine leases was covered by a gravity survey conducted by O. Weiss and Company in 1949. O. Weiss was a consultant geophysicist to the Zinc Corporation. The author believed the accuracy of the gravity data was good. The author believed a Worden gravimeter was used accurate to 0.02 milligals and that staff and level were used for elevation and positional control. In Section 3.3 a brief concerning the likely cause of "noise" observed in detailed gravity profiles (50 and 100 foot spacing) is presented. The author believed that some of the profiles were too short (for example profile 2A, Fig. 9). The author expected the width of the gravity anomaly due to the orebody is around 4500 at half the maximum height and since the shorter O. Weiss profiles were about this length they could not define more than fifty percent of the orebody. Therefore the author presumed that O. Weiss expected the gravity anomaly due to the orebody to be much sharper than the author predicted. This illustrated how a computer could help plan a gravity survey.

After the O. Weiss gravity survey over the Broken Hill orebody had been completed in 1949, density determinations were made on diamond drill core from rocks of the lode sequence. Almost half of these samples were taken from the lode and lode horizon in Section 62 Zinc Corporation. In 1950 and 1951 L.A. Richardson presented the bulk density values. The author believes the data was collected to discover whether an obvious anomaly should have been observed above the orebody. Smellie used this bulk density information to calculate the expected response of the Broken Hill orebodies (Smellie, 1960). He assumed that these orebodies could be satisfactorily represented by a simple rectangular density contrast. As computer technology was not readily available such approximations were necessary to avoid excessively

tedious numerical evaluations.

Smellie inferred that the Broken Hill orebody should be detectable by the gravity method. The author does not agree. Whilst the gravitational anomaly for the lode predicted by the author is of similar magnitude and frequency content, other gravity anomalies interfere and mask the anomaly caused by the Broken Hill Lode. The author has based his conclusions on a detailed study of additional bulk density data, and the use of the University of Adelaide's modern CDC 6400 computer to accurately predict the expected gravity anomaly caused by complex density distributions.

Whilst the rock formations showed density variations which were essentially two dimensional - or even one dimensional - the validity of the Talwani-type subsurface models (Talwani et al, 1959) depends also upon whether the density variations are constant in a direction normal to the section. Since the orebody is known to plunge at around 20 degrees the author used three dimensional prisms to determine whether the plunge would produce an appreciable change in the expected gravity anomaly (Appendix 4 and 5). The results indicated that plunge and strike variations of up to 20 degrees from the normal produce variations less than 0.05 milligals in the expected response to the Broken Hill orebody.

The method of computing the gravitational attraction towards a buried two dimensional, horizontal prism of arbitrary polygonal cross-section is discussed in Appendix 3. The author wrote subroutines to accumulate the contributions from many models towards each gravity station and to compare the value with that observed by O. Weiss gravity traverses. The mismatch between these profiles was called the residual anomaly and was the arithmetic difference. The residual anomaly was then examined to deduce the set of possible causitive bodies. The problem with this inverse process was that the solution was not unique

since theoretically the number of bodies could have been infinite and in practice the types of bodies were often significantly diverse in geological implication. In particular one wished to know whether an orebody could produce a given residual anomaly. However, a suitable distribution of high density material other than lode could be producing this residual anomaly. It remained therefore to gain knowledge of the geological possibilities likely to produce anomalies similar to that of an orebody. Clearly this depended on the locale and the nature of the expected gravitational attraction towards the orebody. In the Broken Hill Lode Sequence the anomaly caused by the lode can be detected. However, only after the good knowledge of the geology and the density distribution for the subsurface country rock has been used.

The author does not believe that the gravity method is a powerful exploration method for the detection of a Broken Hill type orebody, the reason being that in order to detect such an orebody extensive drilling of the country rock must be obtained in order to predict the gravity response caused by the country rock. The author believes that such drilling would have a high probability of intersecting the orebody. Furthermore the presence of the dense Zinc Lode Horizon would cast ambiguity as to whether any residual anomaly had been caused by an orebody or a larger than expected volume of Zinc Lode Horizon.

3.2 Expected Gravitational Attraction Towards the Broken Hill Orebody

In 1950 Smellie used a model of simple geometry and of one density contrast to predict the gravitational attraction at the surface and due to the Broken Hill orebody. Smellie (1960) stated that the orebody should be detected by its gravitational anomaly. He predicted

that the maximum anomaly should be 0.5 milligals and that the width of the anomaly curve at half this value should be 4400 feet. This width is hereafter called the half width. The geometry of this model was that of a right rectangular prism 1500 feet below the surface of width 500 feet and depth 1400 feet. The prism was infinite in extension at right angles to the plane of the profile and was horizontal in attitude. The magnitude of Smellie's expected response curve compared favourably with that predicted by the author's first model for the orebody zone.

This first model used to describe the density distribution near the Broken Hill orebodies was based on the geometry illustrated in the N.B.H.C. geological section number 62 (Folio Fig. 2) and on the average densities found for the different lodes (Table 1). Also included in the density model near the orebody was the Zinc Lode Horizon (Formation number 9, Fig. 1). The density of the Zinc Lode Horizon was found by the author to be just greater than 3.0 gm/cm^3. The total expected response of these bodies is illustrated in Fig. 3. The maximum of the orebody response curve is 0.62 milligals and the width at half this value is only 2800 feet. The reason that Smellie's half-width was greater was that his model had a greater depth to the top of the body. However, even the author's model with an expected response which is sharper, the expected orebody response is broad when compared with the peaks in the observed profile.

Steeper gradients and larger amplitudes can be seen in the observed Bouguer anomaly profile. The residual curve in Fig. 3 also illustrates the relatively broad nature of the expected orebody response. Here the residual anomaly is the difference between the expected gravitational response to the orebody and the observed Bouguer anomaly profile. This residual anomaly is plotted upside down to the observed Bouguer anomaly to avoid fusion of the three curves. It is not possible

to determine the presence or absence of the orebody merely by visual inspection of these curves. One cannot say that the orebody produces an obvious and unmistakeable anomaly. Therefore the author considers it necessary to attempt to predict the observed Bouguer anomaly using all relevant geological knowledge.

Ideally the prediction could be exact. However, in practice it is required that all bodies other than orebodies be sufficiently defined to permit their gravitational effects to be subtracted from the observed Bouguer anomaly thereby leaving a residual which can predict the presence or absence of an orebody. The first paradox which must be tested is whether it is required to so accurately define the country rocks that the presence or absence of the orebody can be determined geologically without the evidence of gravitational anomaly. Secondly the residual is required to unambiguously determine the nature of the high density material. This is impossible. This it must be also tested whether such high density material is likely to be an orebody.

The Zinc Lode Horizon has an expected response of 0.4 milligals in the density model for the orebody just described. By comparison the expected gravity anomaly caused by the orebody is only 0.2 milligals. Therefore if the Zinc Lode Horizon were to have the same density even where the orebody was not present a net difference of only 0.2 milligals might be expected. Furthermore, in Section 92 a high density zone was intersected in DD 130 in a position below the orebody. It is not obvious whether this high density zone corresponds to the Zinc Lode Horizon, Formation 9. The author believes that the high density zone interxected by DD 130 is not related to the Zinc Lode Horizon. The reasons for this opinion were presented in the interpretation of density data from the Broken Hill Lode Sequence. However, it is not necessary to know the origin of the high density zone which occurs where the

orebody might be expected, provided that there is sufficient density information to compare the density of this zone where there is an orebody with the density of this zone where no orebody exists. As discussed in the interpretation of the density of the orebody a model was designed on the basis of the density information only. The expected response of the Broken Hill orebody zone in Section 62 using this model is 1.05 milligals with a half width of 4100 feet. This model includes the lodes, the interlode rocks, the Zinc Lode Horizon and any rock which falls inside the boundaries of this orebody zone (Fig. 4). The author believes that any high density rock below 4000 feet will not contribute greatly to the observed anomaly. Therefore the model is expected to account for all significant density variations except near surface density variations. For example it is not known what density the Zinc Lode Horizon has within 200 feet of the surface. It is predicted that the density of the Zinc Lode Horizon will not be too anomalous near the surface because its density decreases towards the surface in the boreholes below 200 feet. Also the potosi-banded iron high density zone in Section 92 has its equivalent in Section 62 between 0 feet and 200 feet near the surface. Furthermore, the density near the upper amphibolite is not known near the surface. However, the author believes that these near surface density variations will produce only anomalies of small amplitude and very short half-widths. Therefore this model predicts the gross gravitational attraction expected from the lode zone where an orebody is present.

3.3 Expected Response to the Broken Hill Lode Sequence, Section 62

Polygonal outlines of the geometry presented in N.B.H.C. geological section number 62 were used for the first models to represent the subsurface density distribution of the Broken Hill Lode Sequence (e.g. see Fig. 5). As previously discussed in the interpretation of

density no information about the density is known east of Formation 3, the east amphibolite. The residual anomalies over density models for the footwall gneiss Formation number 1 suggested that its density was not very much less than 2.80 gm/cm^3. The maximum gravitational anomaly from these arbitrary models was -2.0 milligals. However, a half milligal residual anomaly at the far east end of gravity profile 1A (at -7000 feet in Fig. 5) suggests that a rock formation of average density lower than 2.80 gm/cm^3 might be present.

No local densities were known also for the potosi gneiss except in DD 130 which is underneath the orebody. Since the potosi gneiss thickens above this intersection and is known to have a variable density (see Section 2.4) it was decided not to put forward an initial model for the potosi gneiss. The small rssidual in Fig. 5 at -50 feet is consistent with the potosi gneiss having a considerable thickness and a density lower than 2.83 gm/cm^3. Subsequent models incorporated a low density model for the potosi gneiss in Section 62.

A model for the east amphibolite, Formation 3, was based on the densities observed in DD 2310, Section 84. The predicted gravitational anomaly towards the east amphibolite is 1.6 mg. and has an almost symmetrical half-width of 1400 feet. In Fig. 5 at -1900 feet a small residual anomaly indicates that Formation 2 has a density slightly more than the standard density of 2.83 gm/cm^3. The residual is small and as density information is available for only a very small part of Formation 2 no model was proposed. It may be noted that examination of all O. Weiss gravity profiles revealed that this small anomaly was almost always present. This indicates that the causative body has a considerable strike extent of at least 16,000 feet. Returning to the residual anomaly profile in Fig. 5 at a position above the east amphibolite at -1400 feet, one can see that the theoretical anomaly matches the observed profile to within 0.1 milligals. The

orebody model was based on the geometry of the lodes and the zinc lode horizon. The response to this body has been discussed in Section 3.2.

The west amphibolite was difficult to model in Sections 62 and 92. One problem was that there were no density determinations for Section 62. Another complication was that the density data from DD 130 Section 92 did not closely correlate with that in DD 1600 and DD 2200, Section 262. The density contrasts for Formations 10, 11 and 12 were less in Section 92 and in particular the density of the west amphibolite was lower. Further complication was that DD 130 lies under the orebody. It is shown on the Section 92 that the garnet quartzite is transgressive. This means that a density contrast observed in DD 13 may not be the same as that near the surface. Yet another complication is that of the relation of the geophysical profile to the geological section. In particular the relation of the residual anomaly to the west amphibolite. Any positive density contrast assigned to the west amphibolite produced an expected peak displaced from the peak in the observed profile. This mismatch is of the order possible from the three degrees between the line of profile and the line of section plus the fact that these lines are not intersecting near the west amphibolite. If one were to assume that the strike of the rocks were normal to the geological section and at an angle of three degrees to the geophysical profile then the distance between the east amphibolite and the west amphibolite would be 2600 feet and the distance between their respective anomaly peaks would be 135 feet greater. It must be pointed out that the author did not have time to verify the actual outcrop position of the west amphibolite in relation to the geophysical profile. This is partly a result of the absence of the original pegs laid in 1949. To emphasize the positional uncertainty one can consider that as the geophysical profile is not exactly adjacent to the geological section then variations in strike can cause further error. There is

no need to postulate that a contribution towards this mismatch may by caused by any error in the position of the west amphibolite as marked on the geological section. Considering the mismatch in the position of the expected anomaly for the west amphibolite and in view of the fact that the average density of Formation 10 and the west amphibolite when combined was 2.83 gm/cm^3 it was decided to omit the model for the west amphibolite from later models for the lode sequence in Sections 62 and 92. The latter fact implies that only a narrow residual anomaly might be expected since the gross anomaly expected from these formations is expected to be zero. Where included the west amphibolite was modelled for Section 62 in Fig. 5. Here a positive density contrast of +0.14 gm/cm^3 was postulated on the basis of densities observed in Section 262 and Section 92 (even though Formation 10 Section 92 contains the apparently transgressive garnet quartzite). At 1200 feet west of the Mine Reference Line a residual anomaly was found above the west amphibolite. This residual of 0.4 milligals has the same magnitude as that predicted from the model for the west amphibolite. Considering problems with the data and the residual anomaly this evidence suggests that the west amphibolite should not be modelled in this position.

Based on O. Weiss and L.A. Richardson's value for the density of the Hanging Wall Gneiss, the models for the Hanging Wall Gneiss produced an excessively large residual anomaly. If the geometry was left unchanged and a density contrast of -0.08 gm/cm^3 was assumed then the residual anomaly was approximately zero. Whilst this may seem to indicate inconsistency between the density data and the observed gravitational attraction it must be remembered that density data is known for only the eastern margin of the Hanging Wall Gneiss. Also it must be noted that R. Wood's average density of 2.74 gm/cm^3 for the Hanging Wall Gneiss would require a density contrast of -0.09 gm/cm^3. This is much closer to -0.08 gm/cm^3, the optimal density contrast, than

is -0.11 gm/cm^3, the density contrast derived from O. Weiss and L.A. Richardson's average density of 2.72 gm/cm^3 for the Hanging Wall Gneiss. It is noted inFig. 1 at feducial 5000 feet that there is an increase in density in the Hanging Wall Gneiss. This can be correlated with the residual anomaly in Fig. 5 at 2250 feet. Furthermore, on the western margin a similar anomaly can be seen at 4000 feet on Fig. 5 which would be consistent with repetition of this high density. No density data from the west side is available for further correlation.

In Fig. 5 the residual anomaly over the Broken Hill Lode Sequence has a maximum absolute value of 0.3 milligals. The observed anomaly over the sequence has a maximum of 2.2 milligals. Thus most of the observed gravity anomaly can be accounted for by the theoretical response of this model. This is a good estimation since the observed profile has 0.1 milligal amplitude noise. In order to estimate what type of noise might be expected in the residual anomaly, Bouguer gravity values from adjacent observed gravity profiles were subtracted. If the profiles lay sufficiently close one assumes that no major density variations will have taken place. It is intended to reveal the type of anomaly which has been caused by error in measurement, variations in the depth of weathering, variations in the depth of cover and those local variations in the density of formations which could not be measured unless boreholes penetrated the weathered layer as often as the profiles occur. Since the noise is random one expects the differences between profiles sufficiently close to contain energy 1.4 times the amplitude of the noise (as previously defined). At the top of Fig. 7 profile 1A minus profile 1 is shown. The comparison of the profiles has been achieved by subtraction of the gravity values observed at locations believed to be in equivalent positions in the Broken Hill Lode Sequence. The strike distance from line 1A to line 1

is only 500 feet. The N.B.H.C. geological sections are 2000 feet apart. Geological mapping does not give sufficiently detailed data to vary the true thickness of units between sections. Nor is there density data between the sections - in fact density data is extended from one section to another because complete density data for the lode sequence is not available for each section. Thus the difference between gravity profiles 1A and 1 gives an estimate of gravity variations which the author could not hope to account for. Anomalies of amplitude 0.2 milligals can be ovserved with half-width of 400 feet. Similarly profile 1A less profile 1C represents differences in gravitational attraction which the author could not hope to account for. However, not so for profile 1A minus 3A, nor profile 1A minus 3. For these latter comparisons in observed gravity profiles a comparison of geological sections is also possible. Therefore an attempt can be made to explain gravity differences in terms of geological differences. For example a positive anomaly on the difference curve means that profile 1A has a greater gravitational attraction in this position. The most striking anomaly in the profile of the difference between profile 1A and profile 3 is at 1000 feet; it is an anomaly of 0.5 milligals in a position above the orebody. Unfortunately three points (circled) on this difference curve are drawn from three points which were linearly interpolated over a gap in the data of profile 3. Even profile 3A has two data points missing between 750 feet and 1050 feet. However, the anomaly in the profile of the difference between profile 1A and profile 3A is sufficiently defined. It is not as large as that in the profile of the difference between profile 1A and profile 3. Although the noise in the profiles is high the author believes that this anomaly is consistent with profile 1A having an increased gravitational attraction at 1000 feet due to the orebody being closer to the surface or the orebody being denser. However, as the anomaly

is small it could not be used as a confident guide as to the presence or shallowing of an orebody. The absence of critical gravity data points weakened the potential of this difference method of detection of the presence of the orebody. The model for the Broken Hill Lode Sequence in Section 62 was revised and this was presented in Fig. 6. The Potosi Gneiss was assumed to have the density of 2.78 gm/cm as found by L.A. Richardson. The geometry was derived from N.B.H.C. geological section 62. The model for the orebody zone was based entirely on density measurements as previously discussed in the interpretation of density.

There is a broad positive residual anomaly of 0.15 milligals above the orebody. This suggests that the predicted anomaly is too high. However, rock of density lower than 2.83 gm/cm^3 may surround the lode zone. Perhaps the depth of weathering is greater. It is not possible to say that the density of the lode zone was overestimated.

The presence of a residual at 900 feet suggests that a high density body two hundred feet wide could be centred at 900 feet. As discussed, it has not been possible to resolve the cause of this anomaly due to the lack of density data for the west amphibolite and due to possible errors in the relative position of the gravity profile.

3.3.1 Section 92

The expected gravitational response to the Broken Hill Lode Sequence in Section 92 is presented in Fig. 8. It must be noted that three points circled in the observed profile 3 (symbol ≠) are interpolated over a gap in the data. The interpolation was essentially linear but with a slight convexity based on the shape of profile 3A. East of Formation 1 the density model has the same density contrast as in Section 62. East of Formation 3 a high density unit has been assumed. It could be an amphibolite stringer or a high density zone

containing banded iron as indications of these possibilities can be found in Section 30 and in geological mapping. These is a mismatch between the position of the expected anomaly of Formation 3, the east amphibolite and the observed anomaly. This leaves the residual anomaly seen at -1600 feet. As the profile does not lie exactly over the section it is likely that the east amphibolite lies under the observed maximum. However, the anomaly in profile 3 is unusually bifurcated at this position. In adjacent profile 3A this is not so and the expected response of the lodes is less in Section 92 and is only 0.3 milligals. Of significant difference to the model for Section 62 is the geometry proposed for the Hanging Wall Gneiss. It is assumed to extend to a depth of at least 10,000 feet. The residual difference profile shows a small anomaly at 3800 feet and a larger one at 5700 feet. The former would require only a small low density zone within the Hanging Wall Gneiss. The later anomaly is outside the Hanging Wall Gneiss and would require another low density zone to be in this position or if the Globe Vauxhall Shear zone has complicated the boundary of the Hanging Wall Gneiss a different geometry of the Hanging Wall Gneiss may be drawn locally to account for the anomaly. This model illustrates how difficult it is to predict the geometry of bodies at depth. The residual anomalies found here in this model are comparable with residual anomalies from locations such as at feducial -3200 feet in Fig. 8. Here also no subsurface density data was available. Clearly unless the density data is available on the western margin of the Hanging Wall Gneiss (at 5000 feet in Fig. 8) the interpretation of the subsurface geometry of major structures would be tentative using the gravity method. This is an example of how measurement of bulk density could have reduced ambiguity in the interpretation of gravity data.

The expected response of Section 92 matches profile 2A better than profile 3. The expected response of the east amphibolite matches

the profile almost exactly. The residual anomaly at -1400 feet suggests a low density body in this position. The Potosi Gneiss lies underneath and it is probable that a model including the Potosi Gneiss would have no residual anomaly in this position. It is of importance that profile 3 does not show a gravity low in this position. The author can suggest that the narrow synform which contains the Banded Iron Formation in N.B.H.C. geological section 92 is not beneath profile 2A but does lie beneath profile 3. Consistent with this possibility is the absence of this synformal banded iron structure in Section 62 where there is also a negative anomaly above the potosi gneiss. Furthermore profile 2A lies between Section 92 and Section 62.

Even without the Potosi Gneiss in the model for Section 92 profile 2A shows a residual anomaly at 5000 feet consistent with the orebody having 0.2 milligals greater anomaly than the 0.3 milligals suggested by the model used for Section 92. It is obvious that inclusion of the Potosi Gneiss would leave an even larger residual anomaly over the orebody. The greater anomaly over the orebody in profile 2A compared with profile 3 would be consistent with the decreas in density of the lode zone towards profile 3. The difference between profile 2A and 3 shows that the presence of a low gravity anomaly over the potosi gneiss suggests a greater anomaly over the lode zone. This emphasizes the need for good geological knowledge on either side of the lode zone or preferably the availability of density information on either side of the lode zone. The author considers the difference between profile 2A and profile 3 to be an indication of the degree of geological or density control necessary for the resolution of anomalies of the size of 0.3 milligals. Here in 500 feet along strike a 400 feet deep synformal structure containing banded iron formation is believed to account for an anomaly of 0.25 milligals. This can be shown consistent with the expected response of a horizontal cylinder of radius 200 feet

near the surface and with a density contrast of 0.1 gm. This assumes the density of 2.93 gm. of the Potosi-Banded Iron high density zone next to the Potosi gneiss with density 2.78 gm/cm^3.

The residual anomaly between profile 2A and the expected response of Section 92 is similar to that for profile 3 which was relevant to the Hanging Wall Gneiss. The anomaly predicted for the Hanging Wall Gneiss on the eastern margin was too great. This could be consistent with the increase in density observed in DD 130 at feducial 950 feet in Fig. 1.

3.3.2 Section 262

Section 262 is a section of the Broken Hill Lode Sequence in which no orebodies have been discovered. Therefore this section was studied to observe whether the bulk density of the formations in the Broken Hill Lode Sequence in Section 262 were similar to that where the orebody exists. If so then the discovery of anomalous high bulk density could be more reliably correlated with the presence of orebodies. It was found that the bulk density of formations were grossly similar along this strike extension of over two miles. Geologically the sequence in Section 262 is similar to that in Section 62. However, the width and dip of formations are both different. In Section 262 the width of the sequence between the east amphibolite and the Hanging Wall Gneiss is approximately 5800 feet as measured from N.B.H.C. geological cross section (Folio Fig. 4). In comparison the width between these formations in Section 62 is measured at only 2800 feet. Because of this variation in width the author has only considered density determinations on core from within Section 262 for the density model of Section 262. Since the density information for the east amphibolite is only available for Section 84 this was an exception. However, this data was modified. The thickness of the east amphibolite as measured in N.B.H.C. geological Section 262 was noted to be about 20% less than

that measured in N.B.H.C. geological section 62. Also it was found that if the density of the east amphibolite was assumed to have a 26% lower density contrast a smaller residual anomaly was apparent.

In Section 262 the dip of the formations is shallower than in Section 62. In Section 262 the dip of the upper amphibolite is approximately 46^{o} whereas the dip of the upper amphibolite is approximately 10^{c} down to about 2000 feet below the surface as measured on the N.B.H.C. geological sections 62 and 92.

The differences in formation thicknesses and the dip of the Broken Hill Lode Sequence between Section 262 and 62 do not permit a simple subtraction of the geophysical profiles in order to compare any differences in the gravity attraction between profiles 1A and profile 13. However, it may be said that a regional gradient of 1.4 milligals per thousand feet exists over section 262. The author has assumed that such a gradient could not be caused by any body less than 5000 feet below the ground and within the Broken Hill Lode Sequence. Thus a straight line regional was removed to facilitate interpretation of the residual anomaly. The observed gravity less regional is plotted in Fig. 17. It is significant that no gravity low is observed east of the east amphibolite in Section 262. In the interpretation of regional gravity data, geological inference is made from this fact. In Section 262 the density east of Formation 1 was assumed the same as the average bulk density of sillimanite gneiss in the lode sequence. As no density information is available no theoretical anomaly can be derived without assumption of the density. However, it can be said that the interpretation of the residual anomaly near the lode zone is not greatly affected by the necessity of this assumption because the lode zone is relatively distant, being 4000 feet to the west. As in Section 62 there is a positive anomaly above the east amphibolite. Just as there is also a gravity low over Formations 4 and 5, sillimanite gneiss and Potosi

gneiss, and there is also a small high above the lode horizon between Formations 5 and 10. Then there is a very small high at the Mine Reference Line zero feet caused by the upper amphibolite which is denser in Section 262 than it is in Section 62. Then finally there is the major gravity low associated with the Hanging Wall Gneiss. Thus there is a qualitative similarity between the shapes of the gravity profiles for the two sections, one containing the orebody, the other not. The author again suggests that the presence of the Broken Hill orebody cannot be inferred merely by inspecting the gravity profiles. The expected response to the Broken Hill Lode Sequence in Section 262 was then examined in order to see how closely one can predict the observed gravitational profile.

The subsurface density model for Section 262 is presented in Fig. 10. On the east end is a high density unit of suspected density contrast of +0.10 gm/cm^3 or equivalently of suspected density of 2.93 gm/cm^3 which is that of the upper amphibolite. This latter comparison is not meant to imply that this high density unit could be the upper amphibolite, but is meant to show that a few twenty foot stringers of amphibolite could cause such an anomaly.

Although no density information is available for the footwall gneiss a model was proposed and the density contrast was varied to minimize the residual anomaly. As in other sections it was found that a very small or zero density contrast produced the smallest residual. The density model for the east amphibolite was as just previously described. It has a theoretical anomaly of 1.1 milligals and a half-width of 1000 feet. The density of Formation 4 is based on density data from DD 1600 and DD 2200. As only the east end of Formation 4 had a low density in both diamond drill holes, it was modelled separately to the more westerly half of Formation 4 in Section 262. The eastern 700 feet of Formation 4 had an average density of 2.805 gm/cm^3

(2.81 gm/cm^3 in DD 1600 and 2.80 gm/cm^3 in DD 2200). It was found better to use 2.80 gm/cm^3 in the model. The rest of Formation 4 was modelled in the upper part, that is the nearer to surface part, by the data from DD 2200 which gave an average density of 2.81 gm/cm^3 over 800 feet. However, it was found better to assume an even lower density of 2.80 gm/cm^3 for this model. The effect of this is not major. However, it is obvious from Fig. 10 that a residual high exists at -2000 feet. This implies a density even lower than the assumed 2.80 gm/cm^3 or perhaps that the depth of weathering is deeper in this part of the profile.

The geometry of this low density unit has been drawn similar to that of the Potosi gneiss in Sections 30, 62 and 92. This shape was defined by the surface, the slope of the drill hole and the local dip of the formations. The combined anomaly for the two sides of Formation 4 in Section 262 has a maximum of 0.4 milligals and a half-width of two-thousand feet.

The next part of the model was the lode zone Formations 6 to 9 and including some high density Potosi gneiss Formation 5. The average density was 2.89 gm/cm^3. The elements used to construct the geometry of the model were the folded dip of the Potosi gneiss, the width of the unit, the surface and a base of 5000 feet. The maximum anomaly attributable to this body was 0.6 milligals with a half-width of 1800 feet. This anomaly is similar to that predicted for the orebody when assuming a model based on the geometry of the lodes and the average density within those lodes. Thus if both models are correct then the gravity method cannot differentiate where the lode zone has an orebody. This problem is discussed again in the re-interpretation of the lode sequence.

The next formation to be represented in the density model for Section 262 was the upper amphibolite. A reasonably small residual

anomaly over this formation was obtained. However, a better residual could be obtained by making the model for the upper amphibolite 25% broader and proportionately less dense. The effect of this was to provide a broader anomaly comparable with that seen in the observed gravity profile. Even so the residual anomaly suggested that the density contrast be higher or that the body was thicker than that modelled. Examination of the residual gravity profile in Fig. 10, S. 262 Broken Hill Density Model shows that the residual is almost a one point anomaly at -450 feet. This residual is too small to postulate further modification to the density model for the upper amphibolite in Section 262.

The last formation to be modelled in Section 262 was the Hanging Wall Gneiss. The N.B.H.C. geological section gives only the eastern boundary of the surface outcrop of the Hanging Wall Gneiss and the dip of this boundary (Folio Fig. 4). The thickness of the Hanging Wall Gneiss was initially modelled as the same as that in Section 92. Also the dip was assumed to be constant as far as 5000 feet below the surface. Early residual anomalies showed that the thickness had to be less than that in Section 92 if the thickness was assumed to be constant as far down as 5000 feet below the surface. This decrease in apparent wi th compares favourably with the suggested width of the Hanging Wall Gneiss as indicated on Zinc Corporation 1" to 2000 feet Geological Plan, Broken Hill District Sheet no. 1. Once again no density information is available west of the Hanging Wall Gneiss, so here an average density of sillimanite gneiss has been assumed. Therefore little can be said about the likelihood of the structure being correct other than it provides an acceptable gravity model. Fig. 10 shows only a very small residual anomaly above the Hanging Wall Gneiss. It should be mentioned that the bulk density of 2.74 gm/cm^3 has been assumed for this density model as this is the average measured by R. Wood and is for samples between Section 262 and Section 92, the section in which

L.A. Richardson measured an average bulk density of only 2.72 gm/cm^3. It is interesting to observe that if the eastern margin of the Hanging Wall Gneiss in Section 92 became progressively more like Formation 12 in composition towards Section 262 then this would explain for the increase in thickness of Formation 12 and the apparent decrease in thickness of Formation 13, the Hanging Wall Gneiss.

SECTION 4 DETECTION OF THE BROKEN HILL OREBODY

4.1 Hypothesis

If one hypothesises that the Broken Hill orebody has not been discovered one can determine whether the gravity data would have indicated the presence of an orebody. Several other assumptions are necessary. Section 62 will be considered in this hypothesis. Figure 11 illustrates the geological model which the author believes could have been presented by geologists from surface outcrop and subsurface drilling without discovering an orebody in Section 62. The orebodies are known to be over 800 feet below the surface in Section 62.

The model is comprised of four separate geological bodies. In the east is supposed a low density formation (probably a large mass of sillimanite gneiss and quartzite) with a density of 2.80 gm/cm^3. As mentioned previously in Section 2.4 minimization of the residual anomaly suggests that 2.80 gm/cm^3 is a close approximation to the average bulk density of this body. Therefore no subsurface drilling or surface costeaning would have been required to arrive at the model for this low density formation.

The second formation to be included in this model would have been the east (lower) amphibolite. The O. Weiss gravity profiles show a positive anomaly over this amphibolite for over two miles - this can be best observed in Broken Hill on Zinc Corporation gravity profiles at a scale of 400 feet to the inch with geological plans at the same scale. Thus it would have been obvious that a large formation of amphibolite was producing this positive gravity anomaly (centred at feducial -1000 feet in Fig. 11). A shallow diamond drill hole less than one thousand feet deep would have allowed accurate near surface density determinations to be made. This would have allowed the density model proposed for the east (lower) amphibolite in Fig. 11 to have been proposed without discovery of the orebody.

Also had this diamond drill hole been shallow it would have also intersected the Potosi Gneiss. Therefore the geological outcrop and shallow near-surface drilling would have suggested the model for the Potosi Gneiss proposed in Fig. 11.

The author then assumes that a diamond drill hole such as DD 130 Section 92 (Folio Fig. 3) was drilled in the vicinity of Section 62. It is important to observe that DD 130 did not intersect the orebodies. Also DD 130 was the diamond drill hole along which density determinations were made by L.A. Richardson (see Appendix 1). This information was used by the author to construct the models for the Broken Hill Lode Sequence in Section 62 (see Figs. 5 and 6). Yet the orebody was not intersected by this diamond drill hole, nor by those in Section 262 which were also useful for the construction of these models.

The average density of the sillimanite gneiss surrounding the Potosi Gneiss was determined from diamond drill holes which did not intersect the orebodies. Also the model for the Hanging Wall Gneiss was determined from diamond drill hole 130 and surface outcrop.

4.2 Model possible prior to Orebody discovery

The author believes that if two diamond drill holes - one penetrating the Potosi Gneiss and the east (lower) amphibolite, the other in a position below where the orebodies are now known - similar to that of DD 130 were drilled near Section 62, the model in Fig. 11 probably would have been constructed. It is important to point out that the geometry of the lower part of the Hanging Wall Gneiss may be substantially deeper without significantly affecting the theoretical gravity profile.

The interpreted residual in Fig. 11 is in fact exactly the expected response of the model for the Broken Hill Lode Horizon in

Section 62 based on density determinations from diamond drill holes through the orebodies. But at first the presence of a high density mass would have been suggested. Now the problem remains to reduce the ambiguity and to suggest the likelihood that an orebody exists under the maximum residual anomaly.

4.3 Ambiguity

If an interpreter were faced with this problem the density data for the Broken Hill Lode Horizon would have been examined in detail. It is relevant that DD 130, DD 1600 and DD 2200 show a high density zone for the Broken Hill Lode Horizon - even when no orebodies are known. Therefore the model proposed for the Broken Hill Lode Horizon (used in Section 662) where no orebody exists would be added to the model in Fig. 11. Thus Fig. 12 represents an attempt to resolve the cause of the interpreted residual anomaly from Fig. 11.

As can be seen in Fig. 12 there is only a small broad anomaly observed in the difference curve. The presence of a sharp residual anomaly at feducial 1000 feet suggests that an additional high density zone is present. The fact that the upper (west) amphibolite is near this position suggests that it may have caused the residual anomaly.

DD 305 penetrates the upper (west) amphibolite and the rock under this residual anomaly. Unfortunately no density determinations were made. However, if the diamond drill hole had been made to resolve the cause of the residual anomaly under discussion then density determinations would have been made and the cause of this relatively sharp residual anomaly would have been resolved. The author mentions that mineralization is noted in DD 305 beyond 1150 feet down hole. This also may have produced higher densities and accounted for this relatively sharp residual anomaly. Thus the cause of this sharp anomaly may have only been attributed to an amphibolite or in the event of a shallow diamond drill hole it may have been attributed to some

uneconomical mineralization.

4.4 Conclusion to Microgravity

The author believes that detection of the Broken Hill orebody by a residual gravity anomaly would have been unlikely. It is important to realize that the lode horizon model in Fig. 12 extends to the surface. If near surface drilling or even deep costeaning had discovered that no high density rock existed near the surface the implication would have been that rock of a higher density than is normal for the lode horizon would exist at depth. In point of fact Potosi Gneiss is mapped in this position (in Section 62, Folio Fig. 2) but Potosi Gneiss sometimes has a low density and sometimes has a iigh density (Section 2.4).

Unfortunately no gravity profiles were made over Zinc Corporation Section 30 where the orebody is shallower than one thousand feet below the surface (Fig. 1). The orebody would be more easily detected in Section 30 where the orebodies are shallower.

The author has shown that the Broken Hill orebody where 1000 feet below the surface, cannot be detected with certainty by the residual gravity method without extensive local subsurface density data. Critical to the interpretation is near surface density information. In the Broken Hill area core densities and residual gravity profiles are expected to indicate the possibility of Broken Hill type orebodies when only a few hundred feet below the surface.

SECTION 5 REGIONAL GRAVITY

5.1 Introduction

The regional gravity section is generally concerned with bodies of smallest dimension between four hudnred feet and two miles. The type of gravity data examined had a station spacing of around four hundred feet. All O. Weiss gravity data was considered since the station spacing for this data was generally 200 feet or less. O. Weiss gravity data, however, cannot be published with the exception of a few profiles previously published (R. Wood, 1972).

Regional gravity profiles were first examined. The author had collected and reduced four hundred and ninety nine gravity stations. For 81 of these stations G. Jenke collected the gravity differences. The author reduced these values from dial division differences to Bruguer gravity values. All stations with relevant data are presented in Appendix 7. Of the 499 gravity sections collected by the author 293 stations were relevant to the following Regional Gravity section. This section mainly concerns the Broken Hill - Little Broken Hill areas and intervening areas between the Thackaringa-Pinnacles Shear and the Wilcannia Highway (see Fig. 18).

Each profile was considered individually. The gravity values were qualitatively correlated with outcrop or subsurface rock type inferred either by colluvium or by along strike outcrop or diamond drill information. Two examples of quantitative interpretations performed at this scale were made and can be seen in Figs. 16 and 17.

The author shows that the gravity values in the Broken Hill - Little Broken Hill area can be correlated with the metamorphic rocks in that area. Many of the major anomalies can be attributed to large masses of rock of known geological type. The best examples are the gravity low over the Hanging Wall Gneiss, the gravity low over the granite gneiss between the Rupee Mine area and the Flying Doctor Base

and the gravity high over the Broken Hill line of lode. Also sparse data indicates that a gravity low can be correlated with the Alma Gneiss.

Of great interest is a very large positive anomaly east of the Broken Hill Airport, the East Airport Gravity High seen in Figs. 16 and 17, and also in Fig. 18. The lineal extent of this anomaly is at least six miles whereupon it is truncated at the south-west extremity. To the north east it continues for six more miles but with diminished magnitude. An amphibolite rich sequence is believed to account for at least part of this anomaly. The Rupee lode sequence is also believed to be part of the rock sequences which have caused this gravity high. The author shows that the trend of gravity anomalies and gradients within the East Airport gravity high suggest that the rock types causing the anomaly are conformable with adjacent rock types.

5.2 Flying Doctor Gravity Traverse

5.2.1 Introduction

The Flying Doctor Gravity Traverse which is illustrated in Fig. 2 was made by the author. Roger Cammel, a surveying student at The Levels Branch of the South Australian Institute of Technology provided expertise and field assistance in the positional and elevation control for the traverse. Particulars relevant to this work and the collection and reduction of the gravity data are in Appendix 7. Bill Laing, a post-graduate student of structural geology at the University of Adelaide provided significant geological mapping and interpretation. A previous study of gravity data from the vicinity of the Flying Doctor Base traverse was made by G. Jenke for his Honours thesis in 1972 (G. Jenke, 1972). This study was observed by the author who had begun a Masters degree in the same Geophysics Department of the University of Adelaide.

It was a purpose of the Flying Doctor Gravity traverse to improve the gravity coverage over the Broken Hill regional gravity high which is approximately ten miles wide. The traverse did not fully transect this regional anomaly which can be conveniently defined by the 15 milligal Bouguer anomaly contour, when the Boug er density of 2.70 gm/cm^3 has been used. Another aim was to delineate rock formation groups of the order of one thousand feet wide and which have density contrasts.

Examples of such rock formation groups are the Hanging Wall Gneiss, the Broken Hill Lode Sequence, the Alma Gneiss and the granite gneiss to the east of the lode sequence in the Northern Leases of North Broken Hill Prop. Ltd. The type of gravitational anomaly produced by such formation groups are over two milligals and have half-widths of over one thousand feet. It was expected that amphibolite formations would produce well-defined anomalies at the station spacing of four hundred feet only if about one hundred feet wide. Generally it is difficult to correlate the gravity anomaly due to an individual amphiboite over along strike distances much greater than a mile. A noteable exception is the lower (east) amphibolite of the Broken Hill Lode Sequence. For example, in the Southern Extensions area a positive anomaly can be followed for four miles in the O. Weiss gravity profiles. This anomaly can be correlated with mapped outcrop of this amphibolite and has been shown to be the expected observed anomaly by calculations made by the author (Residual Gravity Section 3.3). Thus either because of structural and stratigraphic variations along strike or because of random anomalies due to weathering, anomalies due to individual amphibolite formations are difficult to use for regional geological interpretation. Coupled with this fact is the disadvantage of having to make observations at intervals of two hundred feet and preferably one hundred feet or less in order to define the gravity anomalies of individual amphibolite formations.

Some of the geological control was derived from the outcrop along the traverse. William Laing a postgraduate student of structural geology examined the outcrop and made field notes describing the outcrop observed in every fourth subdivision of the station spacing, which was every one hundred feet. The author accompanied this geological reconnaissance. Bill Laing then compiled a geological strip map and interpreted the broad lithological divisions which are seen in Fig. 13 under the heading of generalized geology. The author then compared these divisions with the Zinc Corporation Rupee Area geological surface plan with gravity and magnetic profiles (The Zinc Corporation has this as Sheet 25 at a scale of 1" to 400 feet). This map was especially useful where the Flying Doctor Gravity Traverse crossed colluvium between stations FDB 23 and FDB 33. Since the local strike was normal to the traverse, outcrop mapped along strike was interpreted as being under the colluvium. Unfortunately the Zinc Corporation 1" represents 400 foot scale geological maps only covered areas up to FDB 40. For the remainder of the traverse the Geological Map of the Broken Hill District (1968) was used in conjunction with the geological reconnaissance traverse by Bill Laing.

5.2.2 Details of correlation of anomalies with geology

In Fig. 13 stations FDB 01 to FDB 10 are over granite gneiss and have low Bouguer gravity values. This gravity low has been observed in both O. Weiss gravity profiles nearby and at the end of the Flying Doctor Microgravity profile of North Broken Hill Prop. Ltd. In fact the Flying Doctor Gravity Profile made by the author starts from the end of the Flying Doctor Microgravity profile. This gravity low has been discussed by G. Jenke in his Honours thesis (G. Jenke). He constructed a two dimensional model incorporating the granite gneiss and sillimanite gneisses on either side. His conclusion was that a large granite mass about 2000 feet deep was causing this gravity low.

The author agrees that a large body of granite gneiss has caused this gravity low. However, the author hesitates to accept the model as supporting a synformal geometry for the granite gneiss. This hypothesis is reviewed in the regional geology section (Section 5.8).

5.2.3 Rupee Lode Sequence

A gravity high exists between stations FDB 10 and FDB 36 (see Fig. 13 feducials 3600 to 18,800). This high and the three smaller peaks superimposed on this high were correlated with peaks observed in O. Weiss gravity profiles 96, 97 and others. These geophysical profiles suggest that the rock types between stations FDB 22 to FDB 38 continue towards the north. However, the positive gravity anomaly at FDB 15 to FDB 18 does not continue further north than O. Weiss gravity profile 99, two thousand four hundred fett northeast of the Flying Doctor Base regional gravity traverse.

William Laing mapped amphibolite scree, pegmatite scree, granite scree and sillimanite gneiss and amphibolite outcrop between FDB 16 and FDB 18. This agrees with the geological mapping observed by the author on the Zinc Corporation Ltd. Rupee Area Geological Surface Plan with Gravity and Magnetic Profiles (Sheet 25), scale 1 inch represents 400 feet. This area is in the vicinity of O. Weiss stations 3-853 to 3-860, line 96. A reduced copy of this map was presented as the lower half of Fig. 2A in G. Jenke's Honours thesis (G. Jenke, 1972). The area in question is four thousand feet west of the geophysical base line. In G. Jenke's Fig. 2A the area is at the lowest extremity (towards the south south west). Zinc Corporation mapping showed that the sillimanite amphibolite rich formation under stations FDB 15 to FDB 18 does not appear to continue north of O. Weiss profile 99. Therefore the termination of this gravity peak correlates with the geological inference that this formation does not continue towards the north.

Between FDB 18 and FDB 24 William Laing mapped an area of alluvium and some granite gneiss scree. Then amphibolite with lesser granite gneiss and pegmatite was mapped near station FDB 21 and FDB 22. Finally amphibolite was mapped in outcrop near FDB 24. This outcrop is consistent with Zinc Corporation Geological mapping just north of the Flying Doctor traverse. It is important that this gravity anomaly associated with this formation continues north as far as the Rupee Mine, and also that the Rupee Lode Formation if continued along the local strike would be expected under colluvium mapped by William Laing between FDB 25 to FDB 32.

The author believes that it is most likely that the Rupee Lode Sequence forms at least part of the high density sequence, known to contain sillimanite gneiss and amphibolite, which produces the gravity high between stations FDB 10 to FDB 36. In section 5.8 this gravity high is correlated with gravity highs to the southwest and over a distance of approximately twelve miles.

5.2.4 Darling Range Topographic Corrections

Since the Darling Ranges were rugged and showed a relief in excess of two hundred feet (see Fig. 13) along the Flying Doctor gravity traverse, the author attempted those terrain corrections not accounted for by the Bouguer correction. Elevation contour maps were not available for all of the traverse. However, the ranges were essentially two dimensional and accurate elevation control by staff and level had been secured by R. Cammel and the author, both of the University of Adelaide. Therefore the author compounded a two dimensional model based on elevation data collected along the Flying Doctor Traverse. The author modified program THEORY written by R. Gransbury (R. Gransbury, 1973). This routine allowed for bodies partly above and partly below the plane of observation.

The results indicated that the difference between the two dimensional topographic model and the Bouguer slab model (most commonly used) was less than 0.3 milligals. Generally the difference was less than 0.1 milligals and in particular for adjacent stations the difference of the difference between the two corrections was never more than 0.1 milligals. Therefore since the gravity interpretation always considered gravity anomalies greater than 0.5 milligals, no more detailed terrain corrections were deemed necessary. The author believed that the two dimensional model provided differences of more than half than any refined topographic model when compared with the Bouguer (slab) model for topographic corrections. Hence the author concluded that the gravity values were subject to errors in topographic correction of less than 0.5 milligals. Generally this error was less than 0.2 milligals even in the Darling Ranges.

5.2.5 Main Darling Ranges

The Darling Ranges extend from stations FDB 36 to FDB 60 along the Flying Doctor regional gravity traverse. This part of the traverse is approximately one milligal lower than the adjacent parts. Between stations FDB 36 and FDB 56 the Bouguer values were around 16 milligals (see Fig. 13). Therefore they were still much higher than areas covered by large masses of granite gneiss, such as at the start of this traverse FDB 01 to FDB 10.

Amphibolites and granite gneiss were respectively rare and absent. The first part covered outcrop of mostly retrogressed garnet staurolite schists, with minor pegmatite. The second part of the traverse, that between FDB 48 and FDB 56, covered quartz mica feldspar schists. Also aplite was rare or absent - as can be generally said for areas in the Broken Hill District where the gravitational attraction is greater than 15 milligals. The author believes that the retrogressed quartzofelspathic schists and the quartz mica feldspar

schists of the main Darling Range along the Flying Doctor Traverse have produced the one milligal lower anomaly than the adjacent rock sequences. As mentioned to the west the sequence is amphibolite rich and is largely composed of sillimanite gneisses. Therefore the average bulk density of the western rock sequences would be greater than those in the east.

5.2.6 East Darling Ranges

On the east side of the retrogressed schists and mica schists of the main Darling Ranges a sillimanite gneiss sequence which contains garnetiferous sillimanite gneiss and amphibolites was mapped by William Laing. Outcrops of amphibolite more than 300 feet wide were observed with corresponding local gravity maxima at stations FDB 65 and also FDB 70 to FDB 73. Also outcrop of amphibolite was observed between stations FDB 81 and FDB 82, whilst mostly alluvium was noted between FDB 73 and FDB 81. Therefore the author concluded that a high average density sequence of sillimanite, garnet gneisses and amphibolites has produced the regional gravity high observed in Fig. 13 between stations FDB 56 and FDB 83. A very sharp gravity low was observed between stations FDB 83 and FDB 92. No outcrop or scree of amphibolite was found. Sporadic outcrop of quartz mica feldspar schists, granitic scree and pegmatite were found. However, a most important outcrop of fine grained granite or aplite was found in the centre of the gravity low. As only rare outcrop was found along the traverse no indications of structural control were found. The strike of layering was between 250° and 230° N/N.

However, the density of aplite (2.67 gm/cm^3 L.A. Richardson) is known to be less than that of quartz mica feldspar schists and Potosi Gneiss (2.78). It is expected that at least part of this gravity low is due to the presence of the aplite.

A very sharp positive anomaly was found next over amphibolite

and Potosi Gneiss at stations FDB 94 and FDB 95. The maximum anomaly at FDB 95 although consistently the peak of the anomaly is circumspect because it is very high. However, even without the extreme maximum this anomaly when combined withthe low over the aplite constitutes one of the sharpest anomalies over about one thousand feet that the author has observed in the Broken Hill area. The author postulates that the aplite could be repeated structurally and that if the traverse had continued aplite would have been discovered in outcrop.

5.3 Menindee Highway Gravity Traverse

The author took advantage of the N.S.W. Dept. of Main Roads surveying on a new route for the Menindee Highway. Temporary bench marks were occupied. All elevation control for this traverse was kindly furnished by the Broken Hill Branch office of that Department. Details of positional control and the collection and reduction of gravity data are furnished in Appendix 7. The traverse crossed part of the O. Weiss gravity survey which the B.D.B. traverse also crossed further north. Thus in Fig. 14 the gravity high between stations MEN 10 and MEN 40 can be directly correlated with the gravity high between stations FDB 10 and FDB 40 in Fig. 13. Also assisting comparison between these two regional gravity profiles are two aeromagnetic anomalies and the direction of the local strike which all run almost at right angles to both regional gravity traverses in the vicinity of this gravity high. Geological control was furnished by William Laing who conducted a geological reconnaissance at intervals of a quarter of the station spacing.

As the first part of the Menindee Highway was not being surveyed only the few permanent bench marks could be occupied. The traverse started over the British Shear. A broad positive gravity anomaly is defined by stations MEN 01 to MEN 04. Outcrop noted near

these stations included Potosi Gneiss and amphibolite. O. Weiss gravity data and North Broken Hill Prop. Ltd. microgravity data for the area just to the north were compared with this gravity high. The high is observed over the Broken Hill Lode Sequence and is known to have sharp local maxima over amphibolites.

Then between stations MEN 05 and MEN 09 a gravity low was observed similar to the gravity low on the FDB gravity traverse. Granite gneiss outcrops on the eastern part of the gravity low, the rest is covered by colluvium and alluvium. This apparent correlation of the granite gneisses observed under the gravity lows in both FDB traverse and Menindee Highway traverse will be discussed in the regional gravity section. Between MEN 10 and MEN 29 a gravity high is observed. Near the maximum an amphibolite about two hundred feet wide, and five lesser amphibolites were observed. Thus part of the maximum anomaly is due to these amphibolites.

Whilst there is no outcrop or scree between MEN 29 and MEN 50 the continuity of the shape of the gravity anomaly as observed in O. Weiss data and the continuity of the aeromagnetic anomaly when extrapolated into the north suggest the strike continues southeast from the FDB traverse to the Menindee Highway to the position of the colluvium. Therefore the author suggests that a sillimanite gneiss sequence containing amphibolite stringers lies under stations MEN 29 to MEN 41. This sequence would be expected to contain the Rupee Lode Sequence. Between MEN 41 to MEN 50 the author expects a low density sequence probably rich in granite gneiss. This gneiss would be expected to be the Thorndale Gneiss by the association of the aeromagnetic anomaly and the low density of 2.75 gm/cm^3 reported by O. Weiss. The author conducted a ground magnetic traverse over the first half of the Menindee Highway gravity traverse in order to correlate the gravity data with aeromagnetic anomalies. A 1250 gamma

anomaly in the vertical component of the magnetic field was measured with its peak near station MEN 45. This anomaly was observed by the aeromagnetic survey conducted by Bur. of Min. Res. over the Broken Hill area. The trend of this anomaly labelled D1 has been marked on Fig. 18. The anomaly follows the line ofthe Darling Range scarp. The anomaly is seen to lie closely over the Thorndale Gneiss which also strikes parallel to the Darling Range. Traverse T29 made by G. Jenke over the western margin of the Thorndale Gneiss measured an anomaly similar to that measured by the author. The location of this ground magnetic anomaly also lies under the aeromagnetic anomaly D4 to the north of the Menindee Highway. Thus the magnetic data suggests that the Thorndale Gneiss lies under the colluvium around station MEN 45.

The low density of the Thorndale Gneiss suggests that a gravity low will be associated with this body. This is in fact observed where the O. Weiss gravity profiles (e.g. profiles 97, 103, 106) extend as far east as the Thorndale Gneiss since negative gradient are observed at the contact between sillimanite gneiss (density usually greater than 2.80 gm/cm^3) and the Thorndale Gneiss (2.75 gm/cm^3). Thus the gravity data suggests that the Thorndale Gneiss extends as far as the Menindee Highway.

The second part of the Menindee Highway regional gravity traverse does not correlate with the Flying Doctor Traverse. The second half of the Flying Doctor Base traverse showed a two milligal gravity high for over 8000 feet which was probably due to a sillimanite garnet gneiss rich in amphibolite and then showed a sharp gravity low associated with aplite and quartz-mica-feldspar schists, granitic scree, pegmatite and an absence of amphibolite. However, the second half of the Menindee Highway gravity traverse does not have anomalies greater than one milligal. No aplite was mapped along the traverse. However, two thousand feet south west of station MEN 110 an aplite zone striking

normal to the highway has been mapped on Zinc Corporation 1" to 2000 ft. Geological Plan, Broken Hill District Sheet 1. Mapping to the north of the Menindee Highway suggests that this aplite zone should be the same as that traversed 9000 feet to the north-west by the Flying Doctor Base gravity traverse.

At the end of the Menindee profile there is a suggestion of a positive anomaly at the last station. This would correlate with the anomaly at the end of the Flying Doctor Base traverse. By comparison the end of the Menindee traverse lode horizon and amphibolite also outcrops.

Between stations MEN 50 and MEN 110 no anomaly greater than one milligal was observed. The outcrop consisted mainly of retrograde schists with minor amphibolites and quartz mica feldspar schists. The author believes that the reason why only the Flying Doctor Base traverse and not the Menindee Highway traverse produces a two milligal and eight thousand feet wide gravity anomaly is that structural control near the Flying Doctor Base traverse has brought density contrasts near to the surface. This structure is seen to repeat an amphibolite which is at least three hundred feet wide. The amphibolite is repeated after two thousand feet of traverse. The closure of this amphibolite was not observed near the surface on the Menindee Highway.

5.4 Huonville Gravity Traverse

A regional gravity traverse with a spacing of 400 feet was made by the author across an aeormagnetic boundary believed to be associated with the Redan Gneiss (see Fig. 15). It had been intended to collect ground nagmetic data along this traverse in order to accurately locate any subsurface contact between rocks with different magnetic properties. This would have allowed close correlation between the inflexion of the gravity anomaly and the magnetic anomaly. However, boggy ground prohibited access to this traverse during the time planned

for the ground magnetic traverse and no subsequent time became available. Therefore it is only possible to say that the inflexion point in the gravity profile lies closely over the position of the aeromagnetic boundary.

A six milligal anomaly was observed. The characteristic shape of the response caused by a buried semi-infinite slab-like contact matches the Huonville gravity curve. The data appears to be asymptotic to the west and the gradient is less steep at the east end of the profile when compared to the central part. It would prove useful to extend the Huonville gravity profile particularly to the east as it appears that the anomaly may be greater than six milligals. It is interesting to postulate that if a density contrast of 0.1 gm/cm^3 is assumed the vertical width of the causitive body would be almost one mile. Unfortunately no density information is available in the area. A ground magnetic survey along this profile would help to reduce the number of geological possibilities and would assist in the construction of subsurface density models. Accurate determination of magnetic contacts or magnetic determination of depths to the causitive bodies could then be used as limits for the subsurface density model.

5.5 Airport Gravity

A survey was carried out by the author in and near the Broken Hill airfield. Inside the airfield elevation control was provided by permanent bench marks and the elevation of a few stations were related by barometer. Further details are in Appendix 7. The author is thankful to D.C.A. personnel for letting the author, who is a pilot, conduct this survey. The survey was conducted for two reasons. The first reason was to attempt to fill in knowledge of the gravity field between areas covered by the O. Weiss survey. The second reason was to fill in data for a specific profile, namely the O. Weiss profile 1A. The survey was important because it extended the gravity low associated with the

Alma Gneiss. It has led to the postulation that a gravity low continues north-east to a point on the Menindee Highway (see Fig. 18). This will be discussed in the regional gravity section (Section 5.8).

The author named the gravity high to the east of the Broken Hill airfield the "East Airport Gravity High". E. Cottrell first reported the existence of a five milligal high in this vicinity (E. Cottrell, 1960). The author has since defined a seven milligal excursion over the western extent of this anomaly (see Fig. 16). The eastern extent has not as yet been defined.

5.6 Broken Hill Regional Gravity Profile 1A

The author contoured gravity data observed in the Broken Hill airfield and nearby, then used these contours to define the gravity field over the gap in the O. Weiss gravity data in profile 1A. This revealed a gravity low over an area in which Alma Gneiss on augen granite gneiss is mapped in outcrop by Zinc Corporation ans was seen in outcrop by the author. This has been called the Alma Gneiss Gravity Low 1 in Fig. 16. It must be pointed out that no density measurements are available and also the boundaries of the Alma Gneiss are masked by colluvium. Therefore the gravity low is only inferred as being caused by this granite gneiss.

It is important to observe on profile 1A Fig. 16 that in the east there is a seven-milligal gravity high which the author has called the East Airport Gravity High 1, since it lies just to the east of the Broken Hill Airport. This is the sharpest anomaly over five milligals known in the Broken Hill district. Gradients of over seven milligals in six thousand feet have been measured both by the author and by numerous O. Weiss gravity profiles.

It is significant that sporadic outcrop over the area covered by the East Airport Gravity High and sporadic outcrop in the airfield indicate that this is not likely to be due to a greater thickness of

colluvium over the Broken Hill Airfield. The type of outcrop over the area covered by the East Airport Gravity High is also significant. Much of the outcrop is amphibolite which has a high bulk density. At the time the author proposed a subsurface model to try to account for the East Airport Gravity High no geological sections or maps were available, which were suitable for accurately defining the location and width of amphibolite outcrop across profile 1A. Furthermore, no density information was available for rocks from this area. Therefore the first approach the author used to account for this gravity high was to draw a subsurface model which included an amphibolite rich formation of arbitrary structural attitudes, a limiting maximum effective thickness of eight hundred feet of bulk density 3.3 gm/cm^3. This density of 3.30 gm/cm^3 is the highest density for amphibolites common to the Broken Hill Lode Sequence. The maximum thickness of eight hundred feet for the amphibolite is partly based on estimates given to the author during a discussion with Rowley Brunker, Regional Geologist for the Zinc Corporation (pers. comm.). The author considers this maximum as the maximum possible effective thickness of amphibolite of density 3.3 gm/cm^3 from the Broken Hill Lode Sequence. This includes consideration of the Round Hill amphibolite which is associated with an anomaly of three milligals. 2D Talwani modelling revealed that such an amphibolite rich formation could produce almost all of the East Airport Gravity High if it was assumed that a low density formation five thousand feet wide exists two thousand feet west of the amphibolite rich formation. However, the structural control required is rather limiting. The East Airport Gravity High is 5 miles long and at least six thousand feet wide. The amphibolite rich sequence would have to be near the surface throughout this area. Also it would have to have shallow dips throughout this area because models showed that even a deepening of two thousand feet in the central portion would produce a residual anomaly of over

0.7 milligals. At the boundaries of the East Airport Gravity High this high density formation would have to have near vertical dips. These severe structural demands, required by a model which supposed that a narrow amphibolite rich formation caused the East Airport gravity anomaly, forced the author to consider models which incorporated a high density formation of greater thickness. Such a model would not require shallow dips in the centre of the structure. A model which produced a good match with the observed profile is illustrated in Fig. 16. The model included a high density lode horizon-type formation. On the margins at feducials -21,000 feet and -18,000 feet an amphibolite rich formation has been assumed. The effective anomalous mass represented by this amphibolite rich formation is greater than the anomalous mass of the lower (east) amphibolite of the Broken Hill Lode Sequence. Also the anomalous mass of the model in the region, between feducials -20,000 and -15,000 in Fig. 16, which is the central area of the East Airport Gravity High is greater than the anomalous mass of the Broken Hill Lode Horizon. This region could be a higher density region due to many more amphibolite stringers of widths about 40 feet wide than are in the upper amphibolite of the Broken Hill Lode Sequence. However, as no drilling or costeaning has allowed density determinations in this area it is possible that a very large lode horizon exists with a density of 2.90 gm/cm^3. It is known that the A lode horizon has a density of 2.90 gm/cm^3 in the vicinity of the Broken Hill Lode (see Density Interpretation, Section 2.4). However, this thickness is not very much greater than 400 feet. If the Broken Hill Lode Sequence as it occurs in the west of regional profile 1A were refolded to provide twice the thickness below the surface under the East Airport Gravity High, the author considers that the resultant gravitational anomaly would not be great enough to equal the seven milligal anomaly observed under the East Airport Gravity High. Therefore the author considers

that a sequence denser than the Broken Hill Lode Sequence as observed to the west contributes towards the East Airport Gravity High. The spatial distribution of this sequence is discussed in the section on regional gravity.

The gravity low, between feducials -12,000 and -7,000 feet in Fig. 16, is centred over the Broken Hill airfield along profile 1A. The author refers to this anomaly as the Alma Gneiss Gravity Low since Alma Gneiss outcrops near the minimum and since the Alma Gneiss is expected to have a low bulk density. The bulk density predicted for the Alma granite gneiss is that which is about 2.75 gm/cm^3 the density of the Thorndale Gneiss or the Hanging Wall Granite Gneiss. Subsurface two dimensional Talwani models suggest that the width near the surface would be around five thousand feet along profile 1A if the density of the low density causitive body (thought to be Alma Gneiss) was 2.75 gm/cm^3. Since colluvium masks the boundaries of the Alma Gneiss near profile 1A it is possible that the Alma Gneiss could obtain this width. The author believes that the Alma Gneiss probably does attain this width since about half a mile north of this profile the Geological Map of the Broken Hill District (1968) shows that such a width of Alma Gneiss outcrops. From general experience gained from varying the depths of the model for the Hanging Wall Gneiss the author believes that the depth of the Alma Gneiss should be as great as its width, which is predicted to be 5000 feet at profile 1A.

Sillimanite quartz gneisses are mapped in outcrop west of the Alma Gneiss. These gneisses are thought to contain more quartz and less sillimanite and garnet than the Broker Hill Lode Sequence. This opinion is partly based upon the fact that gravity values decrease over this sillimanite gneiss. As a guide to the selection of a density for the model for this body the author chose the density of quartz rich sillimanite gneiss found in Section 262, Formation 4. This low density

sillimanite gneiss has a density of 2.80 gm/cm^3.

The Broken Hill Lode Sequence was represented by the same models as used in the residual gravity section (see Residual Gravity, Section 3.3). The Hanging Wall Gneiss was also modelled in the same was as in the residual gravity section. It is important to note that gravity high 3 to the west of profile 1A suggests repeated lode sequence. The likely surface lineal extent of the bodies represented by these two-dimensional models for the regional gravity profile 1A is discussed in the regional gravity section.

5.7 Regional Profile 13

The O. Weiss regional gravity profile 13 is presented in Fig. 17. Also presented is the theoretical gravity profile which was predicted from the model also illustrated in Fig. 17. The Broken Hill Lode Sequence was modelled as in Section 3.3.2 (see also Fig. 10).

The East Airport Gravity High can be seen centred around feducial -16,000 in Fig. 17. The absolute value of this anomaly is actually greater than that in profile 1A. This is not apparent from the values which may be read from the curves presented in Fig. 16 and Fig. 17. This is because the base value of these curves has been adjusted to suit plotting of these curves. As the O. Weiss gravity data is not reduced to the sea level direct comparison with gravity curves measured by the author is not possible. Therefore ease of comparison guided the selection of an arbitrary base for these two O. Weiss regional gravity profiles.

The relief of the East Airport anomaly can be seen to be only about four milligals. The author believes that this primarily due to disappearance of the so-called Alma Gneiss gravity low. Theoretical density models suggest that a maximum of two thousand feet of a low density rock (thought to be Alma Gneiss) could exist on profile 13 whilst over five thousand feet of this low density rock is predicted

in profile 1A. The theoretical models take account of the fact that the regional dip is shallower in N.B.H.C. Geological Section 262 (Folio Fig. 4) which underlies this gravity traverse.

In the east of the subsurface density model, a broad high density formation was assumed. This was the same thickness and density as that assumed in profile 1A (Fig. 5). Only one high density amphibolite was assumed since only one sharp anomaly is seen on profile 13. However, in retrospect it seems that the high density sequence seen between feducials -20,000 feet and -16,000 feet at the east end of the East Airport Gravity High of profile 13 should have had a greater anomalous mass. Evidence for this can be seen in the difference curve (the difference between the theoretical curve and the observed gravity profile).

The difference curve also shows a strong negative gradient towards the east indicating that the proposed model has either underestimated the density in the east and/or the model has over-estimated the density to the west, or that the regional gradient is due to rocks below the section which is twelve thousand feet deep. The gradient of this difference curve does not appear to vary greatly and this implies that such an anomaly could be caused by density contrasts below 12,000 feet. The difference between the theoretical gravity profile and the observed gravity profile 13 could be due to errors in the estimation of the density of the rocks shallower than twelve thousand feet. As indicated previously the anomalous mass below the East Airport Gravity High at the eastern side is greater than the assumed density contrast of +0.07 gm/cm^3. Also the Hanging Wall Gneiss at the west end of profile 13 could have been extended deeper and perhaps have been assumed to shallow to the west. As an alternative to this latter alteration it may be supposed that another low density formation such as a pegmatite rich formation exists next to the Hanging Wall Gneiss. These two alterations would have increased the theoretical

gravity values in the east and have reduced them in the west, thereby explaining at least part of the gradient evident in the difference curve of Fig. 17. If extensive sampling of fresh rock ere available for density determinations a more accurate theoretical model for the subsurface rocks down to 12,000 feet would be possible. Density information is available for only five thousand feet of the central portion of this thirty six thousand feet long section. Outside of the lode sequence little is known of the widths of various formations. Even shallow sampling to provide fresh rock would remove ambiguity in the near-surface density distribution.

Whilst the difference curve for profile 13 has larger residual anomalies than the difference curve for profile 1A some limitations can be inferred. The author predicts that no major density contrasts, greater than 0.5 gm/cm^3 and two thousand feet wide near the surface, exist along profile 13, the East Airport Gravity High and the Hanging Wall Gneiss, other than those density contrasts assumed in the model. For example a two thousand feet wide granite gneiss could not exist between the East Airport Gravity High and the Hanging Wall Gneiss, a distance of sixteen thousand feet. The two thousand feet wide body referred to does not include the two thousand feet wide body of low density thought to be the Alma Gneiss and already included in the model for the subsurface geology below regional gravity profile 13.

5.8 Regional Gravity

5.8.1 Introduction

All gravity data from the Broken Hill area were considered where related to any group of rock formations which were of the order of one mile wide. The area covered by this study is approximately twelve miles wide and twenty-four miles long, and is centred between the Broken Hill line of lode and the Little Broken Hill area (see

Fig. 18). The gravity data which is relevant to rock formations greater than a mile wide is discussed in the broadscale regional gravity section (Section 6).

5.8.2 Regional Gravity High

In 1972 a gravity map, which covered this area around Broken Hill, was produced by students under the supervision of Professor D.M. Boyd (G.P. Jenke). This Bouguer Gravity Map indicated that the Broken Hill and Little Broken Hill mines were located on the flanks of a regional gravity high. In order to further define the shape and extent of this gravity high and also to determine whether other such regional gravity highs occurred in the Broken Hill district, the author carried out additional gravity observations along straight line traverses, main roads and access tracks. The author produced a broad scale regional gravity map (Folio Fig. 6). This map suggested that the Broken Hill regional gravity high was not repeated in the Broken Hill District.

The additional gravity data collected by the author also suggested that his regional high was not monotonous, but had significan anomalies superimposed. The O. Weiss gravity data collected for the Zinc Corporation in 1949 was re-examined to determine the detail of the Broken Hill regional gravity high. After consideration of all available gravity data within the Broken Hill area an interpretation of the detail of the regional gravity high was made (see Fig. 18). The data considered includes that from the four regional gravity traverses previously discussed (see Sections 5.2-5.6).

Some of the anomalies superimposed on the Broken Hill regional gravity high extend for over two miles and have been labelled in the plan of interpreted gravity and magnetic features (Fig. 18). In the north-west a gravity high labelled H1 in Fig. 18 has a north-easterly trend. This anomaly can be seen in profile form in Fig. 16

at the western end of profile 1A, and is labelled gravity high 3. The next gravity high to the east (is labelled H2 in Fig. 18) lies over the Broken Hill Lode Sequence. This gravity high is similar to gravity anomaly 2. This similarity is consistent with a repetition of the Broken Hill Lode Sequence. Aeromagnetic anomalies A1 and A2 are also similar and are consistent with the repetition of a magnetic formation within the Broken Hill Lode Sequence. The Geological Plan and Sections of the Broken Hill Mines Area published in November 1972 by the Mine Manager's Association suggests that the Broken Hill Lode Sequence has been repeated. The mechanism is likely to be folding since no fault or shear is mapped between the repetition of the Broken Hill Lode Sequence. It is unfortunate that bulk density data was not sufficiently complete to allow a rigorous subsurface density model to determine whether the fold was synformal or antiformal (see Residual Gravity, Section 2.4.2).

5.8.3 Alma Gneiss

To the east of the Zinc Corporation Mine lease a two milligal gravity low is observed. As discussed in the section on regional gravity profile 1A this gravity low is believed to be caused by the Alma Gneiss. Subsurface density models based on outcrop just to the north of this profile suggest that six thousand feet of near surface Alma Gneiss produces the observed gravity anomaly of 2 milligals. The gravity low diminishes towards the south. As discussed in the section on the regional gravity profile 13 a maxmium thickness of two thousand feet of Alma Gneiss near the surface is all that is possible near the area of Kelly's Creek Shear. This is consistent with geological mapping at a scale of 1" to 2000 feet Sheet No. 1 carried out by the Zinc Corporation. Alma Gneiss is mapped in outcrop of over six thousand feet north of the Broken Hill Airport. However, less than four hundred feet of augen gneiss is mapped near the area of Kelly's Creek Shear.

5.8.4 Correlations with Aeromagnetic Data

The East Airport Gravity High (H3) also diminishes near the area of the Kelly's Creek Shear. Furthermore, the broad area of high magnetic intensity (A4) also ends near this area. The truncation of these geophysical features suggest a change in rock formations across an axis extending along the Kelly's Creek Shear. Geological mapping indicates that outcrop of amphibolite is sparser to the south-west of this axis. It is possible that a steep change in plunge has removed the high density sequence from the near surface. Here the East Airport Gravity High has two maximums which could possibl be due to the exposed limbs of a structure.

Between the East Airport Gravity High and the Alma Gneiss a linear aeromagnetic anomaly (A3) can be observed. This aeromagnetic anomaly has a north-easterly strike for six miles before deviating to the west-south-west. This closure is called the Central Closure and will be discussed more fully later in this section. However, it is important to observe that the aeromagnetic anomaly (A3) has a small flexure to the east along this length which strikes north-east. Also the boundary of the Alma Gneiss is inferred as having a comparable flexure as do the amphibolites to the east of the Alma Gneiss. The East Airport Gravity High also deviates to the east conformably with the features mentioned. Therefore it would appear that the rock formations in this area are conformable. Thus the Alma Gneiss appears conformable with a rock formation which produces an aeromagnetic high. Also these formations are conformable with the rock formation which causes the East Airport Gravity High and which is known to contain at least 1000 feet of amphibolite in outcrop width. A further example of the conformable nature of the East Airport Gravity High is that the anomaly lies to the west of the aeromagnetic area A4 and the aero-magnetic anomaly A6. In fact where the aeromagnetic anomalies A3 and

A6 come close together just south of the Menindee Highway the East Airport Gravity High narrows. It is difficult to decide why the East Airport Gravity High does not increase to the north of the Menindee Highway where the aeromagnetic anomalies become more separated. If formations are assumed to have constant thickness it can be said that a cylindrical fold which repeats a magnetic formation and has a variable plunge could not account for the East Airport Gravity High. The reason for this is that the gravity values do not increase in both directions as the aeromagnetic anomalies become more widely separated.

5.8.5 Area requiring additional Gravity Data

No gravity data has been collected over an area which the author calls the Central Closure. Where the aeromagnetic anomaly swings to the west the East Airport Gravity High weakens to the north-east. The author suggests that this gravity high also turns to the west and connects to a gravity high in the southeast corner of North Broken Hill Mine Lease. E.C. Andrews has mapped an amphibolite-rich sillimanite gneiss sequence as being folded by the Central Closure. Since amphibolites produce gravity anomalies this mapping is another reason why the author expects the gravity high to follow the aeromagnetic anomaly. It is convenient to define the thirteen mile axis between the Darling Range and the Broken Hill line of lode as the Central Axis. The Central Closure lies along the Central Axis two miles north-east of the Menindee Highway. One of the implications of the Central Closure is that the structure about the Central Axis is either a south plunging synform or a north plunging antiform. This implies that the granite gneiss towards the north east could not be equivalent to the Alma Gneiss. Of course it must be assumed also that no faulting has occurred in the "transgressive" area. It is very important to determine whether the gravity high does pass between these granite gneisses.

Therefore a gravity survey should be conducted across the Central Closure. A persistent gravity high which is not substantially reduced in width across the nose of the fold closure would indicate that a formation of constant width passes between these granite gneisses. This formation would be conformable to the aeromagnetic anomaly and therefore conformable to the Alma Gneiss (preceeding discussion).

5.8.5a Northern Granite Gravity Low

North-east of the Central Closure the gravity values are similarly high about a gravity low. The gravity low conforms to the boundary around outcrop of granite gneiss. Also the bulk densities of the sillimanite gneiss formation on either side of this granite gneiss are sufficiently close to allow a synformal subsurface density model to account for the gravity low (G. Jenke, 1972). Whilst the author suggests that there is still some doubt as to whether the structure is synformal or antiformal the author agrees with the notion that the structure is similar along the Central Axis north of the Central Closure. The author agrees also with the interpretation that this structure closes near the Wilcannia Highway. It seems probable that the eastern limb of this structure called the Rupee structure is at least five miles long and continues as far as a west north westerly trending shear near the Rockwell Homestead. This shear is mapped on the Geological Map of the Broken Hill District (1968). The reason for this suggestion is that a linear aeromagnetic anomaly is clearly traceable for five miles as far as this shear. The aeromagnetic map does not prohibit the possibility that the formations on the eastern limb of the Rupee structure continue near the surface towards the south-west. The magnetic intensity is still high to the east. A deviation of one thousand feet towards the east near the Rockwell shear is possible. This deviation is based on the observation that the aero-

magnetic anomalies appear to deviate to the west. Also the difference between the axes of two linear aeromagnetic anomalies thought to be caused by equivalent rock types on either side of the suggested deviation is one thousand feet. O. Weiss gravity data shows that the strike of the East Airport Gravity High has a deviation in the same sense.

Approximately a half mile south-east of the Menindee Highway and the same distance west of the Darling Range Scarp an aeromagnetic anomaly of intensity of 1300 Gammas was found to correlate with a small gravity high. Both anomalies are local extending for only about one mile along strike. At this location the width between aeromagnetic anomalies striking southwest and having an intensity of over 1000 Gammas is one mile. However, to the south-east the separation between these anomalies increases to two miles. In sympathy the East Airport Gravity High widens and becomes more intense. The structure which controls the formations causing the aeromagnetic anomaly must also control the rock which causes the East Airport Gravity High.

Where aeromagnetic anomaly A3 ends towards the south-west the gradient towards the north-west in the gravity values is diminished. This is a further example of the positive correlation between this aeromagnetic anomaly and the high gradient at the margin of the East Airport Gravity High. The fact that the gravity gradient does not continue where aeromagnetic anomaly A3 ends implies that this truncation is not simply the lensing out of a small magnetic horizon.

Gravity anomalies and aeromagnetic anomalies suggest that the regional strike of rock formations between the Broken Hill line of lode and the Darling Ranges is essentially north-east. A local exception occurs in the area of the Central Closure where aeromagnetic data and geological data suggest a closure. A gravity survey over the Central Closure is recommended to confirm this suggestion. The Alma

Gneiss Gravity Low disappears to the south-west and the East Airport Gravity High diminishes in magnitude near the Kelly's Creek Shear. The structural control is not obvious.

5.8.6 High Density Rock Formation

The rock formation causing at least part of the East Airport Gravity High is believed to be conformable to the adjacent rock formations. An amphibolite-rich sequence is known to contribute to the gravity high. However, the author believes that the amphibolite mapped in outcrop cannot account for the maximum anomaly. The possibility of a thick dense lode sequence must be considered since the Rupee Lode Sequence exists along strike. Also the possibility of a dense non-magnetic intrusive being less than one kilometre of the surface cannot be dismissed on the basis of the gravity data. The east-west shear coincides with the disruption of this northwest to southwest trend of gravity anomalies and aeromagnetic anomalies.

The regional trend of geological outcrop, gravity anomalies, and aeromagnetic anomalies becomes westerly between the East-west shear and the Thackaringa-Pinnacles shear. Regional gravity values converge towards the Thackaringa-Pinnacles Shear suggesting closure of the rock types which cause the Broken Hill Area Gravity High. The Little Broken Hill area has gravity values of magnitude similar to the Broken Hill line of lode. This is consistent with the concept that these two areas of mineralization lie in equivalent formations.

5.8.7 Summary

In the Broken Hill area (Fig. 18) gravity highs were correlated with metamorphic rock sequences containing amphibolites, sillimanite gneisses, lode rocks and an absence of granite gneisses and aplites. Conversely gravity lows were correlated with granite gneisses and aplites. The author believes it likely that pelitic rich

metasediments and psammitic rich metasediments are represented by these sequences. That gravity highs can be correlated with thicker piles of metamorphosed pelitic sediments seems likely.

The cause of the strongest positive gravity anomaly in the Broken Hill District has not been fully resolved. This anomaly called the East Airport Gravity High is tentatively correlated with the Rupee Lode Sequence.

SECTION 6 BROADSCALE REGIONAL GRAVITY

This section is meant primarily for the correlation of gravity information with divisions of rock type into areas greater than two miles in smallest areal dimension. Conclusions are drawn from data often spaced as far as one mile apart. The spatial distribution of the data is web-like as access roads and highways were used. To the North of the Broken Hill mine area the data is sparse.

The primary objective of the broadscale regional gravity survey was to determine whether the Broken Hill - Little Broken Hill area was covered by the only regional gravity high in the Broken Hill District. The Broken Hill District is meant by the author to imply that area covered by the Geological Map of the Broken Hill District 1968 (Folio Fig. 7) and lies within longitudes 141^{o} to $141^{o}45'$ and latitudes $32^{o}30'$ to $31^{o}15'$.

The second objective the the broadscale regional gravity was to collect and collate gravity data near areas of outcrop of the Redan Gneiss in the south east of the Broken Hill District. The third objective was to present a regional gravity map of the Broken Hill District to allow correlation between regional gravity, aeromagnetic and regional geologic features. The discussion of the areas covered by the Regional Gravity of Broken Hill 1973 will simultaneously consider all objectives since they are often intimate.

6.1 Broken Hill - Little Broken Hill Area

6.1.1 The Broken Hill - Little Broken Hill area was discussed in the Regional Gravity (Section 5.8). Gravity values in the area were found to be greater than 15 milligals (Bouguer density 2.70 gm/cm^3), except over a few large granite gneiss bodies.

6.1.2 The East Airport Gravity High was over 20 milligals for an area of one mile by three miles with exceptional positive gradients

for an area of two miles by five miles. No other such anomalies have been found in the Broken Hill District with the one exception near Sunnydale Homestead near the Wentworth Highway approximately 50 miles south of Broken Hill (Section 6.3). Redan Gneiss outcrops nearby and is believed to be closely associated with this gravity anomaly. Aeromagnetic evidence suggests that the Redan Gneiss covers an extensive area. On the south eastern margins of this area strong positive gradients have been observed. Unfortunately no aeromagnetic data was available over the Sunnydale Homestead 20 milligal gravity high. Therefore the magnetic properties of the rocks causing this 20 milligal gravity high cannot be compared with those in the Broken Hill - Little Broken Hill area.

The Broken Hill line of lode occurs in an area where anomalie are around 15 milligals. This is also so for the Little Broken Hill area. It was pointed out (Section 5.8.6) that gravity contours closed to the south-west suggesting that geological formations could also close to the south-west thereby implying that the Broken Hill and Little Broken Hill rock types are equivalent. It was also noticed that the Pinnacles Mine and Sentinel Hill area have the same gravity values as the Broken Hill - Little Broken Hill areas (see next section, 6.2). However, no direct correlation of gravity anomalies is possible due to the closure of gravity contours between the two areas. Furthermore no gravity data exists for six miles to the east of the Pinnacles-Sentinnel Hill axis so it is possible that very high gravity anomalies exist. Such anomalies could be compared with the East Airport 20 milligal gravity high. Because of the rarity of such anomalies in the Broken Hill district this would suggest that the Pinnacles-Sentinnel Hill area was of a similar geological environment to the Broken Hill - Little Broken Hill area to the north east.

6.2 Pinnacles - Sentinnel Hill Area

6.2.1 The regional gravity traverse between the Broken Hill railway stockyards and the Middle Pinnacle revealed that gravity values did not vary by more than one milligal until within one mile of Middle Pinnacle. This was consistent with O. Weiss gravity data which covers this area with many traverses having a station spacing of only 200 feet Sillimanite gneiss was mapped in outcrop along this road. (Geological Map of the Broken Hill District, Folio Fig. 7). The gravity data suggests that this sillimanite gneiss could be near surface along the length of the traverse. This would imply that it was equivalent to the sillimanite gneiss which lies west of the Hanging Wall Gneiss.

6.2.2 In the vicinity of the Middle Pinnacle area the regional gravity data shows variations of the order of one milligal. The sparse coverage allows only a broad correlation between higher and lower gravity values with amphibolite and pegmatite outcrop proximal to the station position.

6.2.3 Similarly the values between Middle Pinnacle (Stations P06 to P0 02 in Table 6 in Appendix 10) remain constant to within two milligals. Most of the variations were one point anomalies. Gravity values decreased south of the Middle Pinnacle (P 10 and P 11). However, the paucity of data did not allow a strong correlation with the Thackaringa Shear and pegmatite outcrop in the vicinity. Then a one station gravity high (P 12) was observed.

6.2.4 The Regional Gravity Contours Broken Hill, N.S.W. Sheet 4 of the Zinc Corporation Ltd. shows a gravity traverse near the author's regional station (P 12). A gravity high was observed east of the Pinnacles - Sentinnel Hill area. The total relief of this regional anomaly was four milligals in five miles. By adding a constant equal to the difference between this survey's values and the author's values

near regional stations P 13 and P 14 the maximum gravity value along the Zinc Corporation traverse corrected to similar elevation and Bouguer density datums would have been around 13.7 milligals.

Secondly the Geological Map of the Broken Hill District 1968 shows that amphibolite outcrops in the area near and between the Zinc Corporation's gravity traverse and the author's stations.

6.2.5 In the Sentinnel Hill area gravity values of stations P 001 and P 002 are high (16.0 and 16.9 milligals). These stations are also to the east and near amphibolite outcrop. The author believes it would be important to discover whether a large gravity high exists east of Sentinnel Hill. Therefore a south-easterly gravity traverse should be made across strike and across the area of best outcrop just north of Sentinnel Hill. The station spacing should be four hundred feet so that ten stations would lie over a lode sequence or aplite body about a mile wide. The traverse should extend to meet the Alliance Survey, four miles to the southeast. The survey should also extend to the northwest as far as the sillimanite gneiss mapped in outcrop on the Geological Map of the Broken Hill District, 1968.

6.2.6 The Sentinnel Hill to Edgebak quarry traverse showed that gravity values decreased from 13.95 milligals to 9.18 milligals. This indicates that a major change in rock type has occurred. Although colluvium extensively covers this part of the traverse the author believes that the lower gravity values west of the Pinnacles - Sentinnel Hill axis are related to increased pegmatite and aplite content in the near surface rocks.

6.2.7 The Angus Area Gravity and Geological Interpretation by Entreprise Exploration, March 1960 showed total gravity contours. Locally amphibolites produced positive anomalies of the order of 1.6 milligals over a width of 600 feet and 1.0 milligals over a width of

400 feet. Faulting was mapped by Enterprise Exploration. The mapping was supported by the truncation of linear gravity highs. However, the data covered too small an area to say definitely that a regional gradient can be associated with the larger faults. Offset anomalies could not unambiguously indicate the degree of lateral movement of the faults, since more than one amphibolite appeared in the narrow area covered by the gravity survey.

6.2.8 From Edgebek Quarry to Adelaide Highway 32 there was excellent correlation of the regional gravity with regional geology. Stations TC 3 to TC 8 indicate a gravity low of two milligals over an area where aplite outcrops most extensively. Discussion with Zinc Corporation Regional Geologist, Rowley Brunker, confirmed the author's belief that a major change in rock type exists in this area.

6.2.9 Summary. The author recommends that a gravity traverse be made across the Sentinnel Hill - Pinnacles axis to determine whether any large regional anomalies exist to the east of Sentinnel Hill. The author knows that diamond drilling was being undertaken in this area by Mines Exploration and that fresh core is therefore available for density determinations. This would allow subsurface density modelling to predict the theoretical gravity anomalies near the diamond drill holes. This would then allow the best correlation between gravity data and geological information.

6.3 Copper Blow - Redan Gneiss Area

6.3.1 Introduction

In May 1973 T.V. Harvey of Mines Exploration Pty. Ltd. and the author conducted a gravity traverse along the road from the Broken Hill Airport to eleven miles beyond Copper Blow diggings. The first part of the traverse covered an area already discussed in the Broken Hill - Little Broken Hill area (Section 6.1.1). The second part of

the traverse, between Station CB 09 and the end CB 20 discovered a regional gravity low. The traverse was terminated before the South-eastern end reached a maximum because the gravity meter went off-scale and time did not permit a return to the end of the traverse (station CB 20).

6.3.2 Broken Hill Airport to Copper Blow

The gravity data revealed a monotonic decrease in values away from a maximum of 21.38 milligals (CB 03) from the East Airport Gravity High to a minimum of 7.7 milligals (CB 15) five miles south-east of Copper Blow (CB 10). Between Copper Blow and the East Airport Gravity High a drop in gravity values of 8 milligals was observed. Therefore the gravity data suggests at least one major change in subsurface rock type. Colluvium and sand if present in sufficient thickness would be expected to produce gravity lows because their densities are less than basement rock. Sillimanite gneisses, granite gneisses and amphibolites are some examples of basement rocks in the Broken Hill area. These rock types have densities greater than 2.70 gm/cm^3, whilst sand and colluvium can have densities as low as 1.70 gm/cm^3. The station near Copper Blow (CB 10) was over outcrop so colluvium could not have solely caused the decrease in observed gravity of 8 milligals. However, stations to the south-east of Copper Blow were not noted to be over outcrop. Therefore the hypothesis that sand, colluvium or laterite had caused the drop of 5.5 milligals between stations CB 10 and CB 15 was tested. If a density contrast of 1.00 gm/cm^3 between basement and cover is assumed then the minimum variation in basement relief required to account for the 5.5 milligal anomaly is four hundred and thirty feet. A useful reference on the subject of the effect of overburden on gravity anomalies can be found in "Methods of Geochemistry and Geophysics", 1973, written by D.S. Parasnis. More detail of the nature of cover and overburden in this

area is discussed in Section 6.3.3 and 6.3.4.

It is unlikely that over four hudnred feet of overburden exists in this area. Therefore the author believes that the negative anomaly is caused by change in basement rock type. Pegmatite was mapped in outcrop two miles from the traverse (Geological Map of the Broken Hill District, Folio Fig. 7). Pegmatite has a lower density than the rocks near Galena Hill, which lies two miles to the north-west in an area of higher gravity anomaly.

6.3.3 Galena Hill Overburden.

Galena Hill lies two miles west of Copper Blow. Whilst it is unlikely that variations in the thickness of overburden in the Galena Hill area produce anomalies as large as 5.5 milligals, it is probable that they produce anomalies as large as one milligal with a half width of around one thousand feet. An induced polarization survey was carried out by Austral Exploration in the Galena Hill area on behalf of Conzinc Riotinto (Australia) Exploration (hereafter abbreviated to CRAE). Professor D.M. Boyd used this data to calculate the depth to the bottom of a more conductive overburden which overlies less conductive basement. He predicted that the relief of the basement was about one hundred and fifty feet in the direct vicinity of a positive gravity anomaly. (Professor D.M. Boyd, pers. comm., August, 1974). Also in the area of this anomaly the near surface basement rock was drilled by diamond drill 73 G.H. 1. M. Kirton, a geophysicist with CRAE, measured the bulk density of 73 samples of rock cored in this hole. He gave a list of these bulk densities and their rock type to the author. The average bulk density was greater than 2.80 gm/cm^3. Also laterite of lower density at 2.56 gm/cm^3 was intersected above the basement. The basement rock was composed of sillimanite quartz gneisses, amphibolites and biotite, sericite quartz garnet schists.

Also in the Galena Hill area the author saw some of the

overburden exposed in costeans. Sand and kunkar as well as weathered schists and gneisses were seen by the author. The overburden in the Galena Hill area could have a density as low as 2.20 gm/cm^3. This conclusion is based on the fact that sand and kunkar have low bulk densities (Dobrin, 1960). In the Galena Hill area this implies a density contrast of 0.6 gm/cm^3 between the basement and the overburden. As the topography of the basement is expected to be shallow - as indicated by auger drilling done by CRAE for geochemical sampling - the formula for the gravitational attraction of an infinite slab was a close approximation. This formula gave an anomaly of 1.2 milligals over an area where 150 feet of basement relief had been inferred from resistivity data. This closely matched the CRAE observed gravity profile.

Therefore the author believed that overburden in the Galena Hill area produced gravity anomalies of the order of one milligal with a half width of one thousand feet. This type of anomaly was similar to that produced by the Broken Hill orebody (Section 3.2). Therefore some knowledge of the overburden relief should be gained before inferring, on the basis of gravity data, changes in basement rock type in the Galena Hill area. The author believes that a resistivity survey can provide this knowledge in the Galena Hill area.

6.3.4 Galena Hill Regional Gravity

CRAE produced a Bouguer contour map from a gravity survey of the Galena Hill area. M. Kirton of CRAE supplied subsurface density values and gravity values from extremities of the survey grid. The regional trend of gravity anomalies was east-west in the Galena Hill area. No exact latitude for the base station was available; an approximate value was read from a 1 to 250,000 locality map. It is probable that gravity values as high as 14.8 milligals (Bouguer density 2.7 gm/cm^3) exist in the Galena Hill area. This is significant

since the Broken Hill and Little Broken Hill lines of lode have values near fifteen milligals also.

A negative regional gradient of approximately one milligal per mile towards the south occurred in the Galena Hill area. The densities of subsurface rocks intersected by diamond drilling were often as high as those found in the Broken Hill Lode Sequence. However, at least forty feet of laterite was intersected and was found to have a density of 2.56 gm/cm^3 (M. Kirton, pers. comm.).

As laterite is known to exist south of the Thackaringa - Pinnacles Shear (at Galena Hill, for example), the author considered the thickness of laterite necessary to produce the 5.5 milligal regional gravity low south of the Galena Hill area. Assuming the density of 2.56 gm/cm^3 of the Galena Hill laterite a thickness of two thousand feet would be necessary. As there is no evidence to support such a vast thickness of laterite the author believes that a change in basement rock type caused the gravity low (see 6.3.2).

6.3.5 To the south-east of Station CB 15 (Table 2) a positive gravity gradient was correlated with scattered outcrop of Redan Gneiss. The BMR aeromagnetic survey of the Broken Hill District in 1960 showed increased aeromagnetic intensity which positively correlated with this regional gravity gradient. The sparsity of gravity stations prohibited detailed and conslusive correlation of these facts.

6.3.6 The gravity data along the Wentworth Highway, stations SSM 3694 to SSM 3699, Table 9, confirmed the presence of the regional gravity low south of the Thackaringa - Pinnacles Shear.

6.3.7 The author's Huonville gravity traverse lies to the south of this gravity low. The name of this gravity traverse related to the property belonging to Huonville station; it is unfortunate that the

homestead is more than ten miles northeast of the Huonville gravity traverse. This traverse had a station spacing of four hundred feet. A strong positive gradient towards the south-east was observed (see Table 7). This correlated with the positive gradient observed at the south-eastern end of the Copper Blow gravity traverse (Section 6.3.5).

6.3.8 Summary of the regional gravity values south-east of Broken Hill

The Galena Hill area shows gravity values similar to other areas of mineralization, such as the Broken Hill and Little Broken Hill areas. A basement rock of lower Density exists south of the Galena Hill area. Further to the south-east a positive gravity gradient, a regional aeromagnetic character change occurs in the vicinity of scattered outcrop of Redan Gneiss.

6.4 Silverton - Purnamoota Homestead area

6.4.1 Silverton Gravity Traverse

The author conducted a regional gravity traverse with a station spacing of half a mile along the highway to Silverton. Investigations in the Department of Main Roads in Broken Hill revealed that no permanent bench marks were situated along the Silverton Highway Therefore the author conducted two barometric surveys to determine the differences in elevation between stations and also between a bench mark in Broken Hill and Silverton Tramway Company's McHugh's bridge over the Silverton Creek. The standard deviation of the differences between the elevation of each station as determined by the two barometric surveys was almost eight feet. Therefore despite the large distance of thirty miles between bench marks the elevations are expected to produce errors less than 0.6 milligals in the reduced Bouguer gravity values. Furthermore this error is expected to be random.

6.4.2 The gravity values observed on the Silverton Highway show a steady and monotonic decrease away from Broken Hill (SILV 01 to SILV 09) (Appendix 10).

6.4.3 Then a small positive maximum was observed to have a maximum relief of 1.2 milligals (SILV 11 to SILV 17). This area lies north north east of the Stirling Vale structure which it crosses by the Adelaide Highway 32 where a similar gravity maximum was observed. It is possible therefore that the Stirling Vale structure has produced the distribution of the rock types which caused the gravity high on the Silverton Highway also. The data is not sufficiently close spaced to define repetition of density contrasts across this area.

6.4.4 The rest of the Silverton Highway regional gravity traverse shows a decrease in gravity values towards Silverton. The only exception is an anomaly of at least 0.8 milligals centred over station SILV 20 which occurs along strike from three outcrops of amphibolite east of Nadbuck and Lucky Hit mines as mapped on the Geological Map of the Broken Hill District, 1968.

6.5 Purnamoota Traverse

6.5.1 Introduction

T.V. Harvey and the author conducted a regional gravity traverse with a station spacing of one mile along the Broken Hill to Purnamoota Homestead road and then for seven miles further north towards Brewery Well. The author conducted two barometric surveys to determine the elevation differences between stations and to tie the traverse to a bench mark in Broken Hill. Unfortunately the traverse did not have an elevation tie at the northern end. It is therefore "floating" at the northern end where the elevations are dependent upon preceeding barometric elevation determinations. A third barometric survey was conducted by the author over the northern half of the Purnamoota traverse in order to improve control at that extremity. Differences in elevations found by these surveys suggest that final errors in the Bouguer gravity values could be as high as one milligal. However, relative differences between proximal stations is less than 0.6 milligals.

6.5.2 Decrease away from Broken Hill

Bouguer gravity values show a steady decrease away from Broken Hill. Then a 3.1 milligal anomaly high was observed near Nine Mile Creek (Stations DU 07 to DU 09). As colluvium is mapped near these gravity traverses it is not obvious what is causing this positive anomaly. Further to the north the gravity values fall to the lowest found in the Broken Hill District. The lowest value of 4.0 milligals was found over a post-Wilyama intrusive granite. The author does not consider that the regional gravity low of eight milligals observed towards the end of the Purnamoota traverse has been caused by sand or colluvium. Discussion of this type of problem can be seen in Section 7.3.3 for the Copper Blow gravity low.

The Silverton Highway - Purnamoota Homestead gravity traverses show that regional gravity values decrease away from Broken Hill towards the northwest. Also it appears that the lowest gravity value in the Broken Hill District occurs over a post-Willyama intrusive granite and that a detailed gravity survey over this body may determine the subsurface geometry. The survey would determine the near surface extent of this body under colluvium. However, the author knows of no mineralization along the contact of the post-Willyama intrusive granite and the Willyama complex.

6.6 Tibooburra Road - Wilcannia Highway Area

Except for one gravity station near Golden King Homestead collected by the N.S.W. Geological Survey the available gravity data in the northeast of the Broken Hill District is confined to the Tibooburra Road and the Wilcannia Highway. The gravity stations used by the author were collected by T.V. Harvey and G. Jenke in August 1972 for the Broken Hill Mine Manager's Association. Also at the eastern end of the Wilcannia Highway Alliance gravity data from the

Scopes Range Gravity Survey was used (Alliance, 1967). Gravity data collected by the N.S.W. Geological Survey was superseded by these surveys with closer stations spacings. The author digitized the coordinates from an overlay on which G. Jenke had marked the position of the stations. Also the author reduced the data from raw dial division difference with the drift as yet unremoved since previous reductions did not relate to the International Gravity Formula for the normal geod (Dobrin, 1960).

6.6.1 Tibooburra Road

For the first 24 miles beyond Broken Hill the gravity values along the Tibooburra road are less than 12 milligals. They are therefore three milligals lower than gravity values commonly found in the Broken Hill - Little Broken Hill area. Therefore the near surface rock types are not expected to be equivalent.

Granite Gneiss outcrops in the vicinity of the Stephens Creek Hotel. However, stations in the vicinity of these outcrops do now show significantly lower gravity values than for proximal stations along the Tibooburra Road. Since granite is usually less dense than sillimanite gneisses and schists (which are mapped next to these outcrops of granite) a definite gravity low would have been expected over a granite which encompasses all outcrops of the granite near the Stephens Creek Hotel. Therefore it can be said that the gravity data does not suggest that such a large body of granite exists about the Stephens Creek Hotel.

This gravity low along the Tibooburra Road cannot be correlated with any gravity low to the south-west along the regional geological strike. Insufficient gravity data prohibits correlation or proof of closure of this gravity low.

6.6.2 Although only three stations were located over the Torrowangee

Adelaide sediments a gravity low of at least 0.7 milligals has been established. This suggests that the average bulk density of these Adelaidean sediments is less than the adjacent rocks from the Willyama Complex.

6.6.3 In the Euriowee Inlier the gravity values rise by five milligals. Values as great as those (15 milligals) found along the margins of the Broken Hill - Little Broken Hill area suggest the possibility that rocks equivalent to those in the Broken Hill area may exist along the Tibooburra Road in the Euriowee Inlier. The Geological Map of the Broken Hill District 1968 shows that an amphibolite and granite gneiss sequence occur near the maximum. This sequence is mapped striking north-west.

A map of Bouguer Anomaly Contours and Gravity Stations compiled by the N.S.W. Department of Mines shows that regional gravity values have a north-easterly trend near the Wilcannia Highway and then change to a north-westerly trend where the Tibooburra Road crosses the Euriowee Inlier. The author suggests that the gravity coverage north of the Wilcannia Highway is not sufficiently complete to prove closure of the Broken Hill - Little Broken Hill area gravity high. Gravity values from the O. Weiss survey indicate that the gravity low west of Rupee Mine closes to the north east (Section 5.8.5a). However, this feature is only part of the regional gravity high and does not necessarily imply that the regional gravity high closes.

6.6.4 The Wilcannia Highway gravity traverse was conducted by G. Jenke and T.V. Harvey under a grant to the University of Adelaide from the Broken Hill Mine Manager's Association for a regional gravity survey. The author reduced the raw gravity data. The gravity values show the northernmost intersection with the Broken Hill - Little Broken Hill area regional gravity high - that is for values greater than 15

milligals. Within the regional gravity high there is a local gravity high to the east. The N.S.W. Department of Mines Bouguer Anomaly and Gravity Stations Map correlates this gravity high with that on the Tibooburra Road which was discussed in Section 6.6.3. The author recommends more complete gravity coverage near or just north of the Stephens Creek Reservoir in order to determine the northern extent of the regional gravity high and the relationship of the local gravity maxima.

The decrease in gravity values towards the east along the Wilcannia Highway half a mile past the Stephens Creek crossing coincides with the first outcrop of aplite outside of the Broken Hill - Little Broken Hill Area in which outcrop of aplite is rare. To the east the area is extensively covered by colluvium. Here the gravity data suggests that the underlying rocks are not equivalent to those in the Broken Hill - Little Broken Hill area.

This negative gradient correlates with the gravity low east of the Downfall along the Menindee Highway. The regional gravity trends are in the same direction as the regional geological strike, that is north-east.

6.6.5 Summary of gravity coverage north-east of Broken Hill

The gravity coverage in the Tibooburra road to the Wilcannia Highway arc north-east of Broken Hill is insufficient to suggest whether any rocks of the Broken Hill - Little Broken Hill area can be traced north of the Wilcannia Highway. However, gravity data suggests that the regional geological strike should be northerly and then become north-westerly over a distance of 45 miles north of the Wilcannia Highway and east of the Tibooburra Road.

6.7 Broadscale Regional Gravity Summary

The author believes that the gravity values in the Broken Hill District reflect the density of the subsurface metamorphic rocks seen in outcrop in the District. Sillimanite gneiss and amphibolite rich sequences produce gravity highs which can be traced for miles. Similarly granite gneiss and aplitic rich sequences produce gravity lows. If one postulates that sillimanite gneiss and amphibolite rich sequences are metamorphosed pelitic rich sediments or blanket type lava flows which after metamorphism have a higher bulk density than granite gneiss and aplitic rich sequences postulated to be psammitic rich metasediments, then regional gravity anomalies can be believed to indicate the relative thicknesses of such sequences. For example in Folio Fig. 6 the author's Regional Gravity Map of the Broken Hill District and Eastern Environs those areas where the gravity values are greater than 15 milligals (see Appendix 7 for details of reduction) are shaded. Then these shaded areas could indicate thicker sequences of pelitic rich sediments than those adjacent. Also it is possible that in the south eastern portion a fold system with north east to south-westerly major axes still influences the disposition of a folded sequence of metasediments. It must be pointed out that more gravity stations would better define the gravity field and may modify the regional gravity contours drawn by the author. At present the N.S.W. Department of Mines is collecting additional gravity data in the Broken Hill District.

REFERENCES

(See also References at the back of Appendix 8)

Alliance. 1967. See Scopes Gravity Survey.

Andrews, E.C. 1922. Government Geologist, N.S.W. Geological Map of that portion of the Broken Hill District which contains the principal Silver, Lead and Zinc Deposits. Scale 1" to 2 miles.

Broken Hill Mine Managers' Association. Nov. 1972. Geol. Plan of Sections of the Broken Hill Mines Area. Compiled from mapping by the Zinc Corp. Ltd., New Broken Hill Cons. Ltd., North Broken Hill Ltd., Broken Hill South Ltd., the Central Geological Survey (1936-1939) and the Geological Survey of N.S.W. (1922) by I.R. Johnson and G.D. Klingner. Ground Survey Control drafted by M.L. Brooksby.

Bureau of Mineral Resources. 1960. B.M.R. Published a map showing total magnetic intensity measured by airborne magnetometer and radioactive anomalies in the Broken Hill Area, N.S.W. in August 1960. The map reference number published was G289-11. The areal scale was one inch represents two miles and the contour interval was fifty gammas.

Cottrell, E. 1960. "Final Report on A to P 2056, Rupee Anomaly". Zinc Corporation Report files, Broken Hill.

Dobrin. 1960. Introduction to Geophysical Prospecting. Second Ed. McGraw-Hill Book Co. "International Gravity Formula" p. 234.

Enterprise Exploration Co. Pty. Ltd. "Geology & total gravity contour plan of the Southern Portion of the Broken Hill Area". Scale 1" rep. 2000'. Zinc Corp. Plan No. X27/734.

Fifth Empire Mining and Metallurgy Congress, Australia and New Zealand. 1953. Book entitled "Geology of Australian Ore Deposits".

Gransbury, R.T. 1973. Gravity and Laboratory Induced Polarization investigations in the Eurelia Area, South Australia.

Gunn, P. 1967. M.Sc. "Gravitational and magnetic interpretation of the Middleback Range Area, South Australia".

Jenke, G.P. 1972. "Geophysical Investigations in the Rupee Mine Area, Broken Hill, N.S.W." Hons. Thesis, Department of Economic Geology, University of Adelaide.

Hodge, Dennis S. and Mayewski, Paul A. Journal of the Geological Society of America. Bulletin, Vol. 80, April 1969, pp. 705-714.

King, H.F. and Thompson, B.F. 1953. "Geology of the Broken Hill District". Fifth Empire Mining and Metallurgy Congress, Australia and New Zealand, 1953. Book Entitled "Geology of Australian ore Deposits".

King and O'Driscoll. 1953. From "Geology of Australian Ore Deposits".

Kirton, M. 1973. (pers. comm.) Geophysicist for Conzinc Rio Tinto Aust. Exploration.

Laing, W.P. 1972. (pers. comm.) Ph.D. student, University of Adelaide.

Matheron, G. 1971. "The theory of Regionalized Variables and its Application". Editor, Ecole Nationale Superiere de Mines de Paris, 1971.

Nagy, Dezco. 1966. Geophysics, April. Gravitational Attraction towards a Right Rectangular Prism.

Parasnis, D.S. 1973. Mining Geophysics (second edition). Elsevier Scientific Publishing Company.

Scopes Gravity Survey P.E.L. 82 New South Wales. For Alliance Oil Development Aust. N.L., conducted by Geosurveys of Australia Pty. Ltd., and report written by W.F. Stackler and P.G. Brunt, July 1967.

Copy held in the Geophysics Department of the Univ. of Adelaide.

Smellie, Donald W. 1960. "Applicability of Geophysics in the Broken Hill District of Australia". October 1960. For Consolidated Zinc Propriety Ltd., Melb., Australia.
Copy housed in Zinc Corporation's Geological Office in "Geophysical Papers" cabinet.

Smith, R.A. 1942. "Some Depth Formulae for Local Magnetic and Gravity Anomalies". Geophysics, Vol. 7 No. 1, p. 55.

Talwani, M., Worzel, J.L., and Landisman, M. 1959. "Rapid Gravity computations for two-dimensional bodies with applications to the Mendocino submarine fracture zone". Jour. Geoph. Research, 64, p. 49-59.

Weiss, O. 1949. Unpublished report on the gravity anomaly expected over the Broken Hill orebody. Housed in Zinc Corporation report files, Broken Hill.

Wood, R.J. 1972. "The Interpretation of Ground Magnetic and Gravity Data, and its Correlation with the Geology in the Broken Hill Area, N.S.W.". Hons. Thesis, Dept. of Economic Geology, University of Adelaide.

Zurfluch, E.G. 1967. Applications of Two-Dimensional Linear Wavelength Filtering. Geophysics, Vol. XXXII No. 6, December, 1967.

APPENDIX 1 DENSITY DATA PRESENTED BY L.A. RICHARDSON

In 1950 L.A. Richardson, of the New Broken Hill Consolidated Mine, presented bulk density values measured from diamond drill core taken from the Southern Extensions Area in Broken Hill. The New Broken Hill Consolidated mine reference numbers for these plans are X10/8 and X10/6. The core was sampled at apparently regular ten feet intervals from mine cross-sections 62 and 92. The diagrams showed the ground surface and diamond drill paths. The downhole footage and value of bulk density for each sample were represented by the intersection and length of a line normal to the borehole path. The length of the line was a function of the difference of the density of the sample with 2.80 gm/cm^3 and the scale of one inch equals 0.2 gm/cm^3. Only "dyeline" copies are available and their quality does not allow them to be reproduced photographically.

The author had to measure each density value from these copies. The measurement of the length of the line produced errors of the order of one fortieth of an inch or 0.005 gm/cm^3. Thus the original data is usefully recoverable if one assumes that it was plotted to this accuracy.

APPENDIX 2 FOLIO FIGURE 1: EXPLANATION AND DESCRIPTION

MEASURED BULK DENSITIES OF CORE FROM BROKEN HILL LODE SEQUENCE

On Folio Fig. 1 individual bulk density values are represented sequentially with the horizontal axis representing downhole distance. Bulk densities from the one diamond drill hole are represented by the same symbol. Bulk densities from different diamond drill holes have different symbols as often as the number of suitable symbols in the computer plot routine allowed. The right hand direction indicates more westerly samples. For diamond drill holes in rock other than lode the relative position of the diamond drill holes has been expressed by the relative position of plotting. For example DD 2310 is the most easterly diamond drill which does not intersect the lode. Most of the densities are for east (lower) amphibolite (Formation number 3, Fig. 1). Next starting at feducial -3200 feet is plotted DD 2200 which passes through sillimanite gneisses and as far as the west (upper) amphibolite (Formations 4, 5 to 10, 11 and 12, Fig. 1).

The densities from DD 1600 have been plotted four inches above those for DD 2200. This allows broad correlation for those values for core from equivalent formations from the Broken Hill Lode Sequence (see Section 262, Folio Fig. 4).

The upper half of Folio Fig. 1 was transposed from the right hand side of the lower part in order to make the diagram squarer rather than striplike. Therefore DD 130 is more westerly than either DD 1600 or DD 2200. DD 130 passes into the Hanging Wall Gneiss (Formation number 13). DD 85 passes through Potosi Gneiss and sillimanite and also part of the Broken Hill orebody. DD 85 is plotted with the bulk density base four inches higher than that for DD 130. All other diamond drills intersect part of the Broken Hill orebodies and were arranged so as to occupy spaces between the other diamond drill holes. The reason for including the diamond drill holes which intersected

the orebodies was to provide a comparison of those densities from heavily mineralized rock with those densities from lightly mineralized or unmineralized rock.

APPENDIX 3 SUBROUTINE GUN: METHOD OF CALCULATION OF THEORETICAL GRAVITATIONAL ATTRACTION

The method of calculation of the theoretical gravitational attraction of the subsurface density models, was that of supposing two dimensional geometry, polygonal cross-section with infinite extension normal to the section. The formula for the theoretical gravitational attraction of such a body was given by Talwani, M., Worzel, J.I. and Landisman, M. in 1959 (Talwani, 1959). Peter Gunn wrote a program to perform this computation in 1967 (Gunn, 1967). The author made minor modifications to this program and incorporated it as a library subroutine available on permanent disc file. As discovered by R.J. Gransbury and the author in 1973, P. Gunn's program did not produce correct results for models with horizontal sides. The author pointed out that P. Gunn had quoted that Talwani et al had published a method of calculation which was "effectively a summation of the gravitational attraction of infinite step type bodies (regarding the faces of the polygon as forming the edges of the step)". (Gunn, P., 1967, p. 77). In fact the summation represents successive contributions to the Hubbert line integral (Hubbert, 1949). The author observed that P. Gunn's erroneous assumption led to the conclusion that no contribution to the final summation was made by a face which is horizontal. The author showed that this term was deliberated omitted. Therefore in the use of the program written by P. Gunn the author avoided the contingency of horizontal and vertical sides by making adjacent points at least very slightly different in co-ordinates. Whilst this produced no significant difference in gravitational attraction no models were prone to programming errors.

The validity of the output from this program was checked by using models such as infinite slabs and rectangular shaped models. The latter were checked by the use of the three-dimensional subroutine PRISM (see Appendix 4).

APPENDIX 4 SUBROUTINE PRISM

Subroutine Prism was written by the author to test the validity of using two dimensional models with no plunge to predict the expected gravitational attraction caused by the Broken Hill orebody. A copy of this subroutine is included. The Broken Hill orebody has a plunge of about 20^{o} in the Southern Extensions area (Ian Johnson, Chief Geologist, Zinc Corporation, 1973, pers. comm.). Subroutine PRISM was used to calculate the gravitational attraction of upright rectangular prisms joined together in such a was as to represent the Broken Hill orebody with a twenty degree plunge.

The mathematical formula was checked by the author by taking the vertical component of the fact on a unit mass which is given by the basic formula

$$\text{Force} = G \iiint \frac{\rho(x,y,z)}{r^2} dxdydz$$

where G is the Gravitational constant

$\rho(x,y,z)$ is the density defined in three dimensional space

r is the distance between the unit mass and the unit volume of the disturbing mass

and performing the integration over an upright rectangular prism. The formula was published by Dezco Nagy in Geophysics, April 1966, Vol. XXXI, No. 2. However, several errors were noted by the author in equation (8), p. 364.

The author preferred to use the abbreviated form of the formula for the vertical component of the gravitational attraction of an upright rectangular prism of uniform density. This form was also published by Dezco Nagy in equation (7) (Nagy, 1966). This form is written below

$$F_z = G\rho \left| \left| \left| x\ln(y + r) + y\ln(x + r) - z\arcsin \frac{z^2 + y^2 + yr}{(y+r)\sqrt{y^2+z^2}} \right|_{x_1}^{x_2} \right|_{y_1}^{y_2} \right|_{z_1}^{z_2}$$

The contributions of each term are then computed successively by substitution of the limiting coordinates into the forms of the abbreviated integrand and by varying the signs of these terms depending on whether the sum of the indices of the coordinates is even or odd.

Subroutine PRISM was checked by writing a second version of this evaluation. In this version the integrand was written in expanded form and the substitution of the limiting coordinates was made only once into each term. This version was similar to equation (8) in Dezco Nagy's article (in Geophysics, April 1966, Vol. XXXI, No. 2). Subroutine PRISM was also checked by evaluating the gravitational attraction of a unit mass towards a very broad, thin slab buried at a shallow depth and comparing this attraction with that towards an infinite slab of the same width and density.

APPENDIX 5 SUBROUTINE TEST

Subroutine TEST used subroutine MODEL, a subroutine also written by the author, to represent the Broken Hill orebody in the Southern Extensions Area. Subroutine TEST specified the size of the model, the plunge and also the size of the prisms which make up the model. Subroutine MODEL generated and stored the co-ordinates for every PRISM. Subroutine TEST then called subroutine PRISM to evaluate the gravitational attraction of all prisms at every sensing point.

The gravitational attraction of the model which plunged at 20^{o} was at most 0.04 milligals greater than that for the non-plunging model. This indicated that two dimensional Talwani density models could be satisfactorily used to model the Broken Hill orebodies.

APPENDIX 6 PROGRAM TALW

The calculation of theoretical gravity profiles and their comparison with O. Weiss observed gravity profiles was achieved by a number of subroutines. These were written by the author - with the exception of subroutine GUN which the author modified from program TALW written by P. Gunn (Gunn, 1967) (see Appendix 3). Because the combined length of the subroutines became unmanageable the author created several libraries and stored them on permanent disc file. The libraries were then attached and the subroutines wer accessed when required. The University of Adelaide Computing Centre's Local Publication No. 55 entitled "Introduction to Scope 3.4" provided the information required to create and use libraries.

Program TALW was the master routine. A permanent file on which two records of data were stored were attached. Then two libraries were attached which contained subroutine APLT, subroutine O.WEISS and subroutine GUN. These subroutines were left with the Geophysics Department at the University of Adelaide.

The first record of data contained the gravity values and co-ordinates for the O. Weiss observed gravity profile. The formal parameter NTAPE conveyed the local file number of the first data record to subroutine O.WEISS. This data was arranged as follows.

FIRST CARD

PROFIL: PROFILE NAME OR NUMBER 80 CHARS.

SECOND CARD

BEGIN: IF NON-ZERO, START OF STATIONS SPACED STEP APART

STEP: IF BEGIN NON-ZERO, DISTANCE BETWEEN STATIONS

RESET: OFFSET BETWEEN GEOPHYSICAL BASELINE AND MINE REF. L.

FMG: Factor to convert values to MILLIGALS

REGION: Regional gradient to be removed: MILLIGALS PER UNIT DISTANCE FOOT

SIGN: Positive if the traverse runs in the same direction as the Mine Reference Co-ordinates.

NEXT CARDS

FIVE STATIONS PER CARD (OBS: OBSERVED GRAVITY
(EXOBS: PROFILE (X) CO-ORDINATE OF STATION

LAST CARDS

FILLED BY 99.99

WHICH TERMINATES INPUT OF OBSERVED GRAVITY

EOR: END OF RECORD

Subroutine O.WEISS stored values of gravity and profile co-ordinates related to the Broken Hill Mine Reference Line. The treatment of the co-ordinates suited to arbitrary reference points. The RESET optionally allows for offset in co-ordinate values. The BEGIN value optionally generates the x co-ordinate values for regularly spaced stations.

The second data record contained information for the theoretical subsurface density model. The body corners' co-ordinates were related to the N.B.H.C Mine Reference Line. The data was arranged as follows.

FOR THE FIRST BODY

FIRST CARD

SEXION : SECTION NAME OR NUMBER 80 CHARACTERS

SECOND CARD

JTOT : NUMBER IF BODY CORNERS TO BE READ (AN INTEGER, I5)

DENS : DENSITY OF BODY (ONE SPACE, A REAL DECIMAN NUMBER, F6.3)

THIRD CARD

EXX : X-CO-ORDINATE OF FIRST BODY CORNER (F8.2)

ZEE : 2-DEPTH OF BODY CORNER (F8.2)

DAM : NAME OF BODY (SA10)

NEXT (JTOT-1) CARDS

EXX : X CO-ORD. OF NEXT CLOCKWISE BODY CORNER (F8.2)

ZEE : 2 DEPTH OF NEXT CLOCKWISE BODY CORNER

These formats were repeated for each body for the subsurface density model. Subroutine GUN has a print option, formal parameter NOPRNT, for the printing of the gravitational attraction at each sensing point caused by the body in question. This gravitation attraction is returned to the main routine via array GR in Common Block Two. A description of the use of subroutine GUN is presented in Appendix 3.

The main routine, program TALW, then recalled subroutine GUN until it had reached the total number of bodies to be included in the model. This number is set within program TALW and was stored by the parameter IS. The gravity total for each station was stored in array GRAT. Next the array plotting subroutine APLT was called. This routine was written by the author to plot all gravity profiles used or measured by the author on the ten inch CALCOMP plotter attached to the University of Adelaide's CDC 6400 computer.

Formal parameter ID1 was an option to set the type of plot to be made from subroutine APLT. Program TALW only called on four types of plotting from subroutine APLT. Three options were the plotting of the body corners the individual gravity to a body (see Folio Fig. 5) or the total gravity response caused by all bodies in the model. The latter type included a comparison and difference with the observed gravity. Finally program TALW required the scales to be varied for mine scale to regional type profiles. The most common outputs were at 1000 feet to the inch and 4000 feet to the inch.

Also, through the use of formal parameters (NOPLT) "no plot", subroutine APLT included an option to print the arrays, scale factors and origins before plotting. This had the advantage of inspecting the data before use of the LINE routine which calls the pen plotter. Bad data could be prevented from being plotted on the plotter which was much in demand by the users of the University of Adelaide's computer.

When the data was good the NOPLT option was changed from the value of two in program TALW merely by reversing the order of two cards.

APPENDIX 7 REDUCTION OF GRAVITY DATA

The author wrote subroutines to compute and remove the drift from gravity differences measured in dial divisions by any gravimeter, provided that the calibration factor had been previosuly determined. Provision was made to process field loops which included any station whose absolute gravity was known. The field loop did not necessarily begin or end on such a station. The absolute value of gravity of such stations was known either from a list of base stations established by previous surveys or from stations whose value of absolute gravity had been computed from a previous loop.

For each station the position was fixed by co-ordinates related to the Australian Map Grid. Most of the regional stations along roads and tracks in the Broken Hill District were positioned by the author on Zinc Corporation airphotos scaled at one inch represents one thousand feet. These airphotos were then located on base maps upon which Australian Map grid Co-ordinates were marked. For traverses only a few stations' co-ordinates were determined from airphotos - the other statiors' co-ordinates were found by interpolation. The latitude for each station was calculated using these co-ordinates and a subroutine written by R. Cammel who was a student of surveying in the South Australian Institute of Technology in 1973.

Bouguer gravity values were produced by a subroutine written by the author who used the International Gravity Formula (Dobrin, 1960). The station name, value of absolute gravity, elevation, northing, easting, latitude in radians, and Bouguer value of gravity are presented. Also presented at the front of each table are some details relevant to the collection and reduction of the data. Computer cards (IBM) containing this information less the Bouguer values were left by the author with the Geophysics Department at the University of Adelaide.

APPENDIX 8 VARIATIONS IN THE ABSORPTION COEFFICIENT OF GAMMA-RAYS IN ROCK FROM THE BROKEN HILL LODE SEQUENCE

Evaluation of the feasibility of using absorption of gamma-rays as a measure of the bulk density of core was undertaken by the author. The accuracy of this operation rather than the speed is here discussed. The equipment used belongs to the CSIRO Division of Soils and is in the charge of Mr. C.G. Gurr. All details of the equipment were furnished by Mr. Gurr who also built the apparatus. Drill core was borrowed from the Department of Mines through the courtesy of Bernie Milton whose interest includes the determination of the bulk density of wet porous sedimentary rocks. The experiment measured the absortpion across a standard core cross-section for gamma-rays of two energies, namely the 0.66 MeV peak emitted by Cs 137 and the 59.6 KeV peak emitted by Am 241.

Apparatus

The sources were in turn placed in a lead collimator cum shield for measurement of the complete suite of rock core. Absorption by the atmosphere was considered neglibible. The radiation emitted is in the form of a sliver which fans from 1 cm in breadth to 3 cm over a distance of 20 cm. The core, approximately 4 cm in diameter, was located nearer the source than the detector, which was a Sodium Iodide, thallium doped crystal $1\frac{1}{2}$" in diameter and 1" in height. After a photocultiplier a discriminator passed voltages corresponding to 8% of the width at half the peak height for the Cs source and 30% of the width at half the peak height for the Am source. Normally the check that the bandpass was centred over the peak was done automatically. However, due to an electronic breakdown this had to be checked manually. Drift was checked for by measuring the counts through two A1 standard sheets and fixed places of the core. No significant drift was observed

in the response of the photomultiplier. To calculate the average absorption per core the source-detector geometry was shifted vertically with respect to the core which averaged 40 cm in length. This was done automatically in 5 millimetre increments by the apparatus which can also be preprogrammed for lateral shifts of the material under bombardment. Alignment was achieved by clamping the core to a steel beam, and errors associated with alignment were considered neglibible. The zero absorber count rate was obtained by extrapolation from counts obtained from 1, 2 and 4 standard thicknesses of A1 plate. The dead time per count was taken as 0.00000146 secs. (C. Gurr, pers. comm.).

Theory

For a given thickness of material x composed of materials of absorption coefficients U_i and density P_i the absorption of a beam of intensity N_0 is given by:

$$N = N_0 e^{-x(U_1P_1 + U_2P_2 + ...)} \qquad 1.$$

If the materials have a constant absorption coefficient then the total bulk density can be found. Assuming that a sufficiently homogeneous core is sampled often enough the average density encountered every 5 mm equals the overall bulk density (P_B), which equals that density (P_A) measured using archimedes method provided that the core is not permeable. Reshuffling equation 1 the density across any section P_i is given in equation 2 where U_i is the total absorption coefficient across that section and x_i is the width of that section.

$$P_i = \frac{(\ln N_i - \ln N_o)}{(-Ux_i)} \qquad 2.$$

The average producet of the absorption coefficient with the width (hereafter denoted by $\overline{ux}$) encountered along the n sections of a

core is thus given by equation 3.

$$\frac{\sum_{i=1}^{n} u_i x_i}{n} = \frac{1}{-P_A n} \sum_{i=1}^{n} \ln N_i - n \ln N_o \qquad 3.$$

Reduction of Data

A program was written by the author to correct counts for dead time and to solve for each core's average absorption coefficient times width (i.e. $\overline{ux}$). Also computed was a density section for each core based on the assumption that everywhere the absorption coefficient times the width was a constant equal to $\overline{ux}$. The data were digitized on a fortran card punch despite the availability of paper tape. The amount of data recorded was too small to justify writing a sub program to convert paper tape information to IBM code.

The results for these "standard" absorption coefficients are listed in Table 1. The $\overline{ux}$ for Cs equalled 0.410 and had a std of 0.5%. The $\overline{ux}$ for Am equalled 1.634 and has a much larger std of 3.0%

TABLE 1

Core Label	Archimedes Density	Cs $\overline{ux}$	Am $\overline{ux}$
1555	2.63	0.409	1.597
1573	2.63	0.510	1.616
740	2.67	0.411	1.582
716	2.72	0.408	1.704
Broken core 2.72	2.80	0.413	1.670
		mean = 0.410	mean = 1.634
		std = $\pm$0.002	std = $\pm$0.051
		or std = 0.5%	or std = 3%

Using the average absorption coefficient the density could be computed at each point for Cs. It was noted that the density around the break in the core labelled "broken core" was almost 10 per cent lower for three readings out of the fifty measured. This was similarly

noted for the Americium density profile. This could produce error in the resultant average absorption coefficient in the positive sense as is also observed in Table 1.

The reason for the divergence of values for $\overline{ux}$ for Cs and Am in the case of core labelled 716 is not known. However, it is recorded that large veins occur in this sample. The standard deviation in the number of counts recorded in a given time (about 200,000 in ten seconds for the Cs source used) is the square root of the number of counts. The "statistical" error in the determination of $\overline{ux}$ for one section of core is given in equation 4.

$$(-ux) = \frac{1}{P} \ln (N + N) - \ln (N) \qquad 4.$$

$$= \frac{1}{2.5} \ln (2 \times 10^5 + 500) - \ln (2 \times 10^5)$$

$$= \frac{1}{2.5} \times 2.302 \times 0.0011$$

$$(-ux) = 0.001 \quad \text{or} \quad 0.25\%$$

However, the percentage error due to statistical fluctuations in the determination of the average value of ux ($\overline{ux}$) will be inversely proportional to the square root of the number of individual determinations. This commonly implies a reduction by a factor of six. Therefore, the error due to statistical fluctuations in the determination of $\overline{ux}$ was approximately 0.04% and not significant. The "statistical" error in $\overline{ux}$ for Am 241 was similarly not significant.

The variations in Cs $\overline{ux}$ are small enough to permit a density determination after a ten second count with an accuracy of 0.5%. The Am 241 after a forty second count time (longer than for Cs due to a poorer penetration of the order of $\frac{1}{150}$ compared with 1 in three for Cs 137) provides an accuracy of only 3%. In particular it seems that comparison of the absorption in rocks of the caesium 0.55 MeV peak

with the americium 59.6 KeV peak (see B.D. Soane, 1967) to produce a measure of the water content in rocks is not possible due to the variation of the absorption coefficient for americium. A higher energy source may be substituted for Am. However, accuracy depends on the difference in the energies of the sources. Although the stability of the absorption coefficient is good in the 0.5 MeV to 3.0 MeV range safety considerations became important.

The energies were converted to wavelengths using Plank's relation and some mass absorption coefficients were compared in Table 2 after selection from the Handobok of Chemistry and Physics, the 51st edition of the Chemical Rubber Co.

TABLE 2

	0.024 A^o or 0.6 MeV u (cm^2/g)		0.2068 A^o or 60 KeV u (cm^2/g)
(H)	0.165	(H)	0.375
(C)	0.080	(O)	0.183
(A1)	0.079	(A1)	0.270
(Fe)	0.080	(Fe)	1.10
(Cu)	0.081	(C)	0.63
(Sn)	0.100	(Mg)	0.25
(Pb)	0.210	(S)	0.40

From consideration of these absorption coefficients it is seen that compositional variations affect the Am absorption coefficient far more radically than for Cs. Only the absorption coefficient for heavy metals drastically alter (i.e. over 1%) in the case of Cs. However, variation is not strictly monotonic for increase in atomic number in the light to medium range. Thus one might hope for a change in composition of more than one element producing a situation where

some variations in absorption coefficient are in the opposite sense. Also the composition variation is not expected to be complete and the error in assumed absorption coefficient only acts on the "anomalous" composition.

Bulk Chemistry and Heavy Metal Content

From a study of the bulk chemistry of thirteen areas selected from representative rock types at Broken Hill but not including lobe zones one realizes that variations in heavy metal content are expected to be less than 1,000 ppm as the total heavy metal content recorded is less than 2,000 ppm. The heavy metals listed were Ph, Ni, Co, Cn, Ag, Zn, Sn, Ba and the mean total composition of these heavy metals was 967 ppm with a standard deviation of 351 ppm over twelve areas. The data was incomplete for the thirteenth. Thus using a large deviation of the absorption coefficient such as the difference between lead and iron the maximum likely error in the absorption coefficient due to variations in heavy metal content is 0.25% of the absorption coefficient for light to medium density elements. Thus the presence of heavy metals is not expected to be important due to the low percentage present in the country rock at Broken Hill.

Later work conducted by the author on 15 more samples of diamond drill core confirmed the work presented here. However, time did not permit the presentation of these results. The author concluded that the bulk density of metamorphic rocks from the Broken Hill Lode Sequence could be determined by counting the amount of gamma radiation absorbed by samples. For radiation emitted by CS 137 and core of regular diameter and without cracks ten second counts could be used to compute the bulk density to within half a percent. The percentage composition of heavy metals would have to be that common for rocks in the Broken Hill Lode Sequence but not near the margin of the orebody.

Method of Determination of Bulk Density

The bulk density of core from Broken Hill was measured by the author by using a beam balance and water immersion. Reproducibility of readings from a given core were generally better than 1:250. Exceptions were rare and proved to be weathered and permeable to water. Such samples were soaked to ensure no air was entrapped. The absolute accuracy was considered to be 1:250 since the balance and the density of the fresh water used were more accurate than 1.000 ± 0.002. The scales were accurate to at least 2 grams whilst the density of the fresh water was not considered more different than 1.000 ± 0.002. This accuracy of 1:250 was at least four times the statistical variation in density for individual geologic rock types. All bulk densities presented in other sections of this thesis were determined using the above method.

The gamma ray absorption method was not used because the time and cost of making the equipment was considered excessive when considering the purposes of this project.

Bibliography

Chapell, D.G.: "Gamma-ray attenuation" Nucleonics, 14 No. 1, 40-41. (1956).

Davidson, J.M., Biggar, J.W. and Nielson, D.R.: Gamma Radiation attenuation for measuring bulk density and transient water flow in porous materials. Jour. Geophys. Res. Vol. 68, pp. 4777-4783.

Gurr, C.J. (1962): Use of Gamma Rays in measuring water content and permeability in unsaturated columns of soil. Soil Sc. Vol. 94, No. 4, pp. 224-229.

Gurr, C.J. (1964): Calculation of Soil Water contents from Gamma Ray readings. Aust. Jour. Soil Res. Vol. 2 No. 1, pp. 23-32.

Handbook of Chemistry and Physics. 51st Edition of the Chemical Rubber Company.

Meigh, A.C. and Skipp, B.O. (1960): Gamma Ray and neutron methods of measuring soil density and moisture. Geotechnique, Vol. 10 pp. 110-126.

Price, Horton and Spinney (1957): Radiation Shielding. Pergamon Pr., London.

Soane, B.D.: Dual Energy Gamma Ray transmission for coincident measurement of water content and dry bulk density of soil. Nature Vol. 214, pp. 1273-1274.

Technical Bulletin No. 9, Nuclear-Chicago Corporation, Des Plains, Illinois, (1960).

Van Bavel, C.H.M. (1959): Soil densitometry by Gamma Transmission. Soil Sc. Vol. 87, p. 50.

APPENDIX 9 TABLES OF BULK DENSITY

DIAMOND DRILL HOLE 2200 (APPROX. LENGTH 3250 FT.) N.B.H.C. SECTION 202
DENSITIES COLLECTED AT REGULAR 10 FT. INTERVALS BY H.T.PECANEK
DATA STARTS AT 102 FEET FOR D.D. 2200

2.88	2.89	2.73	2.87	2.84	3.28	3.32	3.30	3.11	3.13
3.06	2.80	2.87	2.88	2.85	2.89	2.90	2.83	2.74	2.79
2.74	2.74	2.82	2.95	2.77	2.85	2.76	2.77	2.86	2.79
2.72	2.74	2.77	2.78	2.80	2.81	2.78	2.77	2.75	2.84
2.77	2.94	2.86	2.76	2.81	2.82	2.80	2.83	2.76	2.79
2.86	2.85	2.75	2.79	2.81	2.84	2.76	2.82	2.88	2.74
2.85	2.85	2.74	2.94	2.88	2.93	2.91	2.77	2.78	2.75
2.99	2.78	2.73	2.77	2.91	2.73	2.82	2.83	2.76	2.88
3.54	2.81	2.79	2.62	2.70	2.80	2.78	2.66	2.87	2.89
2.92	2.94	2.96	2.85	2.88	2.87	2.94	2.83	2.85	2.81
2.97	2.93	2.92	2.94	2.95	2.90	2.94	2.80	2.87	2.91
2.84	2.82	2.83	2.82	2.79	2.89	2.83	2.91	3.00	2.91
2.95	2.84	2.88	2.85	3.05	2.94	2.86	3.01	2.96	2.84
2.88	2.88	2.84	2.77	2.84	2.82	2.97	2.83	2.89	2.86
2.84	2.85	2.78	2.86	2.93	2.96	3.66	2.74	2.88	2.78
2.90	2.86	2.94	2.96	2.72	2.79	2.85	2.96	2.86	2.86
2.83	2.78	2.72	2.71	2.71	2.77	2.73	2.84	2.92	2.84
2.91	2.77	2.87	2.68	2.73	2.76	2.73	2.77	2.72	2.85
2.87	2.76	2.88	2.80	2.85	2.76	2.92	2.96	2.78	2.83
2.83	2.75	2.74	2.76	2.92	2.85	2.74	2.85	2.82	2.86
2.97	2.80	2.85	2.90	2.86	2.69	2.88	2.89	2.76	2.81
2.81	2.75	2.84	2.77	2.79	2.84	2.86	2.84	2.88	2.78
2.84	2.81	2.62	2.75	2.85	2.78	2.87	2.85	2.81	2.79
2.90	2.84	2.77	2.84	2.91	2.81	2.90	2.80	2.81	2.73
2.78	2.77	2.80	2.70	2.79	2.82	2.79	2.82	2.91	2.86
2.80	2.83	2.76	2.79	2.93	2.80	2.76	2.98	2.87	2.85
2.76	2.85	2.72	2.83	2.75	2.74	2.74	2.71	2.82	2.85
2.90	2.75	2.76	2.74	2.79	2.81	2.77	2.67	2.65	2.76
2.72	2.78	2.77	2.84	2.76	2.69	2.69	2.79	2.93	2.81
2.68	2.68	2.69	2.81	3.00	3.38	2.84	2.75	2.78	2.82
2.78	2.81	2.79	2.77	2.84	2.82	2.82	2.80	2.83	2.77
2.77	2.83	2.92	3.19	2.78	2.78	2.83	2.86		

APPENDIX 9

TABLE 1

DIAMOND DRILL 130 N.B.H.C. SECTION 92
DENSITIES ORIGINALLY PRESENTED BY L.A.RICHARDSON- REREAD FROM GRAPHS BY H.T.P.
DATA STARTS AT 120 FEET FOR D.D. 130 ..BAD DATA - 1600 TO 1750 FT. -

2.60	2.92	2.58	2.64	2.70	2.70	2.66	2.74	2.87	2.92
2.64	2.64	2.74	2.74	2.78	2.62	2.78	2.86	2.78	2.72
2.64	2.88	2.71	2.66	2.74	2.65	2.79	2.64	2.78	2.82
2.78	2.80	2.82	2.84	2.78	2.66	2.78	2.57	2.70	2.66
2.62	2.73	2.66	2.68	2.58	2.58	2.78	2.80	2.74	2.74
2.84	2.68	2.62	2.68	2.58	2.68	2.78	2.84	2.80	2.68
2.72	2.68	2.74	2.66	2.78	2.60	2.62	2.80	2.84	2.60
2.74	2.90	2.60	2.62	2.66	2.52	2.62	2.70	2.90	2.78
2.59	2.58	2.92	2.80	2.90	2.66	2.74	2.62	2.68	2.58
2.78	2.58	2.78	2.74	2.64	2.75	2.60	2.72	2.78	2.60
2.72	2.78	2.84	2.66	2.82	2.70	2.78	2.78	2.92	2.82
2.72	2.68	2.80	2.78	2.92	2.66	2.78	2.74	2.70	2.74
2.76	2.72	2.70	2.74	2.68	2.68	2.70	2.73	2.68	2.72
2.68	2.73	2.72	2.74	2.69	2.70	2.76	2.68	2.76	2.72
2.72	2.66	2.70	2.68	2.71	2.71	2.70	2.70	2.68	2.71
2.58	2.62	2.64	2.66	2.58	2.66	2.62	2.64	2.64	2.70
2.70	2.68	2.66	2.68	2.64	2.70	2.64	2.68	2.66	2.70
2.70	2.68	2.66	2.68	2.64	2.70	2.64	2.68	2.66	2.70
2.68	2.78	2.80	2.70	2.66	2.70	2.66	2.78	2.76	2.76
2.80	2.76	2.76	2.80	2.64	2.84	2.86	2.90	2.84	2.58
3.08	2.62	2.84	2.68	2.85	2.86	2.79	2.82	2.86	2.70
2.74	2.72	2.84	3.02	2.70	2.79	3.02	2.96	2.90	2.92
2.76	2.80	2.76	2.88	2.84	2.90	2.78	2.98	3.04	3.30
2.94	3.14	2.76	2.60	2.80	2.76	2.80	2.94	3.40	2.82
2.88	2.88	3.02	3.36	2.92	2.69	2.66	2.84	2.92	2.56
2.72	2.70	2.72	2.84	2.64	2.72	2.66	2.86	2.68	2.64
2.92	2.88	2.74	2.68	2.52	2.90	2.68	2.78	2.82	2.66
2.68	2.64	2.76	2.73	2.82	2.88	2.82	2.70	2.72	2.76
2.66	2.86	2.68	2.70	2.62	2.58	2.94	2.82	2.92	2.86
2.85	2.70	2.60	2.68	2.67	2.66	2.69	2.69	2.68	2.65
2.67	2.69	2.68	2.94	2.84	2.72	2.80	2.90	2.68	2.65
2.94	2.82	2.90	2.76	2.73	2.82	2.88	3.04	3.20	3.02
2.68	2.98	2.96	2.72	2.93	2.98	2.75	2.94	2.84	3.31
2.82	2.86	2.86	2.82	3.03	2.96	3.02	2.97	2.92	2.96
2.86	3.07	2.94	2.78	2.84	2.88	2.94	2.84	2.78	2.78
2.78	2.90	2.94	2.82	2.96	2.88	2.94	2.70	2.92	2.96
2.92	2.78	2.94	2.84	3.32	2.96	2.66	2.78	2.92	2.82
2.84	2.76	2.76	2.78	2.82	2.88	2.74	2.76	2.96	2.78
2.76	2.92	2.94	2.84	2.76	2.96	2.74	2.97	2.88	2.75
2.76	2.83	2.84	2.92	2.78	2.71	2.74	2.78	2.76	2.72
2.64	2.68	2.84	2.94	2.83	2.82	2.79	2.78	2.79	2.79
2.82	2.78	2.78	2.79	2.78	2.72	2.73	2.77	2.68	2.86
3.00	2.98	2.75	3.04	2.74	2.75	2.94	2.84	2.80	2.84
2.78	2.82	2.98	2.92	2.74	2.98	2.90	2.88	2.86	2.91
2.86	2.86	2.92	2.77	3.01	2.87	2.77	2.94	2.68	2.74
2.78	2.68	2.78	2.92	2.86	2.86	2.77	2.78	2.76	2.78
2.78	2.76	3.22	3.07	2.78	2.82	2.64	2.66	2.74	2.81
2.76	2.80	2.77	2.92	2.91	2.83	2.85	2.90	2.84	3.04
2.84	3.00	2.73	2.96	2.83	2.75	2.78	2.77	2.75	2.60

TABLE 2

DENSITIES BROKEN HILL LODE SEQUENCE DATA INTERVAL USUALLY TEN FEET
IND DRILL 142 DENSITIES ORIGINALLY PRESENTED BY L.A.RICHARDSON
STARTS AT 0 FEET FOR D.D. 142

APPENDIX 9

TABLE 3

2.76	2.96	2.85	2.71	2.69	2.81	2.42	2.88	2.93
2.62	2.81	2.84	2.81	2.71	2.90	2.86	2.82	3.00
2.86	2.82	2.96	2.84	3.05	2.96	2.99	2.86	2.87
2.86	2.96	2.93	2.91	2.86	2.68	2.98	2.87	2.86
2.96	2.67	2.83	3.00	2.59	2.64	2.76	2.99	3.00
2.92	2.92	2.92	3.22	3.52	3.06	3.36	2.92	3.29
2.87	2.84	2.86	2.86	2.92	2.96	3.15	2.96	2.96
2.86	2.92	2.87	2.87	3.13	2.93	3.24	3.17	2.74
2.69	2.67	2.70	2.86	3.17	2.76	2.94	2.80	2.98
2.82	2.83	2.87	2.75	2.95	2.83	2.82	2.85	2.86
2.67	2.85	2.92	2.77	2.82	2.83	2.83	2.89	2.83

MOND DRILL 1600(APPROX. LENGTH 5280 FT.) N.B.H.C. SECTION 262
SITIES COLLECTED AT REGULAR 10 FT. INTERVALS BY H.T.PECANEK
A STARTS AT 228 FEET FOR D.D. 1600

TABLE 4

35 2.89	2.84	2.86	2.80	2.77	2.79	2.82	2.77	2.85
33 2.83	2.86	2.76	2.94	2.85	2.86	2.84	2.85	2.71
32 2.87	2.83	2.94	2.81	2.89	2.81	2.81	2.87	2.88
86 2.87	2.87	2.85	2.88	2.91	2.84	2.86	2.83	2.76
79 2.75	2.72	2.72	2.90	2.80	2.79	2.88	2.88	2.72
00 2.72	2.74	2.93	2.70	2.83	2.76	2.97	2.93	2.83
78 2.88	2.84	2.88	2.74	2.84	2.77	2.81	2.84	2.81
80 2.77	2.79	2.71	2.80	2.73	2.80	2.83	2.81	2.78
60 2.91	2.89	2.89	2.81	2.98	2.80	2.78	2.75	2.80
.82 2.77	2.66	2.71	2.70	2.81	2.77	2.87	2.78	2.91
.83 2.73	2.87	2.93	3.14	2.94	2.80	2.83	2.80	3.29
.27 3.27	2.95	2.94	2.93	2.87	2.90	2.74	2.82	2.70
.89 2.83	2.92	2.87	2.92	2.76	2.89	2.86	2.79	2.80
.80 2.81	2.80	2.79	2.92	2.79	2.86	2.87	2.79	2.83
.86 2.88	2.86	2.86	2.77	2.73	2.91	2.77	2.92	2.75
.72 2.85	2.85	2.85	2.82	2.81	2.93	2.71	2.70	2.72
.74 2.82	2.94	2.84	2.71	2.73	2.87	2.97	2.87	2.80
.81 2.90	2.83	2.92	2.81	2.82	2.83	2.83	2.99	3.05
.92 2.86	2.98	3.09	2.97	3.02	2.84	2.83	2.88	2.84
.89 2.88	2.95	2.84	2.94	2.83	2.89	2.77	2.89	2.84
2.77 2.81	2.83	2.85	2.88	2.81	2.94	2.88	3.05	2.79
2.83 2.85	2.86	2.88	2.82	2.88	2.91	3.00	2.95	3.12
2.81 2.78	2.51	2.73	2.73	2.73	2.78	2.78	2.89	2.74
2.77 2.71	2.80	2.76	2.74	2.76	2.72	2.84	2.91	2.77
2.71 2.69	2.88	2.95	2.78	3.46	2.93	2.86	2.74	2.72
2.75 2.73	2.80	2.75	2.87	2.74	2.81	2.80	2.73	2.90
2.71 2.94	2.73	2.86	3.00	2.73	2.74	2.79	2.79	2.72
2.43 2.76	2.87	2.94	2.91	2.74	2.91	2.87	2.83	2.77
2.84 2.85	2.75	2.81	2.86	2.93	2.84	2.88	2.87	2.89
2.82 2.84	2.81	2.79	2.83	2.86	2.89	2.82	2.91	2.79
2.80 2.93	2.88	2.94	2.91	2.82	2.80	2.76	2.84	2.94
2.84 2.74	2.86	2.90	2.89	2.89	2.78	2.76	2.84	2.79
2.75 2.74	2.79	2.78	2.82	2.79	2.76	2.81	2.90	2.92
2.83 2.97	2.83	2.77	2.75	2.86	2.77	2.97	2.91	2.87
2.88 2.84	2.96	2.95	2.91	2.87	2.73	2.75	2.73	2.71
2.79 2.79	2.88	2.86	2.69	2.83	2.74	2.88	2.73	2.98
2.79 2.78	2.79	2.81	3.05	2.87	2.74	2.95	2.81	2.82
2.80 2.81	2.95	2.75	2.84	2.94	2.84	3.04	2.80	2.90
3.10 2.79	2.92	2.83	2.83	2.83	2.81	2.80	2.91	2.83
2.82 2.84	2.86	2.83	2.83	2.80	2.74	2.82	2.78	2.80
2.80 2.78	3.16	2.97	2.85	2.83	2.76	2.81	2.81	2.81
2.80 2.76	2.70	2.73	2.73	2.75	2.74	2.74	2.73	2.76
2.72 2.73	2.94	2.88	2.86	2.94	2.98	2.76	2.84	2.72
2.94 2.73	2.71	2.84	2.73	2.91	2.76	2.78	2.67	2.78
2.81 2.92	2.94	2.88	2.72	2.72	2.86	2.86	2.96	2.83
2.77 2.74	2.79	2.61	2.82	2.87	2.75	2.80	2.93	3.01
3.08 2.93	2.83	2.89	2.84	2.88	2.88	2.88	2.78	2.88
2.82 2.77	2.77	2.85	2.89	2.73	2.91	2.87	3.16	3.27
3.24 2.85	2.88	2.84	2.94	2.93	2.92	2.82	2.89	2.91
2.77 2.80	2.91	2.82	2.86	2.88	2.80	2.86	2.88	2.76
2.91 2.86	2.85	2.93	2.89	2.87	2.86	2.90	2.92	2.93

APPENDIX 9

TABLE 5

n DRILL 131 SECTION 62 THROUGH B.H. OREBODY
IES ORIGINALLY PRESENTED BY L.A.RICHARDSON- REREAD FROM GRAPHS BY H.T.P.
TARTS AT 10 FEET FOR D.D. 131

2.99	3.00	2.92	2.86	2.99	3.00	2.99	2.71	2.74
2.72	2.79	2.80	2.92	2.80	2.66	2.90	2.78	3.00
2.88	3.38	3.32	2.78	2.93	4.28	3.88	3.21	3.17
3.86	4.12	3.09	3.70	3.66	3.33	3.11	3.50	2.88
4.00	4.00	3.66	2.86	3.66	3.75	3.29	3.33	3.84
3.71	3.79	3.64	4.00	4.16	3.49	3.00	3.26	3.18
3.00	3.17	3.00	3.27	3.00	3.15	2.89	2.85	3.10
3.10	3.50	3.00	3.51	3.36	3.18	3.34		

TABLE 6

ND DRILL 92 SECTION 62 THROUGH B.H. OREBODY
TIES ORIGINALLY PRESENTED BY L.A.RICHARDSON- REREAD FROM GRAPHS BY H.T.P.
STARTS AT 60 FEET FOR D.D. 92

3.01	3.17	3.11	3.08	2.93	3.09	2.93	2.90	2.91
2.86	2.70	2.80	3.01	2.78	2.93	3.50	3.31	3.20
3.50	3.01	2.94	3.62	4.24	3.76	3.50	3.38	3.87
3.81	4.42	4.00	4.33	3.01	3.08	3.60	3.86	3.74
4.00	3.94	4.62	3.18	3.43	3.75	4.37	3.01	3.42
3.70	3.31	3.26	3.86	3.27	3.23	2.91	3.33	3.10
3.25	3.30	2.94	3.20	3.30	3.18	3.34	3.20	3.62
3.18	3.10							

TABLE 7

AOND DRILL 110 SECTION 62 THROUGH B.H. OREBODY
SITIES ORIGINALLY PRESENTED BY L.A.RICHARDSON- REREAD FROM GRAPHS BY H.T.P.
A STARTS AT 10 FEET FOR D.D. 110

7	3.44	3.29	3.18	3.35	2.70	2.75	3.31	4.19	3.23
8	3.85	2.93	3.00	3.85	3.31	2.90	4.00	0.00	4.00
8	3.22	3.21	3.06	2.93	2.90	3.09	2.76	3.24	3.19
0	3.43	3.43	3.21	3.16	2.74	3.09	3.00	2.74	2.99
6	3.09	0.00	3.07	3.10	2.80	0.00	2.90	3.00	2.90
9	2.78	2.82	3.30	3.23	3.27	2.84	2.80	3.10	2.74
2	2.92	2.68	2.74	2.75	2.78	2.93	2.55	2.87	3.44
1	2.70	2.76	2.78	2.68	2.67	2.54	2.94	2.68	2.68

TABLE 8

AMOND DRILL 41 SECTION 62 THROUGH B.H. OREBODY
NSITIES ORIGINALLY PRESENTED BY L.A.RICHARDSON- REREAD FROM GRAPHS BY H.T.P.
TA STARTS AT 160 FEET FOR D.D. 41

30	3.34	3.10	3.17	2.92	2.93	3.78	2.81	3.01	2.70
88	2.83	0.00	0.00	0.00	3.00	3.31	3.08	2.90	2.92
82	3.06	3.20	3.66	0.00	0.00	2.86	3.00	2.99	2.76
93	2.61	3.01	2.99	3.00	3.10	3.19	2.83	2.98	2.94
16	2.92	3.29	3.00	3.18	3.72	3.00	3.62	3.60	3.26

TABLE 9

IAMOND DRILL 18A SECTION 62 THROUGH B.H. OREBODY
ENSITIES ORIGINALLY PRESENTED BY L.A.RICHARDSON- REREAD FROM GRAPHS BY H.T.P.
ATA STARTS AT 10 FEET FOR D.D. 18 A

2.86	2.84	2.72	2.86	2.80	2.76	2.81	2.59	2.78	2.92
2.62	2.72	2.55	2.54	2.58	2.52	2.90	2.84	2.90	2.78
2.86	2.79	2.64	2.92	2.86	0.00	0.00	2.71	2.85	2.78
2.64	2.73	2.60	2.42	2.57	2.77	2.81	2.86	2.91	2.77
2.78	2.78	2.92	2.85	2.53	2.80	3.16	2.73	2.76	0.00
2.85	2.99	2.70	2.74	2.70	2.77	2.79	2.79	2.59	2.80
2.40	2.62	2.90	2.80	2.80	2.85	2.83	3.06	3.00	2.80
2.87	2.74	2.94	4.12	3.36	2.92	3.17	2.88	2.80	3.50
2.65	2.65	3.68	2.66	2.85	2.86	2.77	2.76	2.79	2.76
2.91	2.82	2.80	2.68	2.78	2.70	2.78	2.66	2.82	2.81
2.91	2.69	2.80	2.90	2.76	2.86	2.84	2.70	2.80	2.74
2.91	2.90	2.99	2.93	2.90	2.72	3.07	2.86	2.73	2.91
2.92	2.87	3.05	2.77	3.15	2.74	2.80	2.83	2.80	2.99
3.00	2.99	2.62	3.04	2.79	2.93	2.91	2.59	3.06	2.86
2.85	3.06	2.73	2.66	2.80	2.90	2.85	2.85	3.03	3.00
2.99	3.06	2.80	2.78	2.98	2.98	2.94	2.92	3.66	4.12
3.66	3.20	2.77	4.55	3.16	3.36	3.33	3.58	3.98	3.54
2.76	3.86	2.56	0.00	2.72	2.86	3.88	2.92	2.80	3.69
2.82	2.79	2.80	2.82	2.85	2.72	2.91	2.84	2.76	2.80
2.80	2.75	2.64							

DIAMOND DRILL 85 N.B.H.C. SECTION 92
DENSITIES ORIGINALLY PRESENTED BY L.A.RICHARDSON- REREAD FROM GRAPHS BY H.T.P.
DATA STARTS AT 170 FEET FOR D.D. 85

2.74	2.86	2.76	2.83	2.82	2.82	2.89	2.77	2.66	2.74
2.84	2.82	2.70	2.87	2.76	2.72	2.67	2.72	2.84	2.83
2.82	2.72	2.86	2.68	2.74	2.83	2.87	2.74	3.00	2.98
2.76	2.86	3.00	2.83	2.68	2.79	2.71	2.77	2.79	2.73
2.76	2.76	3.00	2.74	2.65	2.88	2.83	2.76	3.20	3.82
2.86	2.82	2.76	3.00	2.94	2.96	2.96	3.00	3.06	2.92
2.89	3.16	2.93	2.93	3.00	3.14	2.90	3.00	2.72	2.82
3.06	2.88	3.01	2.66	2.94	2.73	2.89	2.94	2.72	2.73
2.83	2.77	2.93	2.88	2.78	2.80	2.79	2.73	2.71	2.70
2.82	2.74	2.72	2.74	2.76	2.77	2.81	2.79	2.76	2.76
2.73	2.79	2.82	2.83	2.78	2.82	2.67	3.00	2.94	3.26
2.75	2.73	2.74	2.73	2.71	2.78	2.69	2.88	2.82	2.86
2.70	2.94	2.64	2.61	2.70	2.84	3.02	2.77	2.70	2.78
2.88	2.94	2.74	2.70	2.83	2.74	2.73	2.70	2.74	2.78
2.82	2.88	3.10	2.76	2.66	2.82	2.74	2.94	2.68	2.73
2.71	2.93	2.85	2.74	2.81	2.78	2.81	2.82	2.72	2.88
3.06	2.94	3.02	2.88	2.86	2.60	2.76	2.94	2.88	2.82
3.00	2.70	3.06	2.53	2.83	2.74	2.66	2.95	2.62	2.94
3.07	2.90	2.86	2.83	3.24	3.08	2.94	3.08	2.83	2.94
2.70	2.74	2.72	2.86	2.98	2.90	2.84	3.01	2.91	2.86
3.07	2.75	2.66	2.83	2.91	3.01	2.86	3.00	2.54	2.81
2.86	3.22	2.74	2.82	2.86	2.84	2.86	2.90	2.86	2.82
2.64	2.90	3.40	2.83	2.92	2.84	3.26	3.22	2.94	3.57
3.28	2.90	3.24	3.34	3.12	3.00	2.66	2.83	2.92	3.30
3.40	3.12	2.83	2.81	2.88	2.97	2.90	2.86	3.22	2.91
2.90	3.22	2.86	2.76	2.91	2.99	2.77	2.90	3.38	4.42
3.10	3.00	3.08	2.94	2.91	2.93	2.87	2.95	3.00	3.28
2.84	2.66	2.91	3.00	2.75	2.75	2.84	2.85	2.35	3.00
2.92	4.28	3.26	3.08	2.87	2.92	3.78	3.06	3.10	2.92
3.25	3.26	2.92	3.27	3.16	2.85	3.08	3.16	3.30	3.00
3.40	3.16	3.44	3.10	2.62	2.86	2.70	3.18	2.71	2.86
2.82	3.01	3.20	3.02	2.90	2.92	2.90	3.00	3.22	2.89
2.90	3.01								

APPENDIX 9

TABLE 10

DIAMOND DRILL 2310 N.B.H.C. SECTION 84 ONLY PART THROUGH LOWER (EAST) AMPHIBO
DENSITIES COLLECTED AT REGULAR 10 FT. INTERVALS BY H.T.PECANEK
DATA STARTS AT 1500 FEET FOR D.D.2310

2.88	2.63	2.87	2.81	3.00	2.95	2.90	2.91	2.88	3.17
3.16	3.19	3.22	3.16	3.20	3.19	3.26	3.18	3.20	3.21
3.21	3.14	3.25	3.28	3.26	3.21	3.22	3.21	3.17	3.21
3.21	3.23	2.79	2.88	2.87	3.21	3.21	3.10	3.20	3.26
3.22	3.24	3.26	3.23	3.23	3.06	2.81	3.21	3.07	3.07
2.80	3.00	3.26	3.28	2.84	2.81	2.83	2.84	2.92	2.86
2.82	3.22	2.85	2.83	2.76	2.73	2.74	2.72	2.74	2.73
2.76	2.71	3.09	2.76	2.73	2.76	2.79	2.80	2.77	2.70
3.10	2.76	2.79	2.67	2.78	3.03	2.90	2.98	2.97	3.00
3.02	3.06	3.05	2.70	2.87	2.95				

TABLE 11

DIAMOND DRILL 178 SECTION 62 THROUGH B.H. OREBODY
DENSITIES ORIGINALLY PRESENTED BY L.A.RICHARDSON- REREAD FROM GRAPHS BY H.T.P.
DATA STARTS AT 10 FEET FOR D.D. 178

3.16	2.90	2.84	2.76	2.81	3.00	2.80	3.01	2.86	3.10
2.84	2.74	2.78	3.20	2.77	2.90	2.87	2.97	2.86	2.87
2.92	2.78	2.83	2.86	3.06	2.80	2.78	2.84	2.88	2.86
2.89	2.86	2.85	2.85	2.95	2.83	2.96	2.88	2.81	2.86
2.66	2.54	2.63	2.90	2.89	2.83	2.85	2.87	2.70	2.94
2.63	3.08	3.20	3.02	3.03	2.95				

APPENDIX 9
TABLE 12

DIAMOND DRILL 144 SECTION 62 THROUGH B.H. OREBODY
DENSITIES ORIGINALLY PRESENTED BY L.A.RICHARDSON- REREAD FROM GRAPHS BY H.T.P.
DATA STARTS AT 10 FEET FOR D.D. 144

2.88	2.81	2.77	2.88	2.84	3.19	2.87	2.83	2.74	2.79
2.78	2.64	2.78	2.66	2.66	2.66	2.93	2.90	2.88	2.96
2.87	2.93	2.87	2.86	3.06	2.94	3.07	3.86	3.26	3.67
2.94	2.83	3.03	3.60	3.01	3.30	2.67	2.62	2.57	3.03
3.24	2.84	3.21	3.43	2.87	2.87	2.78	2.77	2.87	2.94
2.78	2.64	2.66	2.79	3.11	2.66	3.14	3.26	2.94	3.35
2.88	3.08	2.83	2.86	2.94	3.38	2.94	2.94	2.96	3.06
2.98	2.84	2.98	3.08	2.98	2.73	2.84	3.06		

TABLE 13

DIAMOND DRILL 15 SECTION 62 THROUGH B.H. OREBODY
DENSITIES ORIGINALLY PRESENTED BY L.A.RICHARDSON- REREAD FROM GRAPHS BY H.T.P.
DATA STARTS AT 10 FEET FOR D.D. 15

3.07	2.82	2.90	2.90	2.92	2.98	2.84	2.90	3.09	2.68
2.82	2.74	2.68	3.17	2.83	2.75	2.78	2.92	2.64	2.75
3.17	2.92	2.91	2.86	2.76	3.29	3.70	3.00	3.10	3.18
3.61	3.00	3.00	3.06	3.09	3.33	3.36	4.00	2.74	3.71
3.09	3.32	3.08	3.62	3.01	3.30	3.36	3.30	3.75	2.79
3.00	3.01	3.30	2.80	2.67	3.01	3.18	2.94	3.16	3.86

TABLE 14

APPENDIX 10 TABLES OF BOUGUER VALUES AND SUBORDINATE DATA

APPENDIX 10

TABLE 1

```
**********************************************************************************
CALITY NAME   ...  FLYING DOCTOR REGIONAL GRAVITY TRAVERSE 1973
ATION SPACING...  FOUR HUNDRED FEET
EVATION CONTROL.  STAFF AND LEVEL.LINE RELATED TO BMS BY STAFF AND LEVEL ALSO
SITIONAL CONTROL  THEODOLITE ST. LINE BET. BASE STATIONS FIXED BY AIRPHOTOS
ID REFERENCE ...  U.T.M. AUSTRALIAN MAP GRID
AVITY METER  ...  WORDEN 368  K=0.0981  OPERATED BY H.T.PECANEK
UGUER DENSITY 1.  2.70 GRAM/ML
UGUER DENSITY 2.  2.40 GRAM/ML
SERVED GRAVITY..  ADD 979000.0 MILLIGALS
ATITUDE       ...  IN RADIANS
EDUCTION      ...  FROM RAW GRAVITY BY H.T.PECANEK
**********************************************************************************
```

TATION	ABS.GRAV.	ELEVATION	NORTHING	EASTING	LATITUDE	BOUGUER 1	BOUGUER 2
FDB001	456.44	820.2	6467068.	550561.	-.5573020	14.09	17.23
FDB002	456.36	820.5	6466974.	550635.	-.5573170	13.96	17.10
FDB003	456.34	821.7	6466879.	550709.	-.5573320	13.94	17.09
FDB004	456.40	823.9	6466785.	550783.	-.5573460	14.06	17.22
FDB005	456.75	824.5	6466690.	550858.	-.5573610	14.38	17.54
FDB006	456.71	827.0	6466595.	550932.	-.5573760	14.42	17.59
FDB007	456.69	827.6	6466501.	551006.	-.5573910	14.37	17.54
FDB008	456.75	830.0	6466406.	551080.	-.5574050	14.51	17.69
FDB009	457.00	830.6	6466311.	551154.	-.5574200	14.72	17.91
FDB010	457.14	830.8	6466217.	551228.	-.5574360	14.80	17.98
FDB011	457.44	835.4	6466122.	551302.	-.5574500	15.31	18.51
FDB012	457.75	842.9	6466028.	551376.	-.5574650	16.00	19.23
FDB013	458.02	843.6	6465933.	551450.	-.5574800	16.24	19.47
FDB014	458.32	843.0	6465838.	551524.	-.5574950	16.43	19.66
FDB015	458.42	847.1	6465744.	551599.	-.5575090	16.71	19.95
FDB016	458.60	845.2	6465649.	551673.	-.5575240	16.71	19.95
FDB017	458.69	846.1	6465554.	551747.	-.5575390	16.78	20.03
FDB018	458.51	846.5	6465460.	551821.	-.5575540	16.56	19.80
FDB019	458.23	848.7	6465365.	551895.	-.5575690	16.34	19.59
FDB020	458.32	851.7	6465271.	551969.	-.5575840	16.54	19.80
FDB021	458.31	855.5	10000000.	500000.	-.5575990	16.69	19.97
FDB023	457.89	873.4	6464987.	552191.	-.5576280	17.20	20.54
FDB024	457.61	873.7	6464892.	552265.	-.5576430	16.86	20.21
FDB025	457.58	877.7	6464798.	552340.	-.5576580	17.00	20.37
FDB026	457.07	884.3	6464703.	552414.	-.5576730	16.82	20.20
FDB027	456.80	889.9	6464608.	552488.	-.5576880	16.81	20.22
FDB028	456.34	896.0	6464514.	552562.	-.5577020	16.65	20.09
FDB029	456.05	900.4	6464419.	552636.	-.5577170	16.56	20.01
FDB030	456.14	904.9	6464324.	552710.	-.5577330	16.84	20.30
FDB031	455.97	911.2	6464230.	552784.	-.5577470	16.98	20.47
FDB032	455.76	916.4	6464135.	552858.	-.5577610	17.01	20.52
FDB033	455.73	920.7	6464041.	552932.	-.5577770	17.17	20.69
FDB034	455.35	926.1	6463946.	553007.	-.5577920	17.03	20.58
FDB035	454.74	931.7	6463851.	553081.	-.5578060	16.70	20.27
FDB036	454.26	936.6	6463757.	553155.	-.5578210	16.44	20.03
FDB037	453.81	947.7	6463662.	553229.	-.5578360	16.58	20.21
FDB038	453.39	953.4	6463567.	553303.	-.5578510	16.43	20.08
FDB039	451.67	977.3	6463473.	553377.	-.5578650	16.07	19.82
FDB040	451.43	980.4	6463378.	553451.	-.5578800	15.94	19.70
FDB041	451.46	978.7	6463284.	553525.	-.5578950	15.81	19.56
FDB042	450.98	988.3	6463189.	553599.	-.5579100	15.83	19.61
FDB043	451.90	974.6	6463094.	553673.	-.5579250	15.86	19.60
FDB044	455.69	911.8	6463000.	553748.	-.5579400	15.84	19.33
FDB046	454.36	938.5	6462811.	553896.	-.5579690	15.96	19.56
FDB047	450.94	995.8	6462716.	553970.	-.5579840	15.89	19.71
FDB048	447.30	1057.9	6462621.	554044.	-.5579990	15.88	19.93
FDB049	446.58	1072.3	6462527.	554118.	-.5580140	15.95	20.06
FDB051	445.01	1089.1	6462337.	554266.	-.5580440	15.24	19.42
FDB052	446.25	1078.8	6462243.	554340.	-.5580580	15.80	19.94
FDB053	448.04	1055.1	6462148.	554414.	-.5580730	16.11	20.15

APPENDIX 10

TABLE 1 (contd.)

FDB054	450.14	1022.1	6462054.	554489.	-.5580880	16.17	20.09
FDB055	450.91	1012.5	6461959.	554563.	-.5581030	16.30	20.18
FDB056	452.05	987.5	6461864.	554637.	-.5581180	15.89	19.67
FDB057	448.76	1047.5	6461770.	554711.	-.5581330	16.10	20.11
FDB058	451.75	998.8	6461675.	554785.	-.5581480	16.12	19.95
FDB059	454.40	960.4	6461581.	554859.	-.5581620	16.41	20.09
FDB060	455.27	947.6	6461486.	554933.	-.5581770	16.45	20.08
FDB061	456.75	930.2	6461391.	555007.	-.5581920	16.83	20.39
FDB062	457.69	919.5	6461297.	555081.	-.5582070	17.06	20.58
FDB064	458.51	925.3	6461107.	555230.	-.5582360	18.09	21.64
FDB065	458.49	918.0	6461013.	555304.	-.5582510	17.57	21.08
FDB066	457.78	926.6	6460918.	555378.	-.5582660	17.30	20.85
FDB067	457.44	932.6	6460824.	555452.	-.5582810	17.25	20.82
FDB068	457.59	934.7	6460729.	555526.	-.5582960	17.45	21.03
FDB069	457.26	942.2	6460634.	555600.	-.5583110	17.50	21.11
FDB070	458.77	925.4	6460540.	555674.	-.5583260	17.94	21.48
FDB071	458.61	924.8	6460445.	555748.	-.5583400	17.68	21.22
FDB072	459.05	920.2	6460350.	555822.	-.5583550	17.77	21.30
FDB073	459.84	911.6	6460256.	555897.	-.5583700	17.98	21.47
FDB074	459.60	908.6	6460161.	555971.	-.5583850	17.50	20.98
FDB075	459.22	907.5	6460067.	556045.	-.5584000	16.98	20.46
FDB076	459.17	908.6	6459972.	556119.	-.5584140	16.93	20.41
FDB077	459.14	915.2	6459877.	556193.	-.5584300	17.22	20.72
FDB078	458.61	916.7	6459783.	556267.	-.5584440	16.71	20.23
FDB079	458.72	923.1	6459688.	556341.	-.5584590	17.14	20.67
FDB080	458.38	929.3	6459594.	556415.	-.5584740	17.10	20.66
FDB081	458.00	933.3	6459499.	556489.	-.5584890	16.88	20.46
FDB082	457.81	938.7	6459404.	556563.	-.5585040	16.95	20.54
FDB083	457.35	939.3	6459310.	556638.	-.5585180	16.46	20.06
FDB084	457.49	935.9	6459215.	556712.	-.5585330	16.32	19.91
FDB085	457.04	941.1	6459120.	556786.	-.5585480	16.12	19.72
FDB086	456.31	948.2	6459026.	556860.	-.5585630	15.74	19.37
FDB087	456.17	946.2	6458931.	556934.	-.5585780	15.41	19.03
FDB088	456.17	941.5	6458837.	557008.	-.5585920	15.06	18.67
FDB089	455.80	944.9	6458742.	557082.	-.5586070	14.83	18.45
FDB090	455.76	950.2	6458647.	557156.	-.5586220	15.03	18.67
FDB091	455.77	957.7	6458553.	557230.	-.5586370	15.42	19.09
FDB092	455.62	963.4	6458458.	557304.	-.5586520	15.54	19.23
FDB093	455.86	966.2	6458363.	557379.	-.5586670	15.88	19.58
FDB094	455.30	984.0	6458269.	557453.	-.5586820	16.31	20.08
FDB095	455.88	996.7	6458174.	557527.	-.5586970	17.58	21.39
FDB096	453.41	1009.9	6458080.	557601.	-.5587110	15.83	19.70
FDB097	453.91	1000.1	6457985.	557675.	-.5587260	15.67	19.51
FDB098	454.34	987.5	6457926.	557721.	-.5587350	15.31	19.10

APPENDIX 10

TABLE 2

```
NAME  ...  COPPER BLOW AND BEYOND  FROM THE B.H. AIRPORT
PACING...  ONE MILE  BROADSCALE REGIONAL TYPE
I CONTROL.  ROVING BAROMETER  CENTRAL BAR. TIE TO GALENA HILL GRID
AL CONTROL  EACH STATION LOCATED ON Z.C. AIRPHOTOS THEN ON BASE MAP
ERENCE ...  U.T.M. AUSTRALIAN MAP GRID
METER  ...  CG-2 NO. 274  K=0.10035 OPERATED BY T.V.HARVEY MINES EXPLOR
DENSITY 1.  2.70 GRAM/ML
DENSITY 2.  2.40 GRAM/ML
 GRAVITY..  ADD 979000.0 MILLIGALS
       ...  IN RADIANS
N      ...  FROM RAW GRAVITY BY H.T.PECANEK
```

	ABS.GRAV.	ELEVATION	NORTHING	EASTING	LATITUDE	BOUGUER 1	BOUGUER 2
	459.60	905.0	6458290.	544110.	-.5586890	15.87	19.34
	463.77	928.0	6456740.	544470.	-.5589320	20.28	23.84
	465.77	928.0	6455500.	545120.	-.5591270	21.38	24.93
	464.93	938.0	6454230.	545680.	-.5593270	20.20	23.80
	465.13	938.0	6452810.	545820.	-.5595500	19.37	22.96
	468.25	861.0	6451310.	546310.	-.5597860	16.80	20.10
	468.32	876.0	6449960.	546640.	-.5599990	16.78	20.13
3	470.33	829.0	6448810.	547010.	-.5601790	15.15	18.33
9	473.20	767.0	6447440.	547820.	-.5603940	13.33	16.27
0	476.36	731.0	6445930.	548460.	-.5606320	13.24	16.04
1	478.41	710.0	10000000.	500000.	-.5608450	13.05	15.77
2	479.15	668.0	6443220.	549230.	-.5610580	10.29	12.85
3	480.18	667.0	6441720.	549610.	-.5612930	10.17	12.73
4	482.10	636.0	6440430.	550060.	-.5614970	9.29	11.73
5	482.66	617.0	6439060.	550740.	-.5617120	7.72	10.08
6	485.65	597.0	6437850.	551360.	-.5619020	8.64	10.92
17	488.95	566.0	6436210.	552180.	-.5621590	8.89	11.06
18	492.35	567.0	6435210.	552910.	-.5623160	11.62	13.79
19	495.37	559.0	6434140.	553500.	-.5624840	13.38	15.52
20	498.19	530.0	6433280.	554750.	-.5626190	13.84	15.87

TABLE 3

```
LITY NAME  ...  BROKEN HILL AIRPORT
OSE        ...  FILL IN BET. O.WEISS DATA--ESP. O.W. PROFILE 1A
ION SPACING...  VARIABLE  STNS. ALONG RUNWAYS AND PERIFERAL
ATION CONTROL.  D. OF CIVIL AVIATION B.MS. --FEW PERIFERAL BAROMETRIC HGHTS
TIONAL CONTROL  D.C.A. COORDINATES TRANSFORMED BY H.T.P. TO U.T.M. A.M.G.
 REFERENCE ...  U.T.M. AUSTRALIAN MAPGRID
ITY METER  ...  WORDEN 368 K=0.0981 OPERATED BY H.T.PECANEK
GUER DENSITY 1.  2.70 GRAM/ML.
GUER DENSITY 2.  2.40 GRAM/ML.
ERVED GRAVITY..  ADD 979000.0 MILLIGALS
ITUDE      ...  IN RADIANS
UCTION     ...  FROM RAW GRAVITY BY H.T.PECANEK
```

TION	ABS.GRAV.	ELEVATION	NORTHING	EASTING	LATITUDE	BOUGUER 1	BOUGUER 2
R001	453.02	952.7	6459868.	545029.	-.5584390	13.29	16.94
R011	455.35	930.7	6459306.	544283.	-.5585280	13.90	17.46
R010	455.19	931.6	6459367.	544548.	-.5585190	13.83	17.40
IR013	454.76	935.5	6459452.	544582.	-.5585050	13.70	17.28
IR015	454.46	937.3	6459544.	544643.	-.5584910	13.57	17.16
IR014	453.87	942.5	6459683.	544733.	-.5584690	13.39	17.00
IR006	456.79	915.6	6458994.	545578.	-.5585770	14.21	17.72
IR002	454.90	935.6	6459444.	544839.	-.5585060	13.84	17.43
IR008	455.48	935.1	6459271.	544994.	-.5585330	14.27	17.85
IR0RP	456.30	924.6	6459106.	544634.	-.5585600	14.34	17.88
AIR003	456.49	922.8	6459063.	544586.	-.5585660	14.39	17.93
AIR009	454.55	950.3	6459487.	545560.	-.5584990	14.40	18.04
AIR004	458.30	912.3	6458682.	544333.	-.5586270	15.29	18.79
AIR0CR	459.14	904.0	6458374.	544119.	-.5586760	15.41	18.87
AIR004	458.30	912.3	6458682.	544333.	-.5586270	15.29	18.79
AIR0.3	456.96	940.0	6459059.	543806.	-.5585680	15.88	19.48
AIR0DR	460.43	907.5	6458205.	544683.	-.5587010	16.79	20.27
AIR0.2	462.07	914.0	6457932.	544854.	-.5587440	18.62	22.12
AIR0GA	463.05	950.0	6457281.	545385.	-.5588470	21.27	24.91
AIR00C	462.93	955.0	6457863.	544614.	-.5587550	21.87	25.53

APPENDIX 10 TABLE 4

ALITY NAME ... SILVERTON HIGHWAY REGIONAL GRAVITY TRAVERSE OCTOBER 1973
TION SPACING... HALF MILE EVERY SECOND STN. NEXT TO MILE POST
VATION CONTROL. BAROMTRIC--BH END TIED TO BM..SILV. END TIED TO RLY APPROX.
ITIONAL CONTROL EACH STATION FIXED ON Z.C. AIRPHOTO THEN ON BASE MAP TRANSP
D REFERENCE ... U.T.M. AUSTRALIAN MAP GRID
VITY METER ... WORDEN 368 K=0.0981 OPERATED BY H.T.PECANEK
GUER DENSITY 1. 2.70 GRAM/ML
GUER DENSITY 2. 2.40 GRAM/ML
ERVED GRAVITY.. ADD 979000.0 MILLIGALS
ITUDE ... IN RADIANS
DUCTION ... FROM RAW GRAVITY BY H.T.PECANEK

ATION	ABS.GRAV.	ELEVATION	NORTHING	EASTING	LATITUDE	BOUGUER 1	BOUGUER 2
ILV01	448.62	1005.0	6463970.	541570.	-.5577960	14.99	18.84
ILV02	445.80	1027.0	6464389.	541010.	-.5577300	13.79	17.72
ILV03	446.58	1003.0	6464968.	540510.	-.5576390	13.56	17.40
ILV04	444.61	1020.0	6465646.	539818.	-.5575330	13.09	17.00
ILV05	444.43	1017.0	6466060.	539066.	-.5574680	13.04	16.93
ILV06	443.76	1024.0	6466560.	538358.	-.5573900	13.14	17.07
ILV07	442.42	1039.0	6466828.	537778.	-.5573480	12.89	16.87
ILV08	441.81	1039.0	6467247.	537080.	-.5572830	12.58	16.56
ILV09	443.56	1001.0	6467525.	536267.	-.5572400	12.27	16.10
SILV10	446.06	981.0	6467798.	535538.	-.5571970	13.78	17.53
SILV11	446.95	952.0	6468111.	534901.	-.5571480	13.17	16.81
SILV12	448.14	927.0	6468490.	534177.	-.5570890	13.14	16.69
SILV13	448.52	922.0	6468889.	533460.	-.5570260	13.51	17.05
SILV14	448.52	914.0	6469075.	532670.	-.5569970	13.17	16.67
SILV15	447.91	920.0	6469192.	531778.	-.5569790	13.00	16.53
SILV16	448.64	900.0	6469525.	531030.	-.5569270	12.78	16.23
SILV17	448.78	889.0	6469731.	530323.	-.5568950	12.41	15.82
SILV18	448.59	895.0	6470030.	529621.	-.5568480	12.80	16.23
SILV19	448.52	893.0	6470292.	528939.	-.5568080	12.80	16.22
SILV20	448.73	894.0	6470641.	528025.	-.5567530	13.32	16.74
SILV21	448.29	877.0	6470924.	527364.	-.5567080	12.08	15.44
SILV22	449.91	851.0	6471234.	526555.	-.5566600	12.37	15.63
SILV23	449.65	857.0	6471435.	525885.	-.5566290	12.61	15.89
SILV24	451.26	834.0	6471525.	524997.	-.5566150	12.91	16.11
SILV25	451.87	807.0	6471580.	524200.	-.5566060	11.96	15.05
SILV26	451.15	803.0	6471680.	523315.	-.5565910	11.07	14.14
SILV27	451.34	795.0	6471860.	522530.	-.5565630	10.91	13.96
SILV28	451.02	785.0	6472025.	521840.	-.5565370	10.12	13.12
SILV29	450.21	790.0	6472145.	521105.	-.5565180	9.69	12.72
SILV30	449.74	790.0	6472230.	520405.	-.5565050	9.28	12.31

TABLE 5

LOCALITY NAME ... PURNAMOOTA HOMESTEAD-BROKEN HILL MAIN ACCESS ROAD MAY 1973
STATION SPACING... ONE MILE BROADSCALE REGIONAL TYPE
ELEVATION CONTROL. BAROMETRIC -ROVING BAROMETER ONLY
POSITIONAL CONTROL EACH STATION LOCATED ON Z.C. AIRPHOTOS THEN ON BASE MAP
GRID REFERENCE ... U.T.M. AUSTRALIAN MAP GRID
GRAVITY METER ... CG-2 NO. 274 K=0.10035 OPERATED BY T.V.HARVEY MINES EXPLOR
BOUGUER DENSITY 1. 2.70 GRAM/ML
BOUGUER DENSITY 2. 2.40 GRAM/ML
OBSERVED GRAVITY.. ADD 979000.0 MILLIGALS
LATITUDE ... IN RADIANS
REDUCTION ... FROM RAW GRAVITY BY H.T.PECANEK

STATION	ABS.GRAV.	ELEVATION	NORTHING	EASTING	LATITUDE	BOUGUER 1	BOUGUER 2
PU01	442.67	1054.0	6466400.	541800.	-.5574130	13.74	17.77
PU02	443.26	1024.0	6467130.	541180.	-.5572980	13.07	16.99
PU03	443.24	1001.0	6468590.	540870.	-.5570690	12.74	16.58
PU04	443.48	983.0	6469930.	540420.	-.5568580	12.89	16.65
PU05	443.33	973.0	6471400.	540105.	-.5566270	13.21	16.94
PU06	443.61	949.0	6472900.	540420.	-.5563910	13.15	16.79
PU07	444.10	939.0	6474290.	540770.	-.5561720	14.06	17.66
PU08	444.43	916.0	6475670.	541060.	-.5559540	14.03	17.54
PU09	443.90	934.0	6477240.	541070.	-.5557070	15.72	19.29
PU10	441.46	904.0	6478743.	540985.	-.5554700	12.58	16.05
PU11	441.46	914.0	6480320.	541120.	-.5552220	14.33	17.83
PU12	438.14	951.0	6481210.	540280.	-.5550820	13.86	17.50
PU13	437.43	944.0	6482660.	540470.	-.5548540	13.79	17.40
PU14	433.34	986.0	6484230.	540330.	-.5546070	13.34	17.12
PU15	431.05	995.0	6485560.	540270.	-.5543970	12.56	16.37
PU16	427.04	1029.0	6486940.	539470.	-.5541800	11.58	15.52
PU17	421.65	1123.0	6488280.	539130.	-.5539700	12.76	17.06
PU18	419.66	1114.0	6489290.	538280.	-.5538110	10.96	15.23
PU19	419.58	1069.0	6490430.	537570.	-.5536320	9.03	13.13
PU20	417.86	1048.0	6491880.	537050.	-.5534040	7.11	11.13
PU21	418.84	1014.0	6493195.	537155.	-.5531970	7.02	10.91
PU22	417.17	1017.0	6494510.	537260.	-.5529900	6.48	10.38
PU23	417.49	984.0	6495730.	537010.	-.5527980	5.72	9.49
PU24	417.34	975.0	6497190.	536820.	-.5525680	6.10	9.83
PU25	416.74	973.0	6498870.	537170.	-.5523030	6.60	10.33
PU26	415.42	983.0	6500170.	536590.	-.5520990	6.82	10.58
PU27	413.39	958.0	6501140.	537090.	-.5519460	4.00	7.67

APPENDIX 10

TABLE 6

LOCALITY NAME ... B.H.-PINNACLES-SENTINNEL -HILLSTON-EDGEBEK-MAIN ROAD
STATION SPACING... ONE MILE BROADSCALE REGIONAL TYPE
ELEVATION CONTROL. EXTREMELY LONG BAROMETRIC LOOPS -ERROR APPROX. TWENTY FEET
POSITIONAL CONTROL EACH STATION LOCATED ON Z.C. AIRPHOTOS THEN ON BASE MAP
GRID REFERENCE ... U.T.M. AUSTRALIAN MAP GRID
GRAVITY METER ... CG-2 NO. 274 K=0.10035 OPERATED BY T.V.HARVEY MINES EXPLOR
BOUGUER DENSITY 1. 2.70 GRAM/ML
BOUGUER DENSITY 2. 2.40 GRAM/ML
OBSERVED GRAVITY.. ADD 979000.0 MILLIGALS
LATITUDE ... IN RADIANS
REDUCTION ... FROM RAW GRAVITY BY H.T.PECANEK

STATION	ABS.GRAV.	ELEVATION	NORTHING	EASTING	LATITUDE	BOUGUER 1	BOUGUER 2
P01	454.01	941.0	6460580.	540295.	-.5583300	14.09	17.70
P02	456.57	914.0	6459700.	538900.	-.5584700	14.39	17.89
P03	457.83	903.0	6458980.	537905.	-.5585840	14.47	17.93
P04	459.62	888.0	6457770.	536480.	-.5587750	14.48	17.88
P05	462.34	853.0	6456880.	535450.	-.5589160	14.46	17.73
P06	464.38	828.0	6455900.	534420.	-.5590710	14.29	17.46
P07	466.06	803.0	6455100.	533390.	-.5591970	13.89	16.97
P08	464.49	849.0	6454260.	532060.	-.5593300	14.45	17.70
P09	467.64	804.0	6453450.	531110.	-.5594580	14.32	17.40
P10	467.90	802.0	6452380.	531480.	-.5596270	13.68	16.75
P11	462.66	840.0	6451740.	530180.	-.5597280	10.23	13.45
P12	468.46	842.0	6450460.	529710.	-.5599300	15.21	18.44
P13	467.62	826.0	6449530.	528650.	-.5600760	12.74	15.91
P14	472.95	740.0	6448030.	528320.	-.5603130	11.85	14.68
P15	471.61	773.0	6447130.	527450.	-.5604550	11.81	14.77
P16	473.05	758.0	6446090.	526330.	-.5606190	11.60	14.50
P17	474.71	759.0	6445190.	525590.	-.5607610	12.66	15.56
P18	475.80	735.0	6443890.	525670.	-.5609660	11.36	14.18
P19	473.48	781.0	6442700.	525100.	-.5611540	10.91	13.90
P20	473.46	815.0	6441400.	525610.	-.5613580	11.97	15.09
P21	474.35	838.0	6440300.	525150.	-.5615320	13.42	16.63
P22	476.30	813.0	6439360.	523320.	-.5616800	13.19	16.30
P23	475.31	837.0	6438330.	522370.	-.5618420	12.87	16.08
P24	477.82	780.0	6437470.	522290.	-.5619780	11.35	14.34
X1	479.92	790.0	6436640.	524230.	-.5621080	13.45	16.47
X2	482.00	762.0	6435750.	522710.	-.5622490	13.20	16.12
TC20	481.98	780.0	6434920.	521840.	-.5623800	13.64	16.63
P001	482.64	785.0	6436880.	524060.	-.5620700	16.04	19.05
P002	476.28	887.0	6438495.	524220.	-.5618160	16.94	20.34
TC02	450.87	1009.0	6454220.	517820.	-.5593420	10.30	14.17
TC03	450.95	1050.0	6453243.	517450.	-.5594960	12.11	16.14
TC04	452.99	1017.0	6451722.	516474.	-.5597360	11.07	14.97
TC05	454.40	973.0	6450090.	515940.	-.5599930	8.67	12.39
TC06	454.13	996.0	6448516.	515485.	-.5602410	8.61	12.43
TC07	458.78	956.0	6447010.	515680.	-.5604780	9.78	13.44
TC08	455.34	1035.0	6445740.	514990.	-.5606780	10.12	14.08
TC09	459.65	975.0	6444120.	515000.	-.5609330	9.67	13.40
TC10	457.64	1020.0	6442910.	514050.	-.5611240	9.45	13.36
TC11	455.95	1060.0	6441600.	513280.	-.5613300	9.18	13.24
TC12	460.04	1034.0	6440190.	513610.	-.5615520	10.69	14.65
TC13	460.62	1018.0	6439110.	514270.	-.5617220	9.53	13.43
TC14	467.22	992.0	6438390.	515730.	-.5618350	14.05	17.85
TC15	471.89	871.0	6436900.	516250.	-.5620700	10.42	13.76
TC16	472.39	873.0	6436140.	517250.	-.5621890	10.48	13.83
TC17	476.90	834.0	6435090.	518020.	-.5623540	11.90	15.10
TC18	476.67	862.0	6434350.	519970.	-.5624710	12.79	16.10
TC19	478.48	850.0	6434430.	520570.	-.5624570	13.95	17.21
TC20	482.11	780.0	6434920.	521840.	-.5623800	13.77	16.76

APPENDIX 10

TABLE 7

CALITY NAME...	HUONVILLE GRAVITY TRAVERSE 1973
PPOSE ...	TO TRAVERSE AEROMAGNETIC BOUNDARY NEAR REDAN GNEISS
ATION SPACING...	FOUR HUNDRED FEET
EVATION CONTROL.	LEVELLED BY R.CAMMELL AND H.T.P.-TIED TO B.M. BY BAROMETER.
SITIONAL CONTROL	THEODOLITE ST. LINE AND INTERPOLATION BET Z.C. AIR PHOTOS
ID REFERENCE ...	U.T.M. AUSTRALIAN MAP GRID.
AVITY METER ...	WORDEN 368 K=0.0981 OPERATED BY H.T.PECANEK
UGUER DENSITY 1.	2.70 GRAM/ML.
UGUER DENSITY 2.	2.40 GRAM/ML.
SERVED GRAVITY .	ADD 979000.0 MILLIGALS.
TITUDE ...	IN RADIANS
DUCTION ...	FROM RAW GRAVITY BY H.T.PECANEK

TATION	ABS.GRAV.	ELEVATION	NORTHING	EASTING	LATITUDE	BOUGUER 1	BOUGUER 2
HUON01	480.63	613.0	6436728.	540478.	-.5620860	3.71	6.06
HUON02	483.35	612.4	6436640.	540570.	-.5621000	6.33	8.68
HUON03	483.62	611.3	6436552.	540662.	-.5621130	6.47	8.82
HUON04	483.68	610.8	6436465.	540755.	-.5621270	6.44	8.78
HUON05	483.85	611.7	6436377.	540847.	-.5621410	6.60	8.94
HUON06	483.82	613.6	6436289.	540940.	-.5621550	6.62	8.97
HUON07	483.97	613.2	6436201.	541032.	-.5621680	6.68	9.03
HUON08	484.22	611.6	6436113.	541125.	-.5621830	6.77	9.11
HUON09	484.44	610.1	6436025.	541217.	-.5621960	6.84	9.17
HUON10	484.65	608.8	6435937.	541310.	-.5622100	6.90	9.24
HUON11	484.92	607.3	6435850.	541402.	-.5622240	7.02	9.35
HUON12	485.11	605.4	6435762.	541495.	-.5622370	7.04	9.36
HUON13	485.27	603.7	6435674.	541587.	-.5622520	7.02	9.34
HUON14	485.38	602.2	6435586.	541680.	-.5622650	6.98	9.29
HUON15	485.56	600.7	6435498.	541772.	-.5622790	7.01	9.31
HUON16	485.71	599.0	6435411.	541865.	-.5622930	6.99	9.29
HUON17	485.87	597.2	6435323.	541957.	-.5623060	6.99	9.27
HUON18	486.04	596.4	6435235.	542050.	-.5623200	7.04	9.33
HUON19	486.16	596.5	6435147.	542142.	-.5623340	7.10	9.39
HUON20	486.37	595.2	6435059.	542235.	-.5623480	7.17	9.45
HUON21	486.63	594.0	6434972.	542327.	-.5623610	7.30	9.57
HUON22	487.00	590.6	6434884.	542420.	-.5623750	7.40	9.66
HUON23	487.15	589.0	6434796.	542512.	-.5623890	7.39	9.65
HUON24	487.37	588.0	6434708.	542605.	-.5624020	7.49	9.74
HUON25	487.58	586.5	6434620.	542697.	-.5624160	7.55	9.79
HUON26	487.65	585.2	6434532.	542790.	-.5624300	7.47	9.72
HUON27	487.75	583.5	6434445.	542882.	-.5624440	7.41	9.64
HUON28	487.83	583.4	6434357.	542975.	-.5624580	7.42	9.65
HUON29	487.93	582.2	6434269.	543067.	-.5624710	7.38	9.61
HUON30	488.11	581.1	6434181.	543160.	-.5624850	7.43	9.66
HUON31	488.47	580.0	6434093.	543252.	-.5624990	7.66	9.88
HUON32	488.72	579.7	6434006.	543345.	-.5625130	7.83	10.05
HUON33	489.13	578.0	6433918.	543437.	-.5625270	8.07	10.29
HUON34	489.15	580.9	6433830.	543530.	-.5625400	8.21	10.43
HUON35	489.60	576.0	6433741.	543623.	-.5625540	8.30	10.50
HUON36	489.79	574.6	6433653.	543716.	-.5625680	8.34	10.54
HUON38	490.52	572.5	6433476.	543901.	-.5625960	8.81	11.01
HUON39	490.90	570.9	6433387.	543994.	-.5626100	9.03	11.22
HUON40	491.26	570.2	6433298.	544087.	-.5626240	9.29	11.47
HUON41	491.68	570.2	6433210.	544180.	-.5626380	9.64	11.83
HUON42	492.18	566.9	6433121.	544272.	-.5626520	10.00	12.18
HUON43	492.68	568.1	6433033.	544365.	-.5626650	10.39	12.57
HUON44	493.21	567.1	6432944.	544458.	-.5626790	10.80	12.97
HUON45	493.72	565.3	6432855.	544551.	-.5626930	11.13	13.30
HUON46	494.09	565.1	6432767.	544644.	-.5627070	11.43	13.59
HUON47	494.31	564.7	6432678.	544736.	-.5627210	11.56	13.72
HUON48	494.42	564.0	6432590.	544829.	-.5627350	11.56	13.72
HUON49	494.34	565.2	6432501.	544922.	-.5627490	11.49	13.65
HUON50	494.30	566.3	6432412.	545015.	-.5627630	11.45	13.62
HUON51	494.61	563.7	6432324.	545108.	-.5627760	11.54	13.70
HUON52	494.94	560.5	6432235.	545200.	-.5627900	11.61	13.76
HUON53	495.19	559.5	6432147.	545293.	-.5628040	11.74	13.88
HUON54	495.56	556.3	6432058.	545386.	-.5628180	11.85	13.99
HUON55	495.93	553.0	6431969.	545479.	-.5628320	11.96	14.08
HUON56	496.04	552.7	6431881.	545572.	-.5628460	11.99	14.11
HUON57	496.21	552.3	6431792.	545664.	-.5628600	12.07	14.19
HUON58	496.46	551.2	6431704.	545757.	-.5628740	12.19	14.30
HUON59	496.89	549.9	6431615.	545850.	-.5628870	12.48	14.59

APPENDIX 10

TABLE 8

****

CALITY NAME ... MENINDEE HIGHWAY GRAVITY TRAVERSE 1973
ATION SPACING... VARIABLE BUT ABOUT 400 FEET ON AVERAGE
EVATION CONTROL. N.S.W. D.M.R. SURVEY PEGS FOR REROUTE MENINDEE HWY
SITIONAL CONTROL Z.C. AIRPHOTOS AND MILEAGE ON N.S.W. D.M.R. SURVEY PEGS
ID REFERENCE ... U.T.M. AUSTRALIAN MAP GRID
AVITY METER ... WORDEN 368 K=0.0981 OPERATED BY H.T.PECANEK
UGUER DENSITY 1. 2.70 GRAM/ML
UGUER DENSITY 2. 2.40 GRAM/ML
SERVED GRAVITY.. ADD 979000.0 MILLIGALS
TITUDE ... IN RADIANS
DUCTION ... FROM RAW GRAVITY BY H.T.PECANEK

****

ATION	ABS.GRAV.	ELEVATION	NORTHING	EASTING	LATITUDE	BOUGUER 1	BOUGUER 2
MEN001	451.52	978.0	6464165.	545030.	-.5577630	16.43	20.18
MEN002	452.44	972.0	6464025.	545200.	-.5577850	16.89	20.62
MEN003	455.99	935.0	6463475.	545710.	-.5578710	17.84	21.42
MEN004	457.16	912.8	6462980.	546430.	-.5579490	17.33	20.82
MEN005	458.29	893.0	6462490.	547080.	-.5580250	16.93	20.35
MEN006	458.33	888.0	6462270.	547210.	-.5580600	16.50	19.91
MEN007	458.70	884.6	6461855.	547740.	-.5581250	16.37	19.76
MEN008	458.64	887.0	6461800.	547900.	-.5581330	16.42	19.81
MEN009	458.71	889.0	6461770.	547940.	-.5581380	16.58	19.99
MEN010	458.80	892.0	6461710.	548025.	-.5581480	16.81	20.22
MEN011	458.98	897.0	6461650.	548120.	-.5581570	17.24	20.68
MEN012	458.81	884.0	6461850.	547790.	-.5581250	16.45	19.83
MEN013	459.03	897.0	6461680.	548060.	-.5581520	17.31	20.75
MEN014	459.47	897.0	6461620.	548180.	-.5581610	17.71	21.15
MEN015	459.62	899.0	6461540.	548320.	-.5581740	17.92	21.37
MEN016	459.83	898.0	6461475.	548390.	-.5581840	18.03	21.47
MEN017	459.44	902.0	6461404.	548516.	-.5581950	17.82	21.28
MEN019	459.68	906.0	6461263.	548766.	-.5582170	18.20	21.67
MEN020	459.92	907.0	6461218.	548845.	-.5582240	18.47	21.94
MEN021	459.84	908.0	6461190.	548895.	-.5582290	18.42	21.90
MEN022	460.02	910.0	6461179.	548942.	-.5582300	18.72	22.20
MEN023	459.93	913.0	6461164.	549005.	-.5582320	18.80	22.29
MEN024	459.86	919.0	6461146.	549082.	-.5582350	19.07	22.59
MEN025	459.46	928.0	6461124.	549175.	-.5582390	19.19	22.74
MEN026	458.85	936.0	6461105.	549260.	-.5582420	19.04	22.63
MEN027	458.90	932.0	6461073.	549395.	-.5582470	18.83	22.40
MEN028	458.57	933.0	6461040.	549538.	-.5582520	18.54	22.11
MEN029	458.46	941.0	6461018.	549631.	-.5582550	18.89	22.49
MEN030	458.81	930.0	6460881.	549795.	-.5582770	18.48	22.04
MEN031	458.15	950.0	6460811.	549921.	-.5582870	18.97	22.61
MEN032	458.72	932.0	6460740.	550020.	-.5582990	18.41	21.98
MEN033	458.68	933.0	6460675.	550112.	-.5583090	18.38	21.96
MEN034	458.70	936.0	6460599.	550218.	-.5583200	18.53	22.11
MEN035	458.55	940.0	6460505.	550350.	-.5583360	18.54	22.14
MEN036	458.16	945.0	6460423.	550465.	-.5583480	18.40	22.02
MEN037	457.98	945.0	6460394.	550564.	-.5583520	18.20	21.82
MEN038	457.79	950.0	6460374.	550620.	-.5583560	18.29	21.93
MEN039	456.83	952.0	6460336.	550735.	-.5583620	17.42	21.06
MEN040	457.24	950.0	6460356.	550667.	-.5583580	17.73	21.37
MEN041	456.55	954.0	6460317.	550792.	-.5583640	17.25	20.90
MEN042	456.40	956.0	6460298.	550850.	-.5583680	17.20	20.86
MEN043	456.14	959.0	6460269.	550935.	-.5583720	17.10	20.77
MEN044	455.94	961.0	6460240.	551021.	-.5583760	17.00	20.68
MEN045	455.74	963.5	6460211.	551107.	-.5583810	16.92	20.62
MEN046	455.63	966.5	6460183.	551193.	-.5583860	16.97	20.67
MEN047	455.40	976.0	6460145.	551273.	-.5583910	17.28	21.02
MEN048	454.80	984.5	6460125.	551333.	-.5583940	17.18	20.95
MEN049	454.20	996.4	6460106.	551393.	-.5583980	17.27	21.08
MEN050	453.73	1007.0	6460087.	551453.	-.5584000	17.42	21.28
MEN051	453.92	1005.0	6460077.	551484.	-.5584020	17.48	21.33

APPENDIX 10

TABLE 8 (contd.)

N052	454.02	1004.0	6460067.	551514.	-.5584040	17.51	21.36
N053	454.41	1000.0	6460048.	551574.	-.5584060	17.65	21.48
N054	454.53	999.1	6460039.	551604.	-.5584080	17.71	21.54
N055	454.63	998.6	6460029.	551634.	-.5584100	17.77	21.60
N056	455.01	992.4	6460010.	551695.	-.5584120	17.77	21.57
N057	455.05	988.3	6459987.	551766.	-.5584160	17.55	21.34
N058	455.02	987.7	6459952.	551846.	-.5584220	17.46	21.24
N059	455.10	988.0	6459921.	551923.	-.5584260	17.54	21.32
N060	454.93	990.8	6459862.	551976.	-.5584350	17.49	21.29
N061	454.46	999.3	6459801.	552028.	-.5584450	17.48	21.31
N062	454.59	999.6	6459741.	552080.	-.5584540	17.59	21.42
N063	454.84	993.7	6459694.	552120.	-.5584610	17.45	21.26
N064	454.91	991.6	6459634.	552172.	-.5584710	17.35	21.15
N065	454.27	1001.0	6459573.	552225.	-.5584810	17.22	21.06
N066	454.44	997.0	6459526.	552266.	-.5584880	17.12	20.94
N067	454.38	998.4	6459473.	552312.	-.5584960	17.11	20.94
N068	454.77	992.0	6459614.	552384.	-.5584740	17.22	21.02
MEN069	455.16	992.0	6459809.	552215.	-.5584430	17.75	21.56
MEN0XX	454.82	998.0	6458877.	553678.	-.5585890	17.09	20.92
MEN070	455.10	993.0	6459711.	552299.	-.5584590	17.68	21.48
MEN071	455.02	992.0	6459541.	552447.	-.5584850	17.42	21.22
MEN072	454.82	994.0	6459482.	552498.	-.5584950	17.29	21.10
MEN073	454.96	993.0	6459409.	552562.	-.5585060	17.32	21.13
MEN074	454.51	1006.0	6459310.	552635.	-.5585220	17.57	21.43
MEN075	454.32	1009.0	6459226.	552691.	-.5585350	17.50	21.37
MEN076	454.05	1018.0	6459106.	552772.	-.5585540	17.68	21.58
MEN077	453.78	1025.0	6459018.	552830.	-.5585670	17.77	21.69
MEN078	453.31	1027.0	6458980.	552902.	-.5585730	17.39	21.32
MEN079	452.60	1037.0	6458942.	552974.	-.5585790	17.24	21.22
MEN080	451.58	1057.0	6458903.	553046.	-.5585850	17.39	21.44
MEN081	451.51	1050.0	6458864.	553120.	-.5585910	16.87	20.90
MEN082	451.60	1054.0	6458827.	553191.	-.5585970	17.17	21.21
MEN082	451.60	1044.0	6458827.	553191.	-.5585970	16.58	20.58
MEN083	452.42	1040.0	6458839.	553308.	-.5585950	17.17	21.15
MEN084	453.59	1020.0	6458851.	553427.	-.5585940	17.15	21.06
MEN085	454.20	1009.0	6458863.	553544.	-.5585910	17.12	20.99
MEN086	454.75	1000.0	6458876.	553670.	-.5585890	17.14	20.98
MEN087	455.19	994.0	6458887.	553774.	-.5585870	17.24	21.04
MEN088	455.18	998.0	6458874.	553833.	-.5585900	17.45	21.27
MEN089	455.29	998.0	6458853.	553845.	-.5585930	17.55	21.37
MEN090	456.73	975.0	6458801.	553905.	-.5586010	17.58	21.31
MEN091	457.06	968.0	6458757.	554137.	-.5586080	17.46	21.17
MEN092	457.51	962.0	6458712.	554183.	-.5586150	17.52	21.20
MEN093	457.73	959.0	6458655.	554241.	-.5586230	17.52	21.20
MEN094	458.06	956.0	6458592.	554286.	-.5586340	17.62	21.29
MEN095	457.99	952.0	6458477.	554346.	-.5586520	17.23	20.88
MEN096	457.98	951.0	6458395.	554389.	-.5586640	17.11	20.75
MEN097	457.87	952.0	6458314.	554431.	-.5586770	17.00	20.64
MEN098	458.03	952.0	6458232.	554474.	-.5586900	17.10	20.74
MEN099	458.18	951.0	6458151.	554518.	-.5587030	17.13	20.77
MEN100	458.25	952.0	6458069.	554560.	-.5587160	17.19	20.84
MEN101	458.36	955.0	6457988.	554603.	-.5587280	17.43	21.09
MEN102	458.50	954.0	6457906.	554646.	-.5587410	17.45	21.10
MEN103	458.43	956.0	6457826.	554688.	-.5587540	17.44	21.10
MEN104	458.25	959.0	6457744.	554731.	-.5587660	17.38	21.05
MEN105	458.25	962.0	6457663.	554774.	-.5587790	17.50	21.18
MEN106	458.15	963.0	6457614.	554800.	-.5587870	17.42	21.11
MEN107	457.95	966.0	6457532.	554842.	-.5588000	17.34	21.04
MEN108	457.63	969.0	6457451.	554886.	-.5588120	17.14	20.85
MEN109	457.46	971.0	6457370.	554926.	-.5588250	17.03	20.75
MEN110	457.20	976.0	6457288.	554971.	-.5588380	17.01	20.75
MEN111	457.13	982.0	6457207.	555014.	-.5588510	17.24	21.00
MEN112	456.85	982.0	6457200.	555020.	-.5588520	16.95	20.71
MEN113	456.59	999.0	6456998.	555124.	-.5588840	17.56	21.38
MEN114	455.98	1012.0	6456855.	555200.	-.5589060	17.62	21.49
MEN115	458.88	978.0	6456557.	555338.	-.5589530	18.27	22.02

****

START AND FINISH ON 1 116

APPENDIX 10

TABLE 9

****

ALITY NAME ... B.H. REGIONAL GRAVITY SURVEY AUGUST 1972..U. OF ADELAIDE
TION SPACING... APPROXIMATELY TWO MILES
VATION CONTROL. D. OF LANDS OR HIGHWAY BENCH MARKS
ITIONAL CONTROL G.JENKE MARKED STNS. ON B.H. INCH TO 2 M. GEOL
ITIONAL CONTROL COORDINATES THEN DIGITIZED BY H.T.PECANEK
D REFERENCE ... U.T.M. AUSTRALIAN MAP GRID
VITY METER ... CG-2 NO.174 K=0.10035 OPERATED BY T.V.HARVEY MINES EXPLOR.
JGUER DENSITY 1. 2.70 GRAM/ML
JGUER DENSITY 2. 2.40 GRAM/ML
SERVED GRAVITY.. ADD 979000.0 MILLIGALS
TITUDE ... IN RADIANS
DUCTION ... FROM RAW GRAVITY BY H.T.PECANEK

****

ATION	ABS.GRAV.	ELEVATION	NORTHING	EASTING	LATITUDE	BOUGUER 1	BOUGUER 2
M3690	458.40	915.1	6459029.	541383.	-.5585740	15.80	19.31
M3691	465.70	842.9	6456139.	539828.	-.5590300	16.69	19.91
M3692	468.56	833.9	6453140.	538603.	-.5595030	16.81	20.01
SM3693	474.10	758.3	6450117.	537795.	-.5599800	15.64	18.54
SM3694	474.91	779.3	6446825.	538432.	-.5604970	15.29	18.28
SM3695	477.65	728.8	6443801.	537564.	-.5609740	12.81	15.60
SM3696	480.63	658.1	6440741.	536216.	-.5614570	9.33	11.85
SM3697	483.92	624.0	6438136.	537018.	-.5618670	8.68	11.07
SM3698	484.68	603.0	6436146.	539046.	-.5621790	6.73	9.04
SM3699	494.44	571.8	6430228.	540148.	-.5631090	10.30	12.49
M 5497	489.83	583.4	6433333.	540021.	-.5626210	8.65	10.89
SM5263	458.24	885.2	6462235.	547134.	-.5580650	16.23	19.62
SM5262	457.80	938.1	6460724.	550011.	-.5583010	17.84	21.44
SM5261	451.41	1031.8	6459114.	552753.	-.5585520	15.87	19.82
PM 3682	455.47	989.1	6457286.	554859.	-.5588380	16.06	19.85
SM5259	466.53	760.9	6454555.	556499.	-.5592670	11.53	14.44
SM5258	470.60	695.5	6453079.	559241.	-.5594970	10.63	13.30
SM5257	473.23	630.0	6451635.	562130.	-.5597210	8.32	10.73
SM5256	474.21	587.1	6450141.	565055.	-.5599540	5.66	7.91
SM5255	473.33	630.0	6449166.	568116.	-.5601040	6.64	9.06
SM5254	477.45	566.4	6447678.	570882.	-.5603350	5.90	8.07
SM2989	452.50	972.6	6454640.	518614.	-.5592760	10.07	13.80
PM 4810	449.19	1034.0	6454359.	516642.	-.5593200	10.22	14.18
SM2988	452.58	960.6	6454847.	515651.	-.5592440	9.59	13.27
PM3683	451.54	965.6	6464393.	544735.	-.5577280	15.88	19.58
SM3002	456.69	876.1	6465137.	546926.	-.5576080	16.25	19.61
SM3003	457.13	850.9	6465857.	548261.	-.5574940	15.72	18.98
SM3004	457.30	829.6	6466759.	549497.	-.5573510	15.28	18.46
PM 4819	457.49	821.8	6467795.	550023.	-.5571880	15.76	18.91
SM3005	456.61	818.0	6468953.	551664.	-.5570040	15.51	18.64
SM3006	457.51	776.9	6469490.	553353.	-.5569180	14.36	17.34
SM3007	456.20	810.8	6469831.	554553.	-.5568630	15.32	18.43
PM 4820	457.73	768.6	6470441.	555936.	-.5567660	14.79	17.73
SM3008	458.04	769.9	6470307.	557405.	-.5567860	15.08	18.03
SM3009	458.70	778.2	6469795.	558567.	-.5568660	15.87	18.85
SM3010	462.42	714.0	6469807.	560159.	-.5568630	15.78	18.51
PM 4821	463.86	688.0	6469538.	562044.	-.5569030	15.48	18.11
SM3011	464.96	682.3	6469721.	563403.	-.5568730	16.38	18.99
SM3012	462.80	672.7	6469782.	564847.	-.5568620	13.70	16.28
PM 4822	461.50	659.4	6470709.	567907.	-.5567120	12.30	14.83
SM3014	460.54	652.1	6471123.	569486.	-.5566460	11.21	13.71
SM3015	459.48	667.2	6471538.	571041.	-.5565790	11.36	13.92
SM3016	456.76	674.1	6471916.	572608.	-.5565180	9.33	11.92
SM3013	462.78	663.1	6470197.	566402.	-.5567950	13.42	15.96
PM5496	451.15	982.3	6461260.	543401.	-.5582220	14.19	17.96
PM 3683	452.13	965.6	6464358.	544749.	-.5577320	16.45	20.15
SM5263	458.83	885.2	6461354.	543418.	-.5582070	16.16	19.55
PM 5418	449.97	942.2	6466478.	545176.	-.5573990	14.44	18.05
PM 4816	447.77	1002.3	6464942.	543548.	-.5576420	14.69	18.53

APPENDIX 10

TABLE 9 (contd.)

4815	446.92	1019.3	6467222.	542838.	-.5572830	16.52	20.42
3001	451.38	983.6	6462796.	540194.	-.5579810	15.61	19.38
5418	449.35	942.2	6466478.	545176.	-.5573990	13.82	17.43
13689	450.94	851.2	6469136.	547159.	-.5569790	11.93	15.19
13688	450.66	817.4	6472013.	548040.	-.5565250	11.74	14.87
13687	448.39	815.0	6475366.	547832.	-.5559970	11.77	14.90
53686	444.81	831.2	6478780.	548603.	-.5554590	11.65	14.83
43685	438.81	889.4	6482182.	549325.	-.5549230	11.59	15.00
M3684	431.07	989.1	6485144.	550452.	-.5544560	11.95	15.74
M3683	429.02	971.2	6487644.	552505.	-.5540600	10.67	14.39
M3682	428.79	904.1	6492480.	557004.	-.5532960	9.97	13.43
M3681	429.03	885.2	6495040.	558981.	-.5528900	10.95	14.34
M3680	427.24	895.8	6497575.	560193.	-.5524900	11.64	15.07
M3679	421.45	972.1	6501010.	560439.	-.5519490	12.89	16.61
,M3678	420.60	960.5	6504178.	560578.	-.5514500	13.65	17.33
;M3677	419.09	971.0	6507245.	561148.	-.5509670	14.99	18.71
;M3000	453.53	932.9	6462199.	538627.	-.5580770	14.30	17.88
;M2999	454.57	908.4	6461577.	537024.	-.5581750	13.43	16.91
8-7705	454.82	890.0	6460846.	535677.	-.5582910	12.04	15.45
M 4813	457.45	861.9	6460212.	534637.	-.5583920	12.53	15.83
;M2997	454.84	919.7	6460455.	532790.	-.5583540	13.54	17.06
SM2996	451.48	981.1	6460443.	531199.	-.5583570	13.82	17.58
SM2995	451.53	973.5	6459663.	529986.	-.5584800	12.85	16.58
8-7706	449.19	990.0	6458931.	528822.	-.5585960	10.96	14.75
SM2994	448.05	1016.0	6458480.	527255.	-.5586680	11.03	14.92
SM2993	448.20	1029.0	6457749.	525689.	-.5587840	11.42	15.36
;SM2992	449.11	1029.0	6456749.	524771.	-.5589420	11.59	15.54
'M 4811	452.32	968.3	6456164.	523241.	-.5590340	10.76	14.47
;SM2991	452.21	972.4	6461988.	521924.	-.5581170	15.15	18.87
;SM2991	452.21	972.4	6455713.	521772.	-.5591060	10.56	14.29
;SM2990	452.74	963.6	6455298.	520513.	-.5591710	10.26	13.96

APPENDIX 11 LOCATION OF GRAVITY TRAVERSES AND GEOLOGIC CROSS SECTIONS

1. The location of O. Weiss gravity traverses 1C, 1A, 1, 2A, 3 and 13 along with geologic sections 30, 62, 92 and 262 are marked on folio figure 8, a copy of the Broken Hill Mining Managers' Association Line of Code map on a scale of 1:25000 published in 1972 by I.R. Johnson and G.D. Klingner.

2. The location of regional gravity traverses discussed in the text are marked on folio figure 7. Here some individual gravity stations have been plotted to help identify the traverses.

FIGURE I

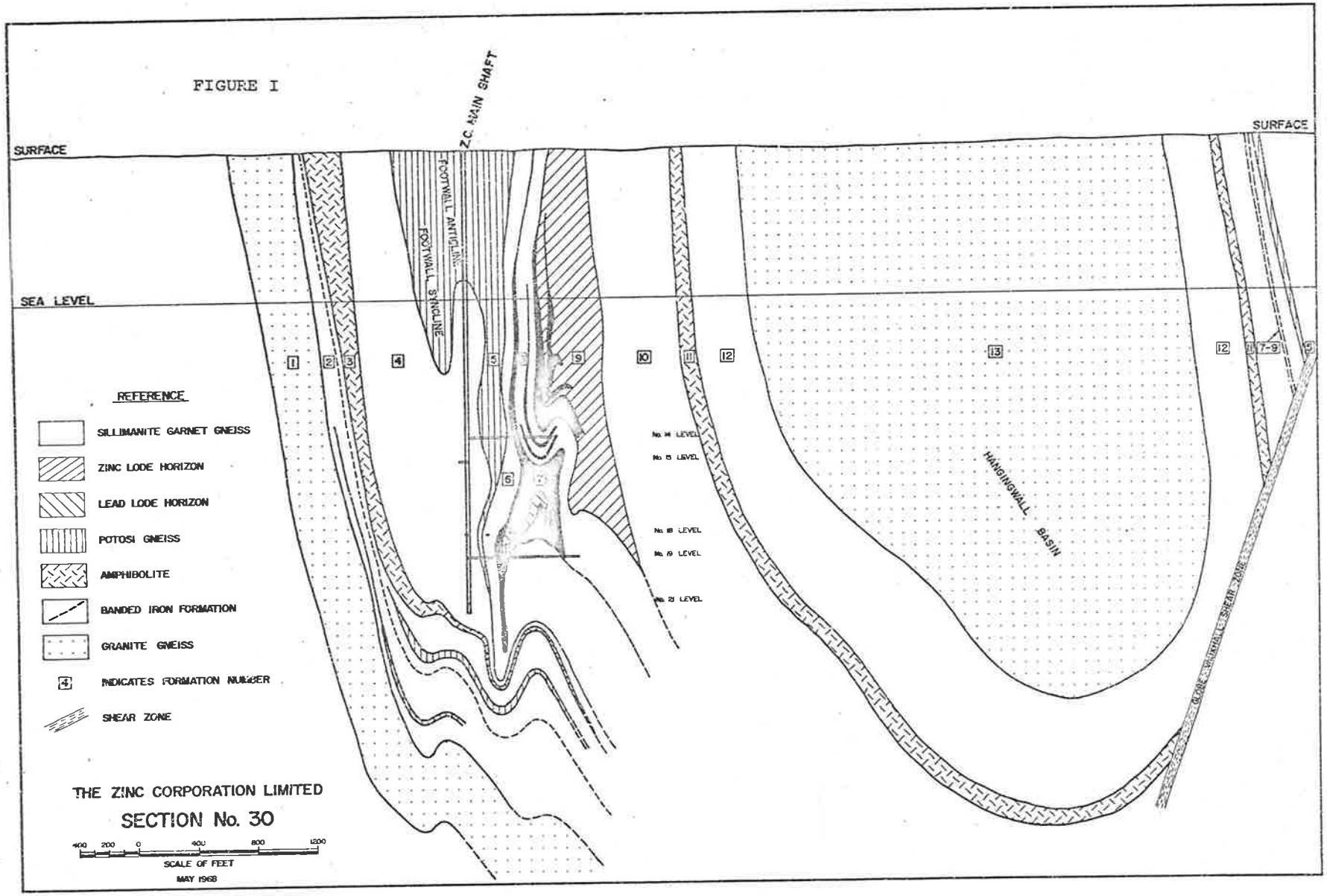
SURFACE
SEA LEVEL
Z.C. MAIN SHAFT
FOOTWALL ANTICLINE
FOOTWALL SYNCLINE
SURFACE
HANGINGWALL BASIN
CORE OF HANGING WALL SHEAR ZONE
No. 14 LEVEL
No. 15 LEVEL
No. 18 LEVEL
No. 19 LEVEL
No. 21 LEVEL
1
2
3
4
5
9
10
11
12
13
12
7-9
5
REFERENCE
SILLIMANITE GARNET GNEISS
ZINC LODE HORIZON
LEAD LODE HORIZON
POTOSI GNEISS
AMPHIBOLITE
BANDED IRON FORMATION
GRANITE GNEISS
INDICATES FORMATION NUMBER
SHEAR ZONE
THE ZINC CORPORATION LIMITED
SECTION No. 30
400 200 0 400 800 1200
SCALE OF FEET
MAY 1968

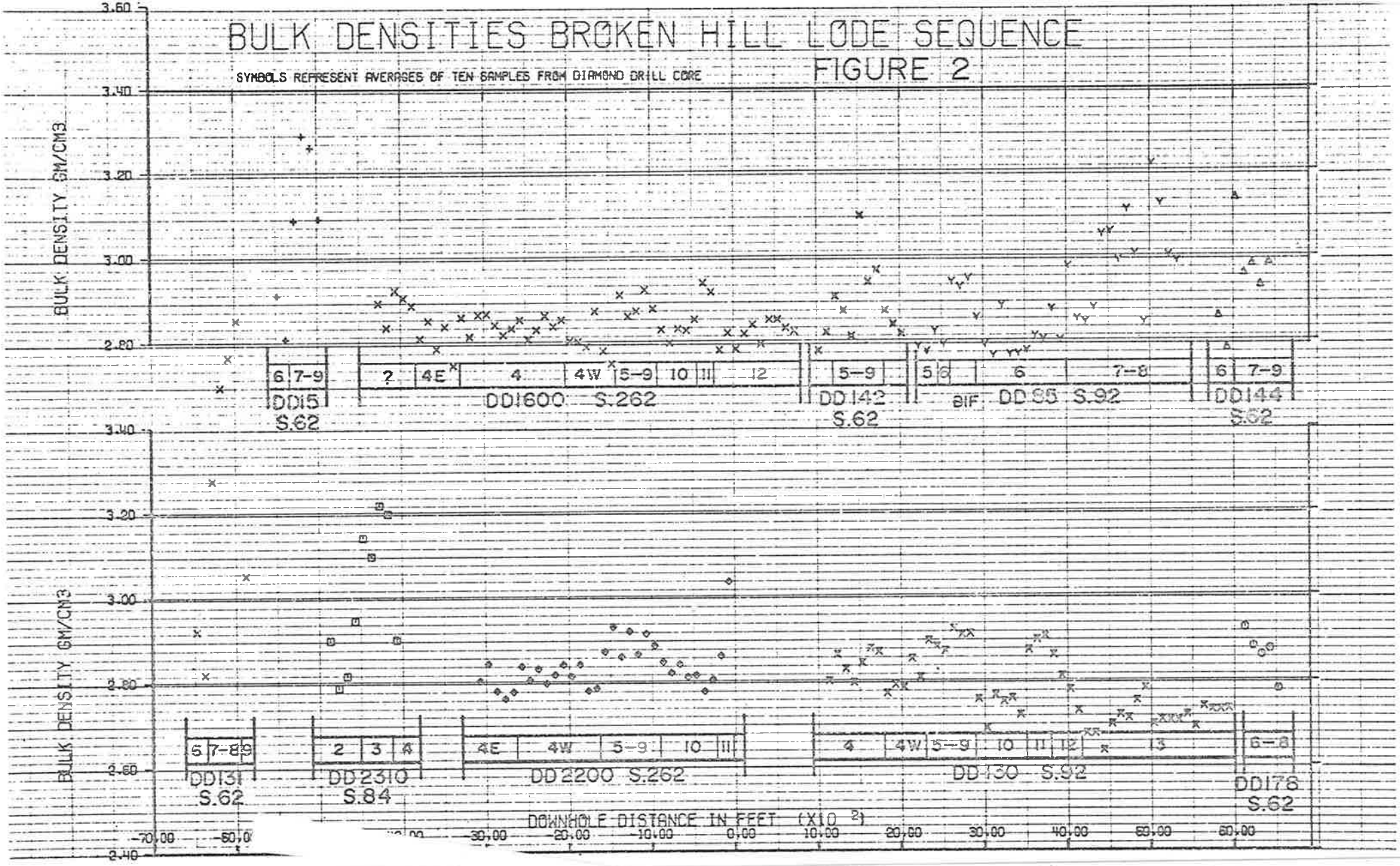
BULK DENSITIES BROKEN HILL LODE SEQUENCE
FIGURE 2
SYMBOLS REPRESENT AVERAGES OF TEN SAMPLES FROM DIAMOND DRILL CORE
BULK DENSITY GM/CM3
3.60
3.40
3.20
3.00
2.80
2.60
2.40
6 7-9
DD15
S.62
2 4E 4 4W 5-9 10 11 12
DD1600 S.262
5-9
DD142
S.62
5 6 6 7-8
BIF DD85 S.92
16 7-9
DD144
S.62
5 7-8
DD131
S.62
2 3 4
DD2310
S.84
4E 4W 5-9 10 11
DD2200 S.262
4 4W 5-9 10 11 12 13
DD130 S.92
6-8
DD178
S.62
DOWNHOLE DISTANCE IN FEET (X10 2)
-70,00
-60,00
-30,00
-20,00
-10,00
0,00
10,00
20,00
30,00
40,00
50,00
60,00

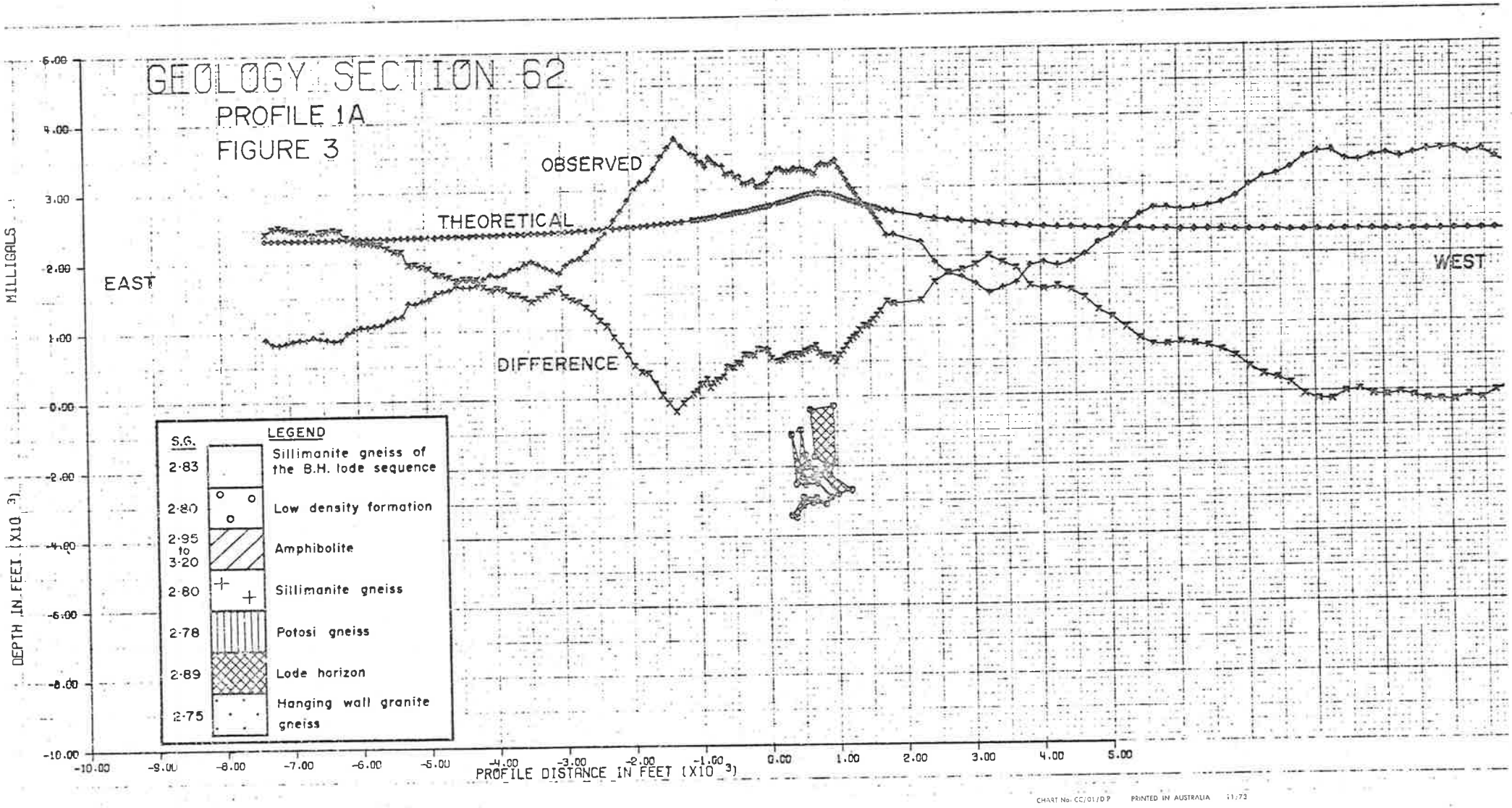

CHART No. CC/01/D.P PRINTED IN AUSTRALIA 11.73

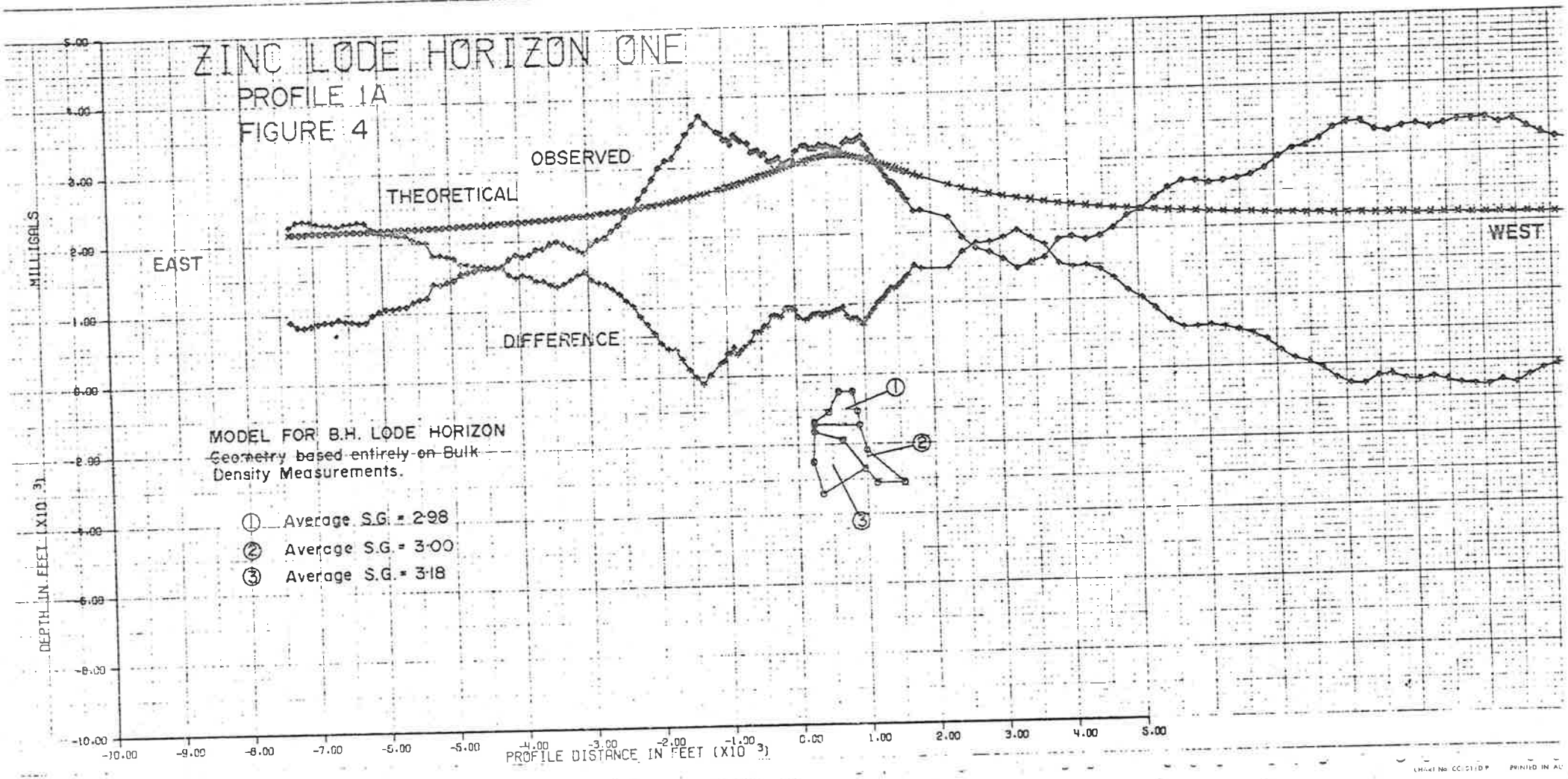
ZINC LODE HORIZON ONE
PROFILE 1A
FIGURE 4
OBSERVED
THEORETICAL
DIFFERENCE
EAST
WEST
MILLIGALS
DEPTH IN FEET (X10 3)
PROFILE DISTANCE IN FEET (X10 3)
MODEL FOR B.H. LODE HORIZON
Geometry based entirely on Bulk Density Measurements.
① Average S.G. = 2·98
② Average S.G. = 3·00
③ Average S.G. = 3·18

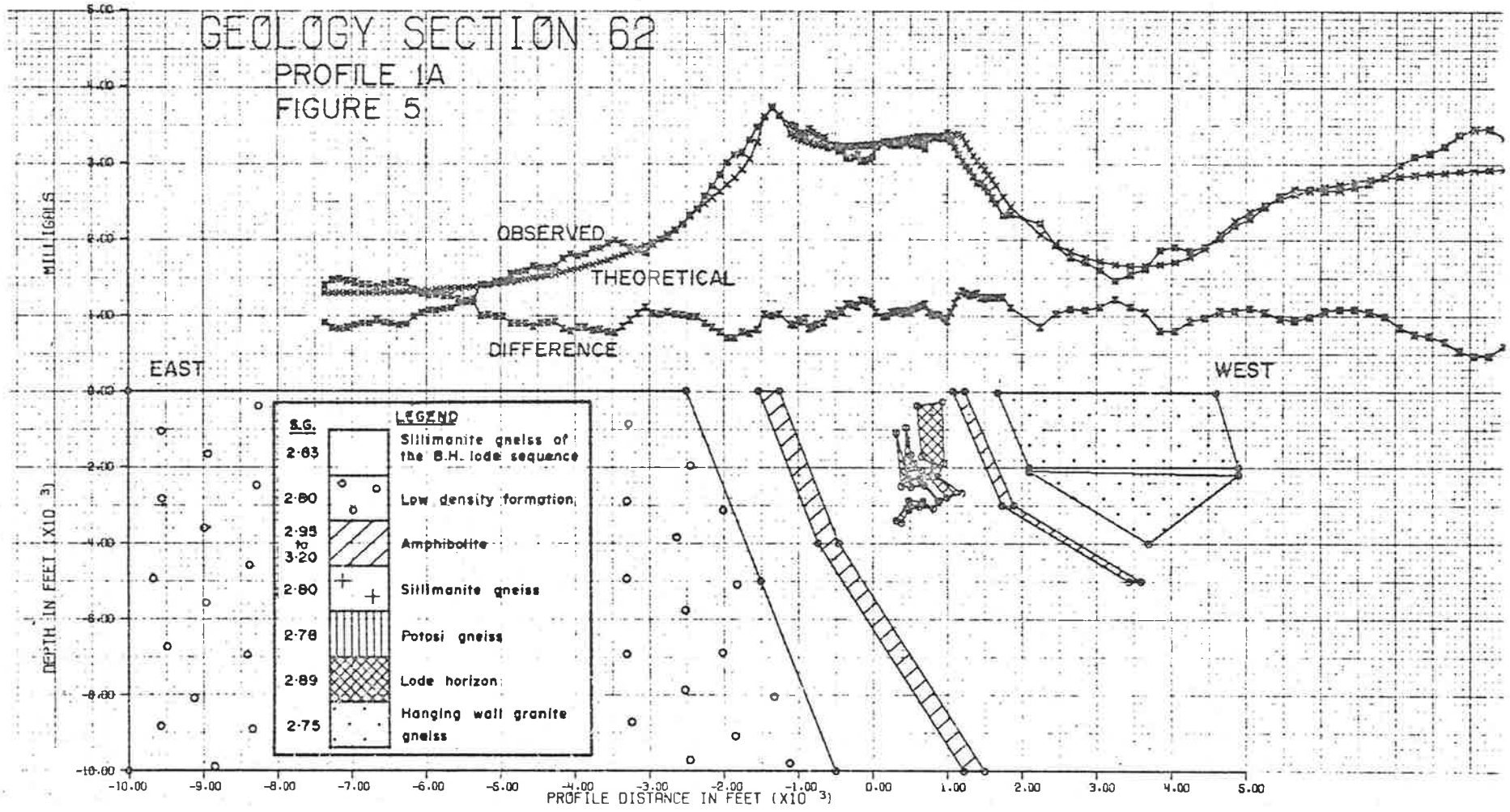
GEOLOGY SECTION 62
PROFILE 1A
FIGURE 5
OBSERVED
THEORETICAL
DIFFERENCE
EAST
WEST
MILLIGALS
DEPTH IN FEET (X10 3)
PROFILE DISTANCE IN FEET (X10 3)
LEGEND
S.G.
2·63 Sillimanite gneiss of the B.H. lode sequence
2·80 Low density formation
2·95 to 3·20 Amphibolite
2·80 Sillimanite gneiss
2·78 Potosi gneiss
2·89 Lode horizon
2·75 Hanging wall granite gneiss

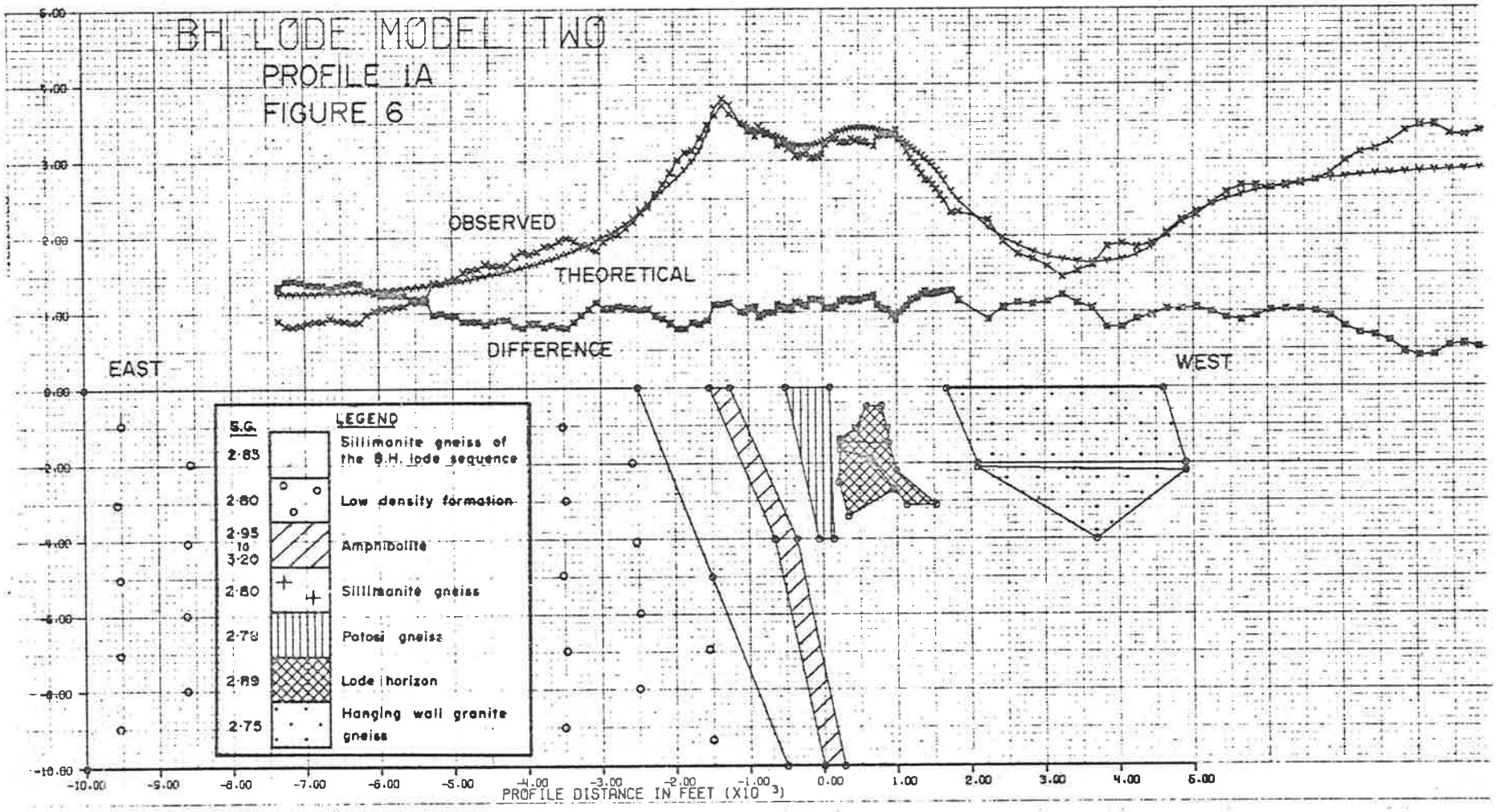
BH LODE MODEL TWO
PROFILE 1A
FIGURE 6
OBSERVED
THEORETICAL
DIFFERENCE
EAST
WEST
LEGEND
S.G.
2·85 Sillimanite gneiss of the B.H. lode sequence
2·80 Low density formation
2·95 to 3·20 Amphibolite
2·80 Sillimanite gneiss
2·78 Potosi gneiss
2·89 Lode horizon
2·75 Hanging wall granite gneiss
PROFILE DISTANCE IN FEET (X10 3)

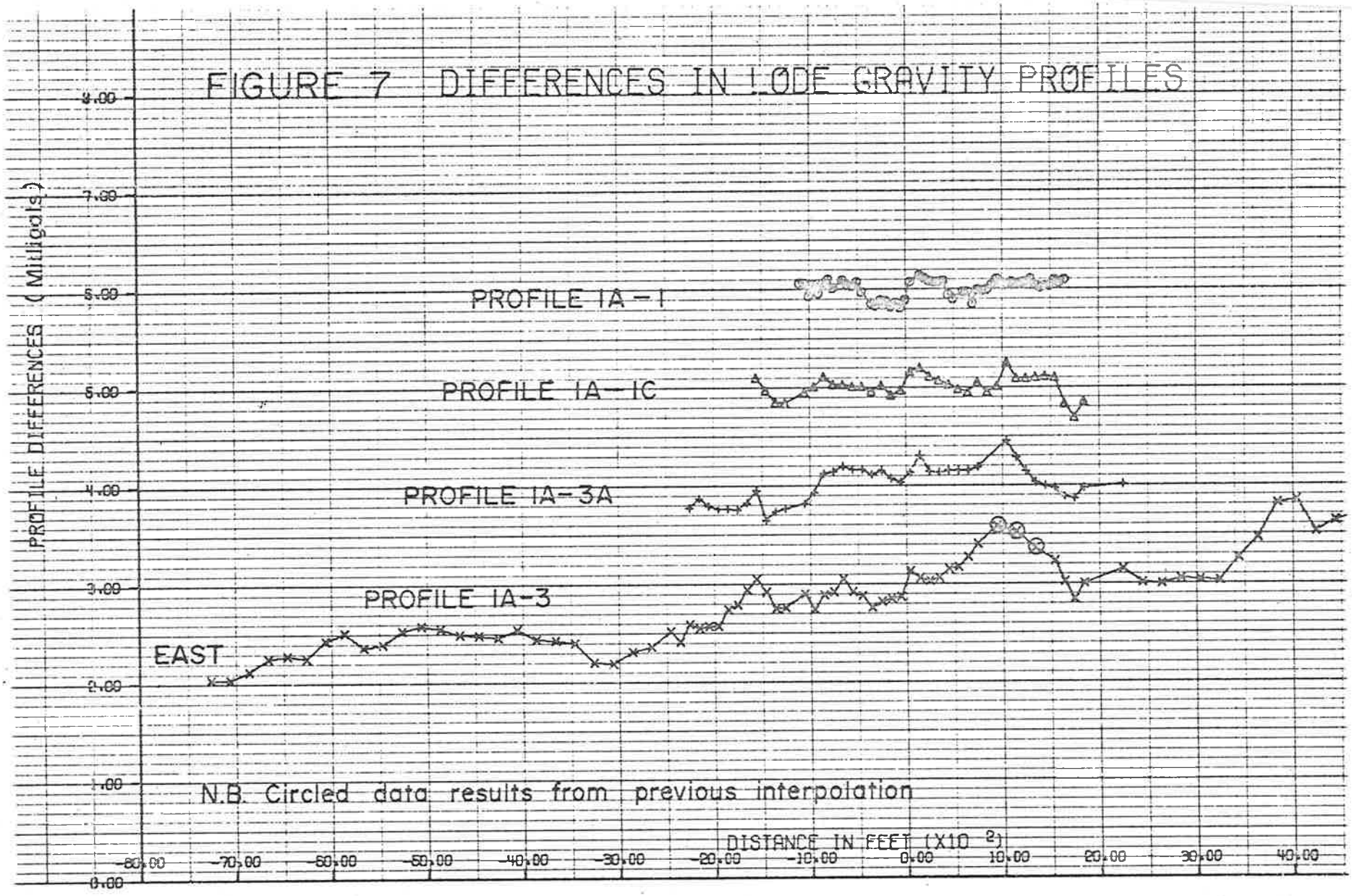
FIGURE 7 DIFFERENCES IN LODE GRAVITY PROFILES
PROFILE DIFFERENCES (Milligals)
8.00
7.00
6.00
5.00
4.00
3.00
2.00
1.00
0.00
PROFILE IA-1
PROFILE IA-IC
PROFILE IA-3A
PROFILE IA-3
EAST
N.B. Circled data results from previous interpolation
DISTANCE IN FEET (X10 2)
-80.00
-70.00
-60.00
-50.00
-40.00
-30.00
-20.00
-10.00
0.00
10.00
20.00
30.00
40.00

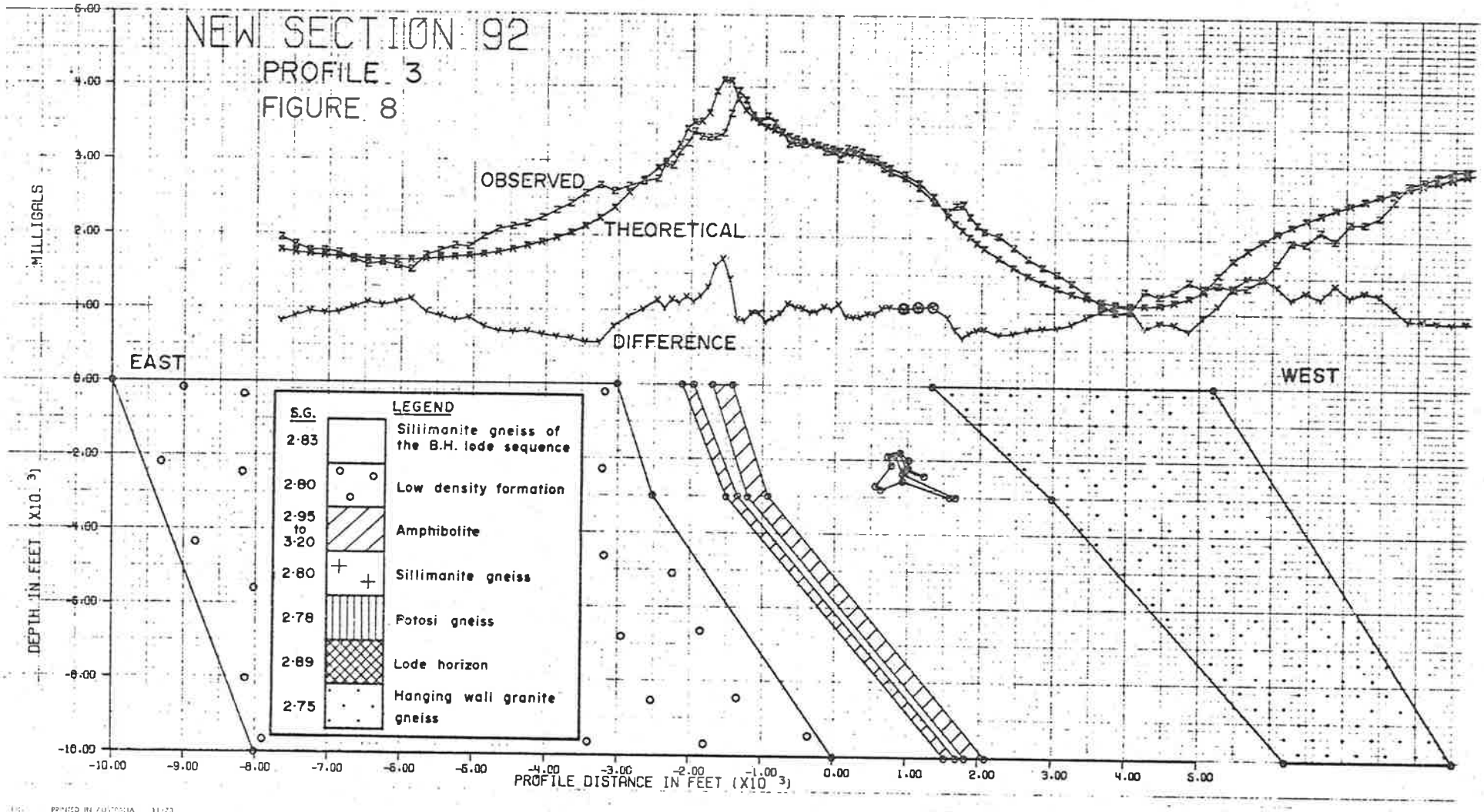
NEW SECTION 92
PROFILE 3
FIGURE 8
OBSERVED
THEORETICAL
DIFFERENCE
MILLIGALS
EAST
WEST
DEPTH IN FEET (X10 3)
PROFILE DISTANCE IN FEET (X10 3)
S.G.
LEGEND
2·83
Sillimanite gneiss of the B.H. lode sequence
2·80
Low density formation
2·95 to 3·20
Amphibolite
2·80
Sillimanite gneiss
2·78
Potosi gneiss
2·89
Lode horizon
2·75
Hanging wall granite gneiss

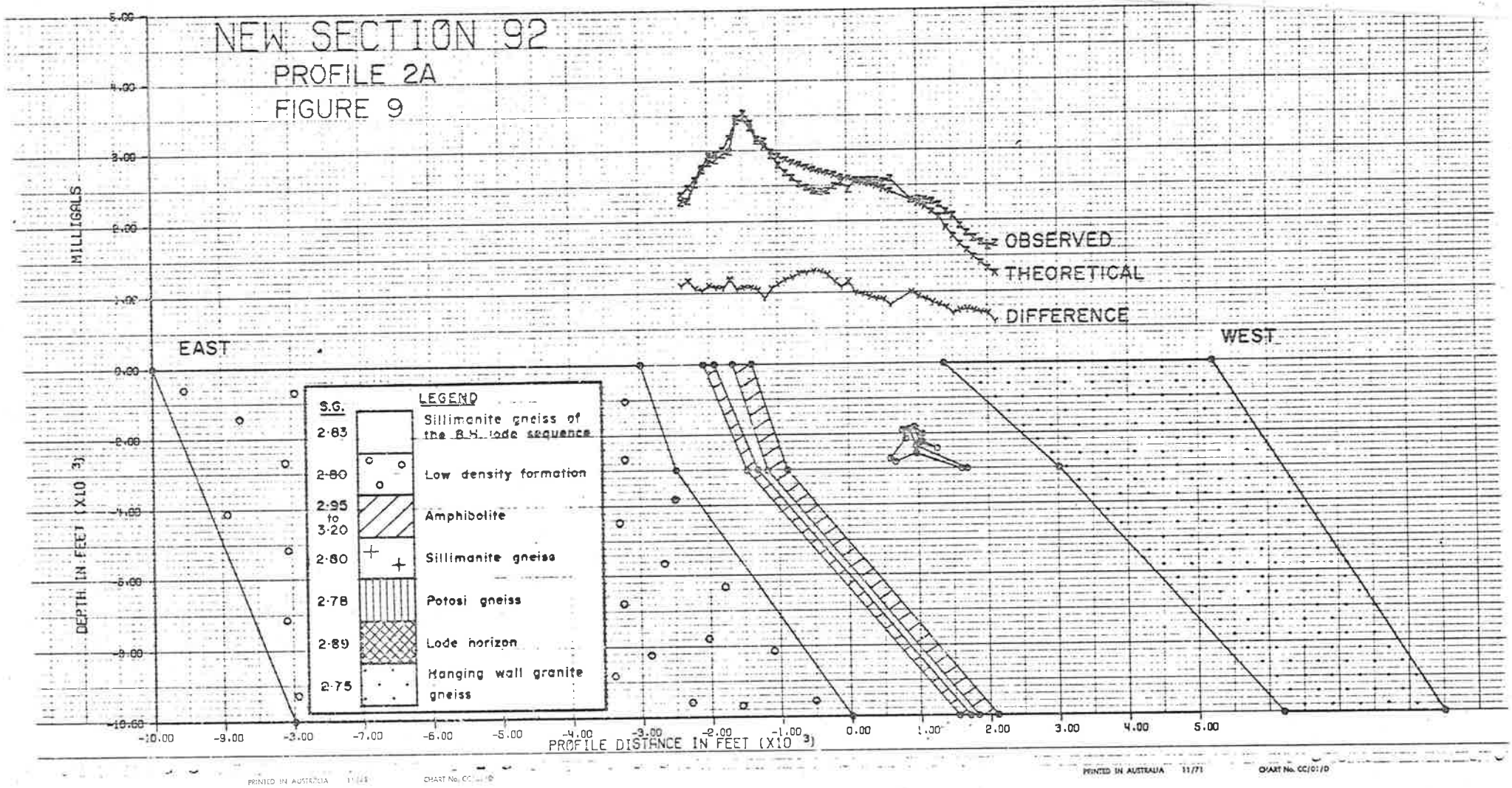

PRINTED IN AUSTRALIA 11/71 CHART No. CC/01/D

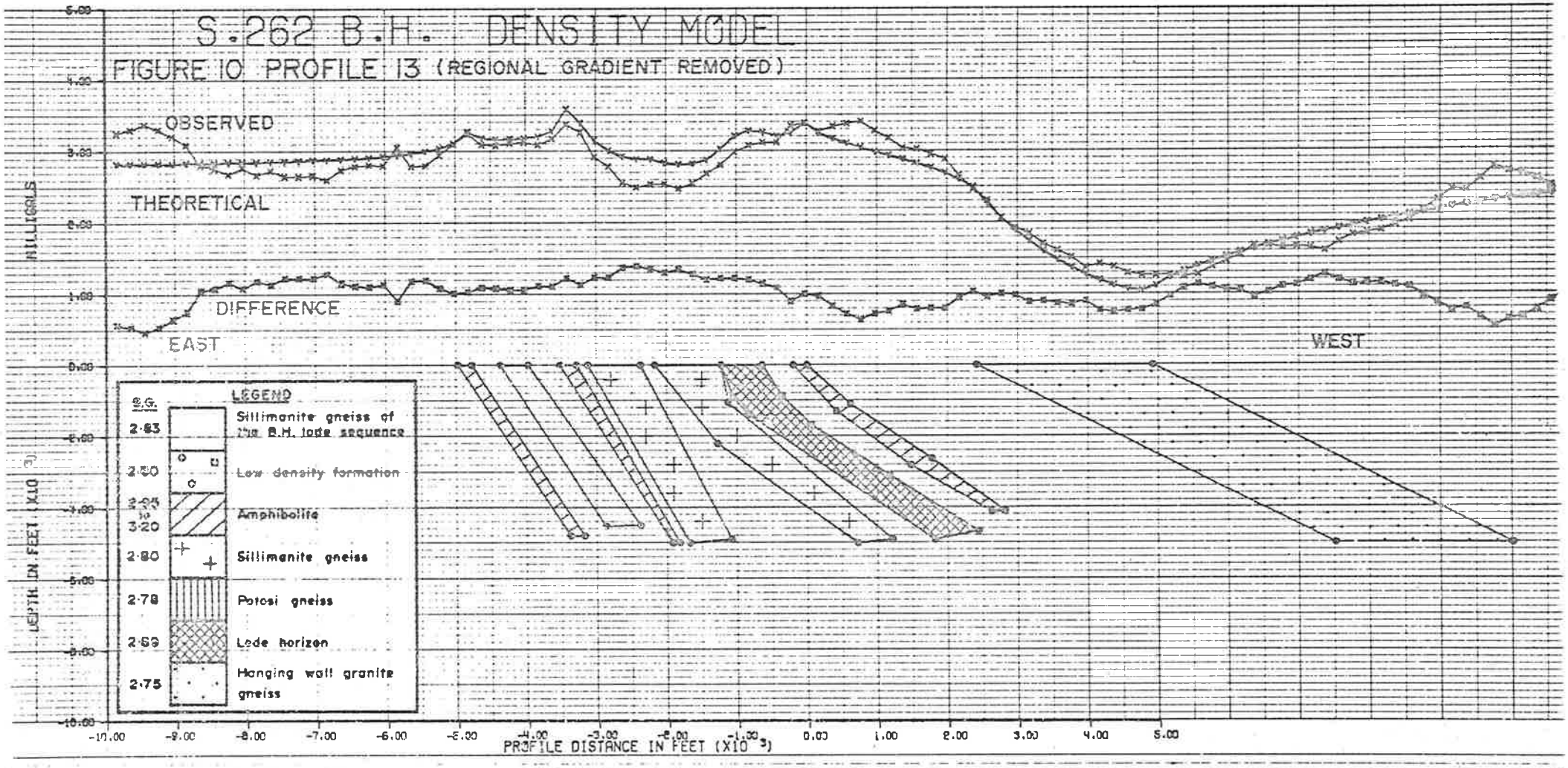

PRINTED IN AUSTRALIA 11/71 CHART No. CC/01/D

PRINTED IN AUSTRALIA 11/71 CHART No. CC/01/D

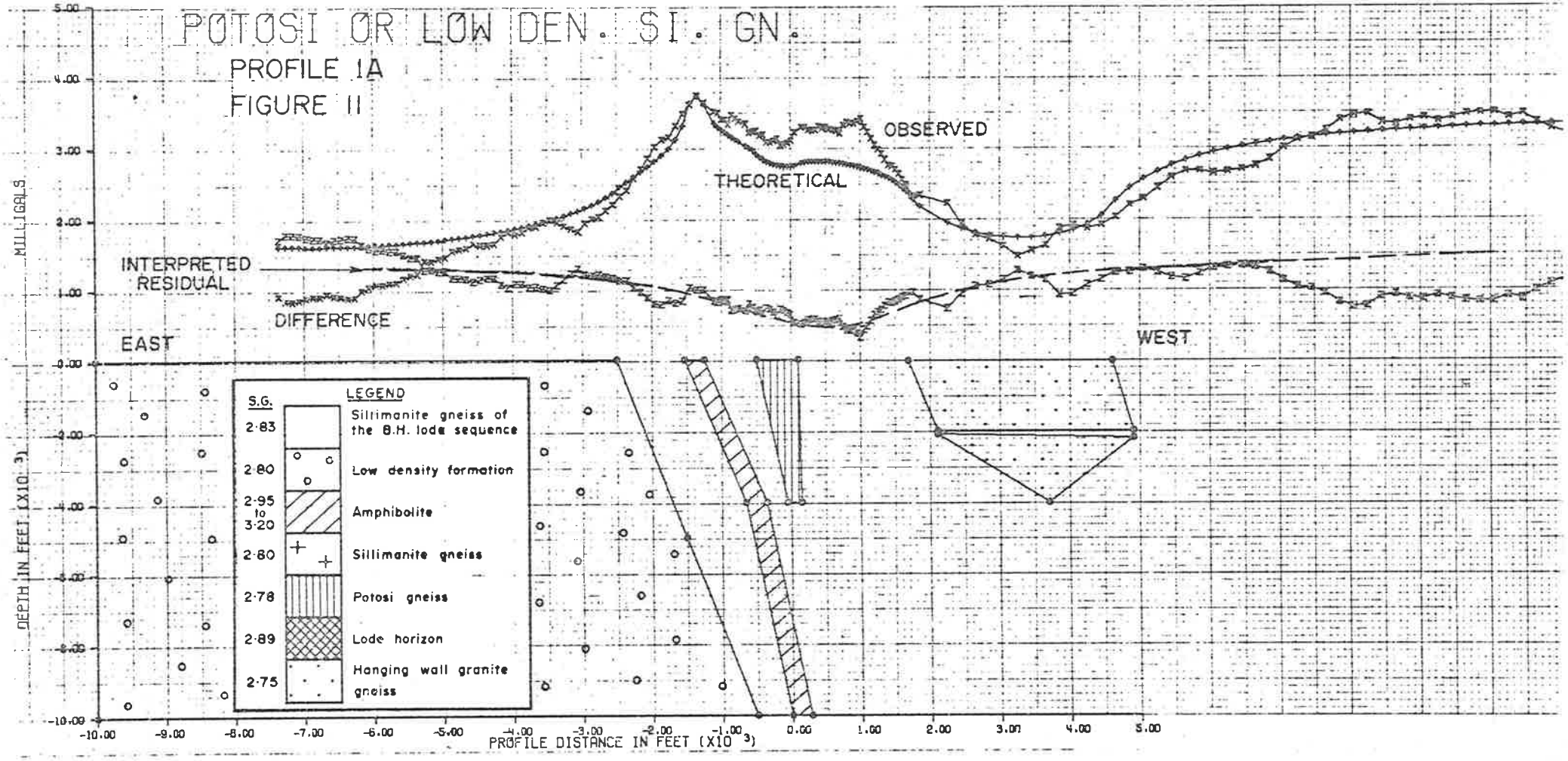
POTOSI OR LOW DEN. SI. GN.
PROFILE 1A
FIGURE 11
OBSERVED
THEORETICAL
INTERPRETED RESIDUAL
DIFFERENCE
EAST
WEST
MILLIGALS
DEPTH IN FEET (X10 3)
PROFILE DISTANCE IN FEET (X10 3)
LEGEND
S.G.
2·83 Sillimanite gneiss of the B.H. lode sequence
2·80 Low density formation
2·95 to 3·20 Amphibolite
2·80 Sillimanite gneiss
2·78 Potosi gneiss
2·89 Lode horizon
2·75 Hanging wall granite gneiss

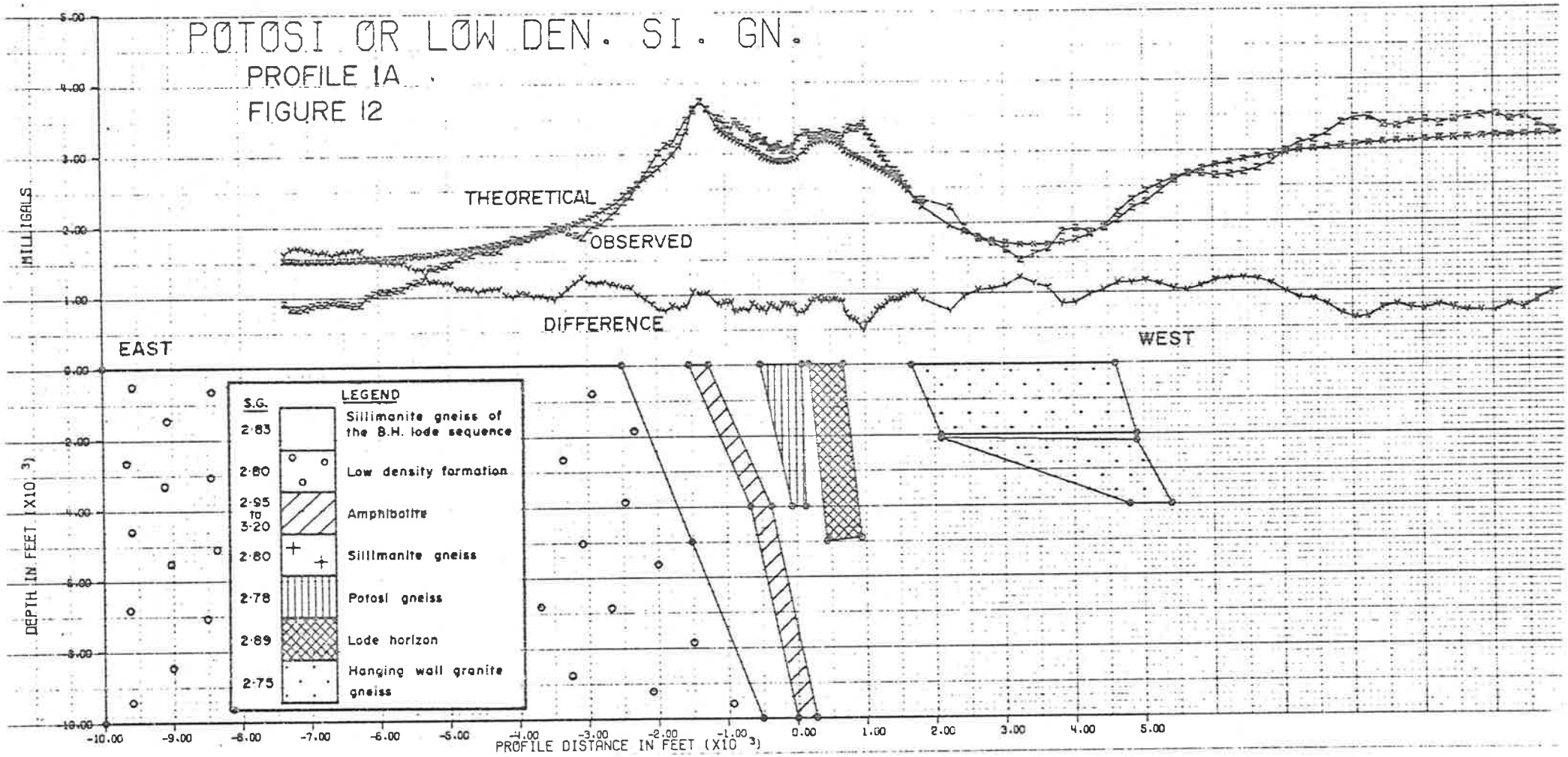
POTOSI OR LOW DEN. SI. GN.
PROFILE 1A
FIGURE 12
THEORETICAL
OBSERVED
DIFFERENCE
EAST
WEST
MILLIGALS
DEPTH IN FEET (X10 3)
PROFILE DISTANCE IN FEET (X10 3)
LEGEND
S.G.
2·83 Sillimanite gneiss of the B.H. lode sequence
2·80 Low density formation
2·95 to 3·20 Amphibolite
2·80 Sillimanite gneiss
2·78 Potosi gneiss
2·89 Lode horizon
2·75 Hanging wall granite gneiss

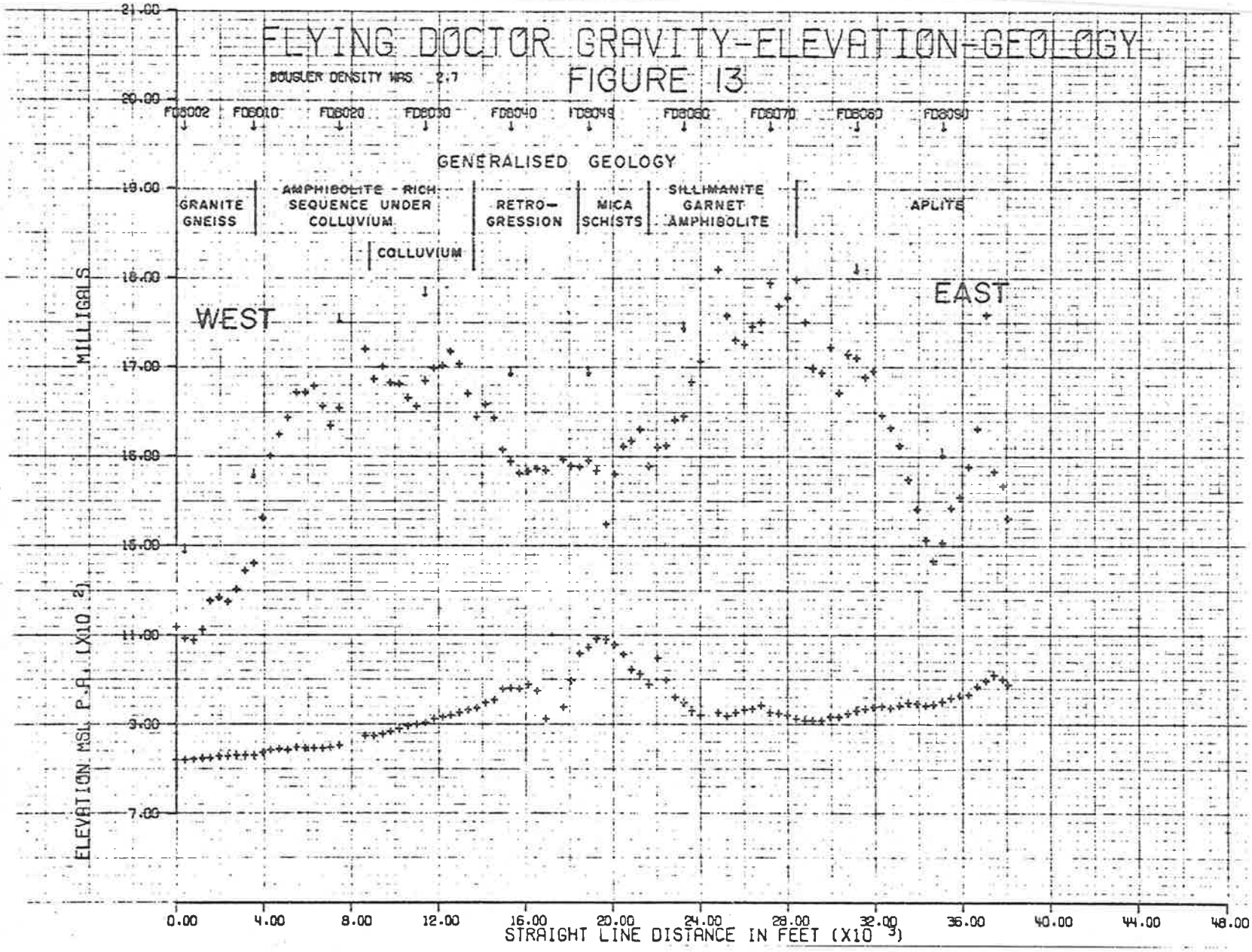
FLYING DOCTOR GRAVITY-ELEVATION-GEOLOGY
FIGURE 13
BOUGUER DENSITY WAS 2.7
FD8002
FD8010
FD8020
FD8030
FD8040
FD8049
FD8060
FD8070
FD8080
FD8090
GENERALISED GEOLOGY
GRANITE GNEISS
AMPHIBOLITE - RICH SEQUENCE UNDER COLLUVIUM
COLLUVIUM
RETRO-GRESSION
MICA SCHISTS
SILLIMANITE GARNET AMPHIBOLITE
APLITE
WEST
EAST
MILLIGALS
ELEVATION MSL P.A. (X10 2)
21.00
19.00
17.00
15.00
11.00
9.00
7.00
0.00
4.00
8.00
12.00
16.00
20.00
24.00
28.00
32.00
36.00
40.00
44.00
48.00
STRAIGHT LINE DISTANCE IN FEET (X10 3)

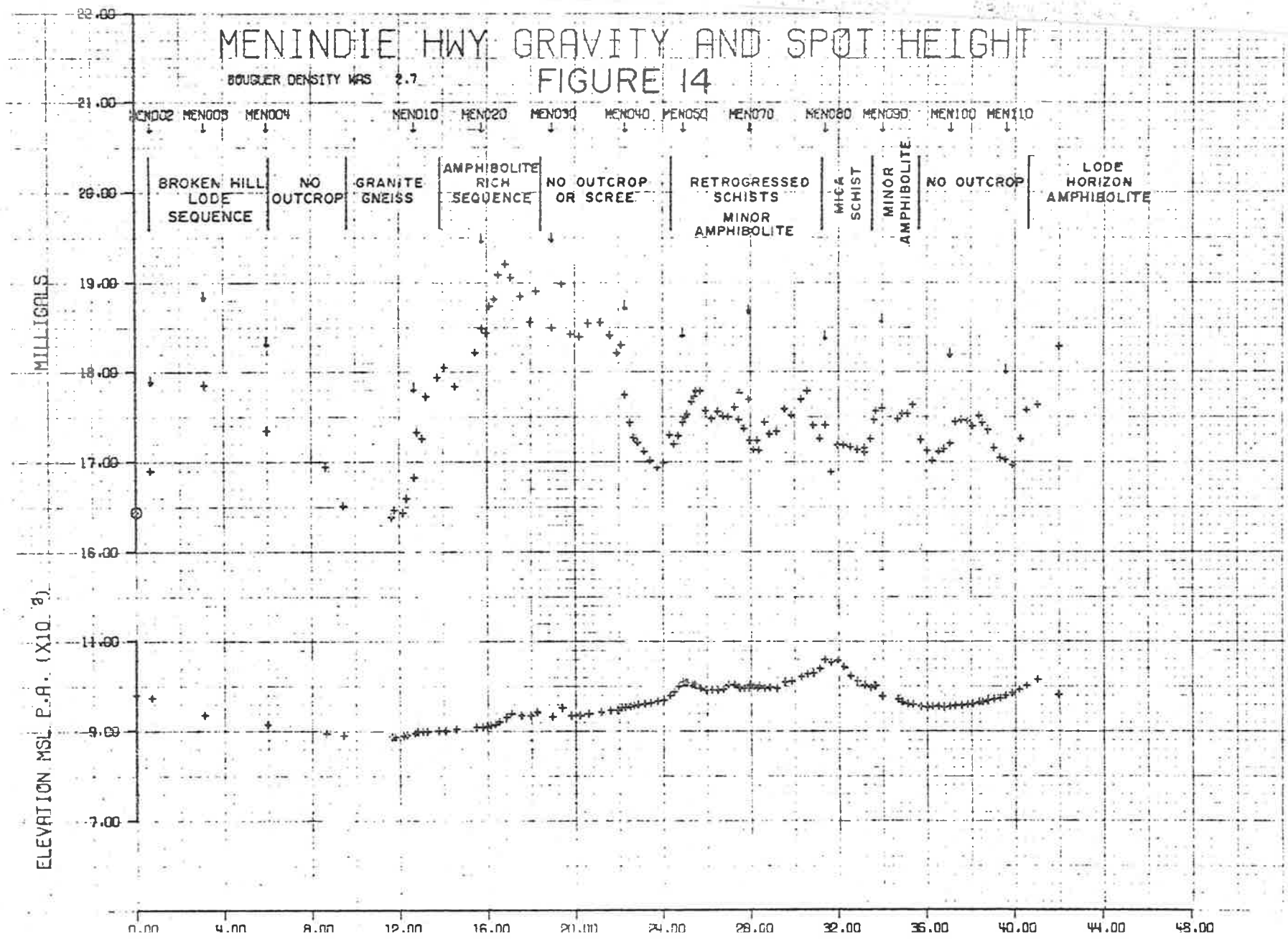
MENINDIE HWY GRAVITY AND SPOT HEIGHT
FIGURE 14
BOUGUER DENSITY WAS 2.7
MEN002 MEN003 MEN004 MEN010 MEN020 MEN030 MEN040 MEN050 MEN070 MEN080 MEN090 MEN100 MEN110
BROKEN HILL LODE SEQUENCE
NO OUTCROP
GRANITE GNEISS
AMPHIBOLITE RICH SEQUENCE
NO OUTCROP OR SCREE
RETROGRESSED SCHISTS
MINOR AMPHIBOLITE
MICA SCHIST
MINOR AMPHIBOLITE
NO OUTCROP
LODE HORIZON AMPHIBOLITE
MILLIGALS
ELEVATION MSL P.A. (X10. 8)
22.00
21.00
20.00
19.00
18.00
17.00
16.00
11.00
9.00
7.00
0.00
4.00
8.00
12.00
16.00
20.00
24.00
28.00
32.00
36.00
40.00
44.00
48.00

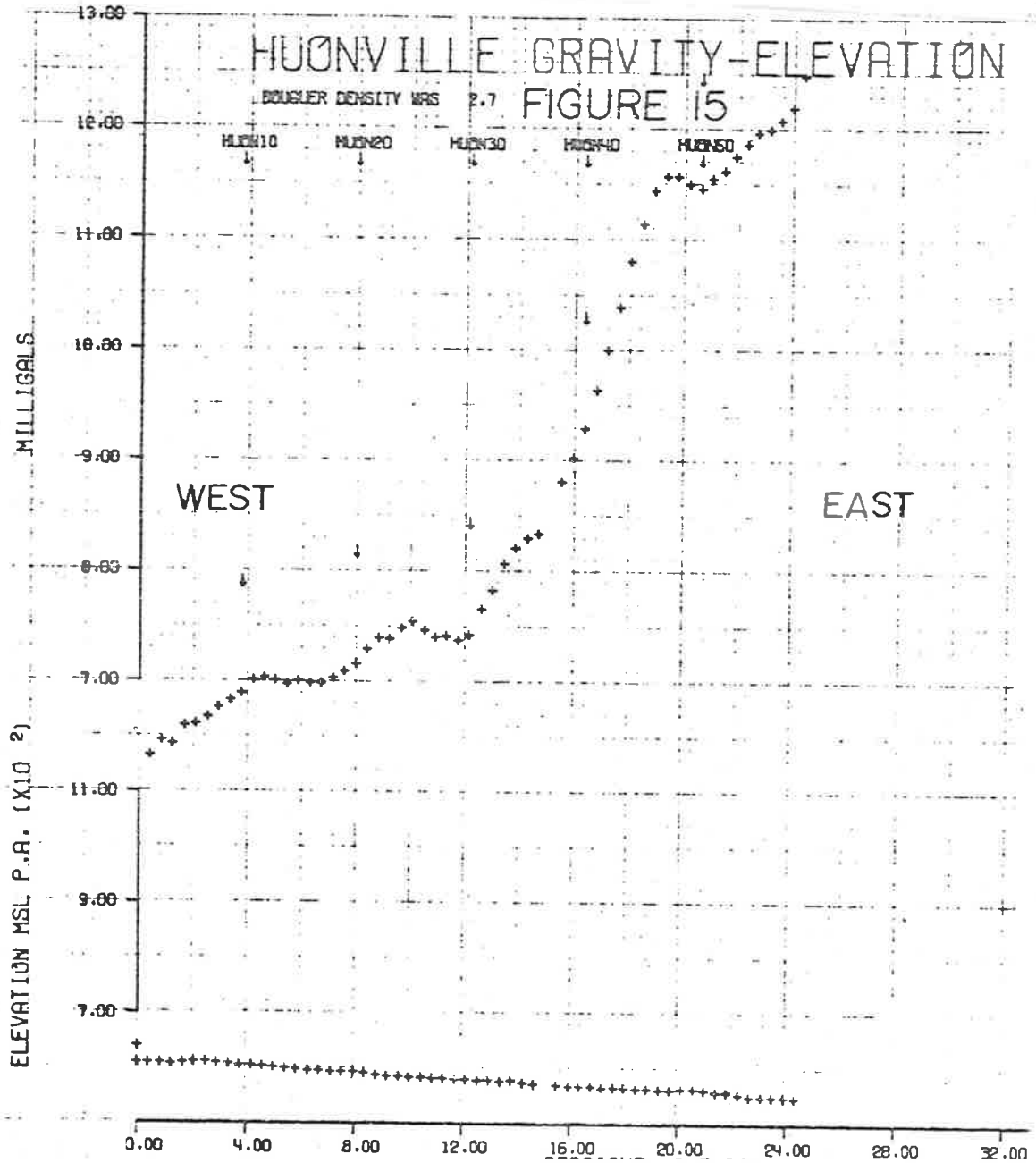
HUONVILLE GRAVITY-ELEVATION
BOUGUER DENSITY WAS 2.7
FIGURE 15
HUON10
HUON20
HUON30
HUON40
HUON50
WEST
EAST
MILLIGALS
ELEVATION MSL P.A. (X10 2)
13.00
12.00
11.00
10.00
9.00
8.00
7.00
11.00
9.00
7.00
0.00
4.00
8.00
12.00
16.00
20.00
24.00
28.00
32.00

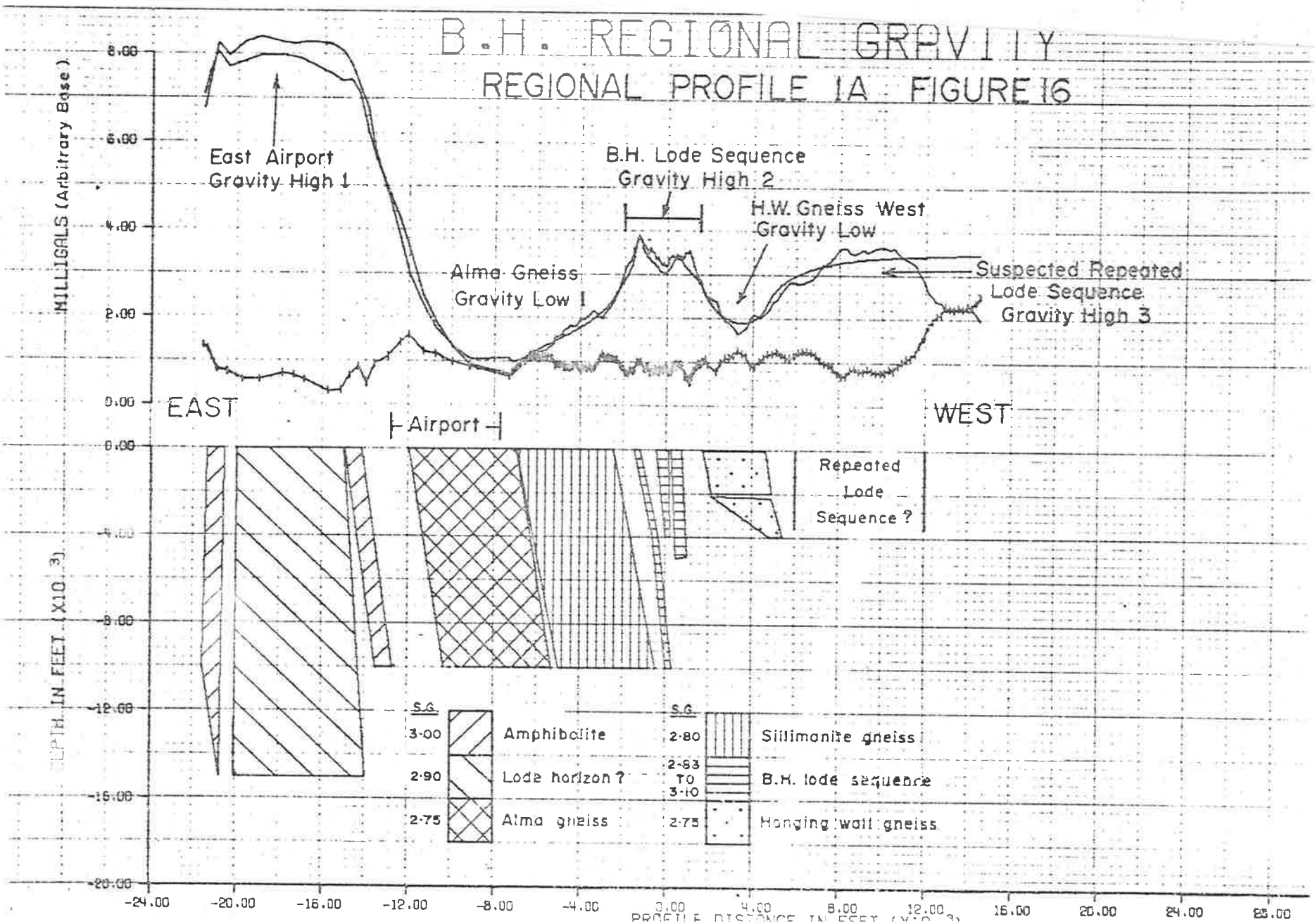
B.H. REGIONAL GRAVITY
REGIONAL PROFILE 1A FIGURE 16
MILLIGALS (Arbitrary Base)
East Airport Gravity High 1
B.H. Lode Sequence Gravity High 2
H.W. Gneiss West Gravity Low
Alma Gneiss Gravity Low 1
Suspected Repeated Lode Sequence Gravity High 3
EAST
WEST
Airport
Repeated Lode Sequence ?
DEPTH IN FEET (X10 3)
S.G.
3·00 Amphibolite
2·90 Lode horizon ?
2·75 Alma gneiss
S.G.
2·80 Sillimanite gneiss
2·83 TO 3·10 B.H. lode sequence
2·75 Hanging wall gneiss
PROFILE DISTANCE IN FEET (X10 3)

S. 262 B.H. DENSITY MODEL
REGIONAL GRAVITY PROFILE 13
FIGURE 17

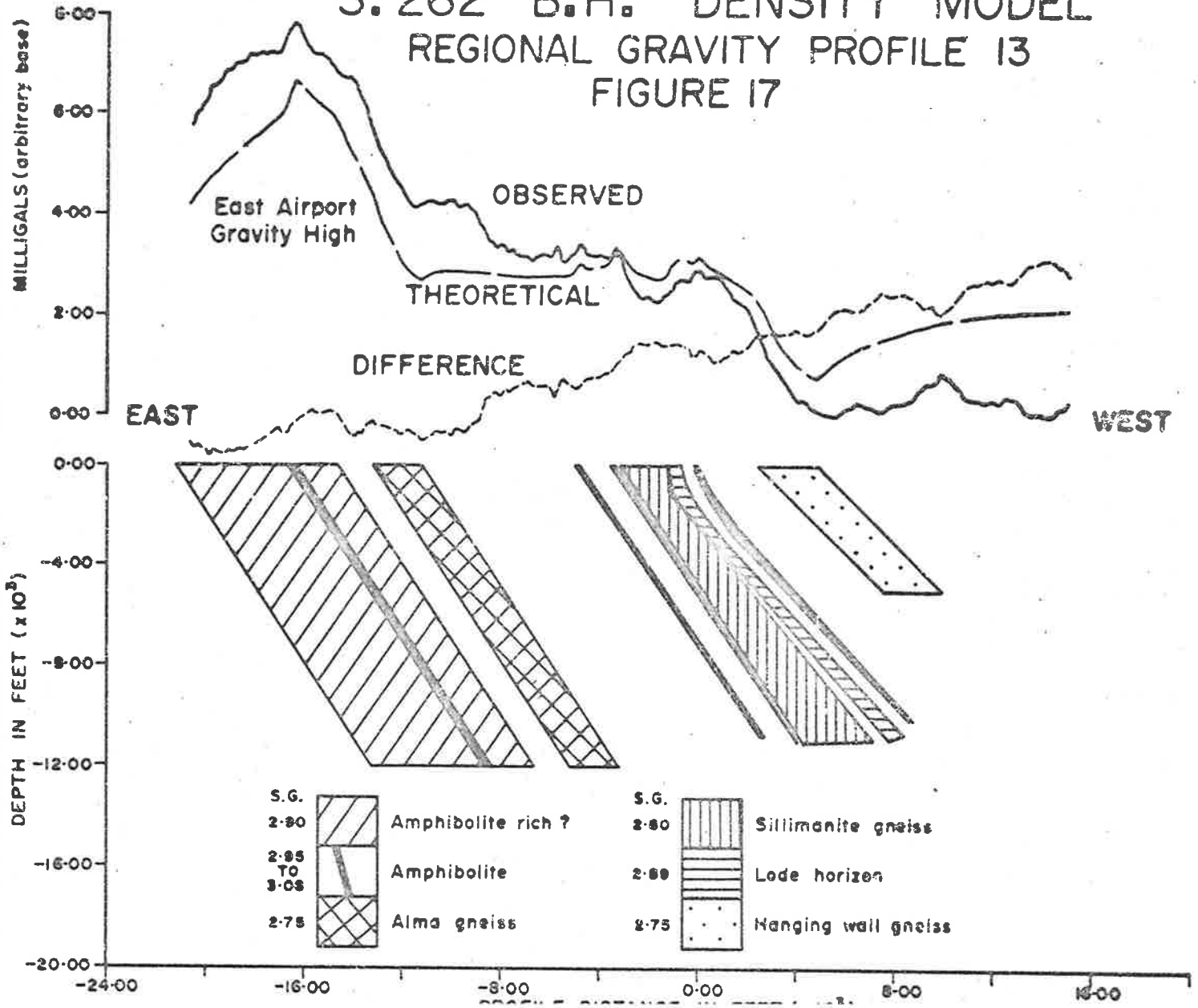

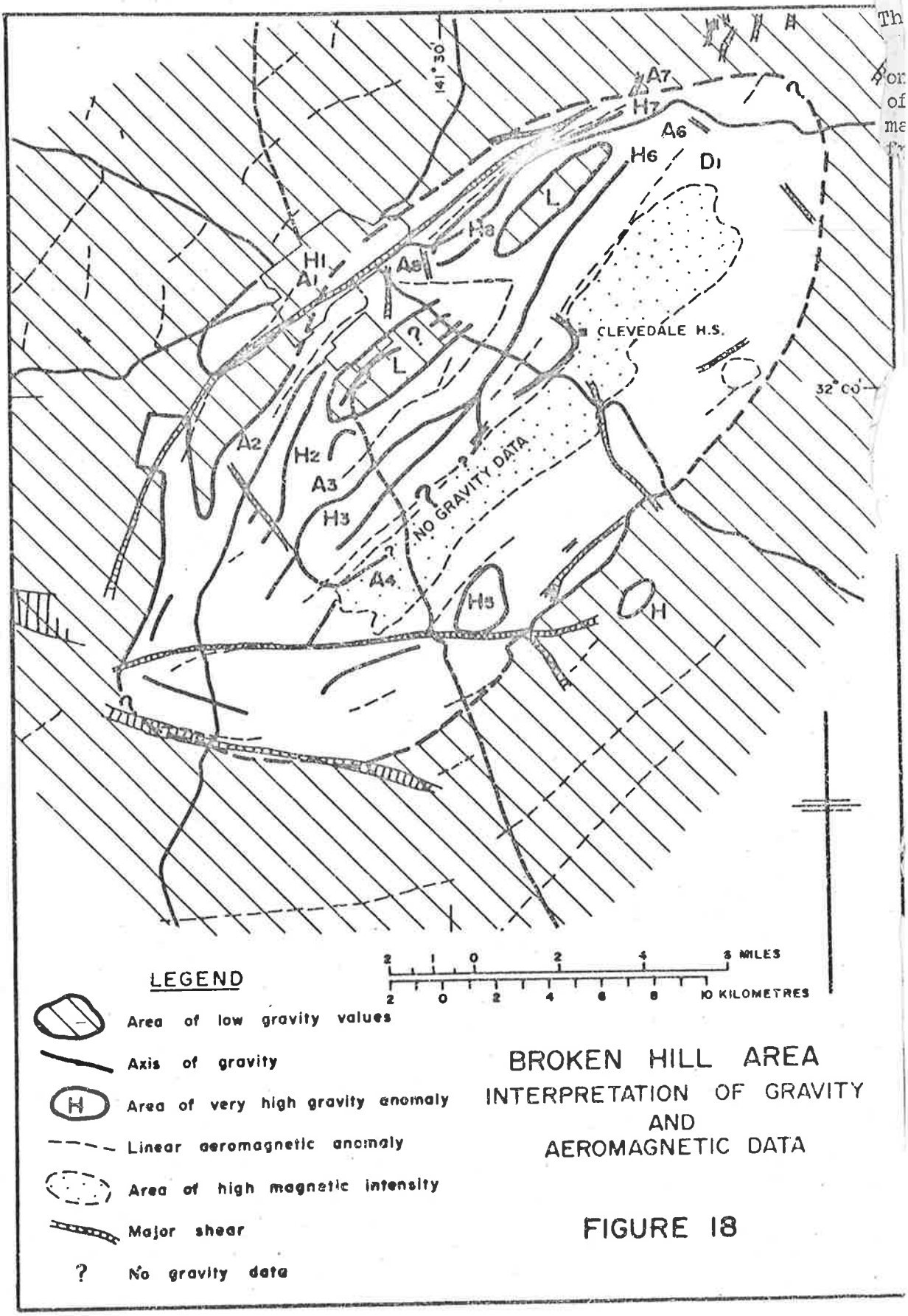

BROKEN HILL AREA
INTERPRETATION OF GRAVITY
AND
AEROMAGNETIC DATA

FIGURE 18